Université de Montréal

Characterization of two sorting nexins: sorting nexin-11 and sorting nexin-30

par Michel Cameron

Département de Pharmacologie, Faculté de Médecine

Thèse présentée à la Faculté de Médecine en vue de l'obtention du grade de Doctorat en Pharmacologie

Octobre, 2014

L’identification du jury

Président : Dr Éric Thorin

Membre du jury : Dr Gregor Andelfinger (Directeur de recherche)

Membre du jury : Dr Sylvain Chemtob (Co-directeur de recherche)

Membre du jury : Dr Stéphane Lefrançois

Examinateur externe : Dr Stéphane Angers

Résumé français

À l'intérieur de la cellule sillonnent d'innombrables molécules, certaines par diffusion et d'autres sur des routes moléculaires éphémères, empruntées selon les directives spécifiques de protéines responsables du trafic intracellulaire. Parmi celles-ci, on compte les sorting nexins, qui déterminent le sort de plusieurs types de protéine, comme les récepteurs, en les guidant soit vers des voies de dégradation ou de recyclage. À ce jour, il existe 33 membres des sorting nexins (Snx1-33), tous munies du domaine PX (PHOX-homology). Le domaine PX confère aux sorting nexins la capacité de détecter la présence de phosphatidylinositol phosphates (PIP), sur la surface des membranes lipidiques (ex : membrane cytoplasmique ou vésiculaire). Ces PIPs, produits de façon spécifique et transitoire, recrutent des protéines nécessaires à la progression de processus cellulaires. Par exemple, lorsqu'un récepteur est internalisé par endocytose, la région avoisinante de la membrane cytoplasmique devient occupée par $PI(4,5)P_2$. Ceci engendre le recrutement de SNX9, qui permet la progression de l'endocytose en faisant un lien entre le cytoskelette et le complexe d'endocytose.

Les recherches exposées dans cette thèse sont une description fonctionnelle de deux sorting nexins peux connues, Snx11 et Snx30. Le rôle de chacun de ces gènes a été étudié durant l'embryogenèse de la grenouille (*Xenopus laevis*). Suite aux résultats *in vivo*, une approche biomoléculaire et de culture cellulaire a été employée pour approfondir nos connaissances.

Cet ouvrage démontre que Snx11 est impliqué dans le développement des somites et dans la polymérisation de l'actine. De plus, Snx11 semble influencer le recyclage de récepteurs

membranaires indépendamment de l'actine. Ainsi, Snx11 pourrait jouer deux rôles intracellulaires : une régulation actine-dépendante du milieu extracellulaire et le triage de récepteurs actine-indépendant. De son côté, Snx30 est impliqué dans la différentiation cardiaque précoce par l'inhibition de la voie Wnt/β-catenin, une étape nécessaire à l'engagement d'une population de cellules du mésoderme à la ligné cardiaque. L'expression de Snx30 chez le Xénope coïncide avec cette période critique de spécification du mésoderme et le knockdown suscite des malformations cardiaques ainsi qu'à d'autres tissus dérivés du mésoderme et de l'endoderme.

Cet ouvrage fournit une base pour des études futures sur Snx11 et Snx30. Ces protéines ont un impact subtil sur des voies de signalisation spécifiques. Ces caractéristiques pourraient être exploitées à des fins thérapeutiques puisque l'effet d'une interférence avec leurs fonctions pourrait être suffisant pour rétablir un déséquilibre cellulaire pathologique tout en minimisant les effets secondaires.

Mots clés : Sorting nexin, trafic intracellulaire, embryogenèse, cardiogénèse, somitogenèse, Wnt/β-catenin, actin

English Summary

The intracellular milieu is housed by countless numbers of intracellular molecules travelling by diffusion or along transient paths, which are regulated by specific trafficking proteins. Among these traffic regulators are the sorting nexins that determine the fate of internalized proteins by directing toward a defined path, which can lead to either degradation or recycling. To date, 33 sorting nexins (Snx1-33) have been identified, which all share a common characteristic, the presence of a PX (PHOX-homology) domain. The PX domain is a phosphatidylinositol phosphate (PIP)-binding domain, which helps bring sorting nexins to PIP-enriched areas of lipid membranes. For example, during receptor endocytosis, the surrounding membrane becomes transiently occupied by $PI(4,5)P_2$. $PI(4,5)P_2$ is then recognized by Snx9, which contributes to the progression of endocytosis by linking the receptor complex to the actin cytoskeleton.

The research presented in this thesis is the first to investigate the functions for two sorting nexins, Snx11 and Snx30, during embryogenesis and endosomal protein trafficking. Results obtained from knockdown experiments in the frog (*Xenopus laevis*) were combined with data from cell culture and biomolecular experiments to propose a function for these two proteins. The data presented here suggest that Snx11 is involved in somitogenesis, and regulates actin-dependent and -independent processes. Snx11 could serve as a scaffolding protein, linking the extra-cellular matrix to the actin cytoskeleton and could also function in actin-independent receptor recycling. On the other hand, Snx30 is implicated in early cardiogenesis and promotes the commitment of a population of mesoderm cells to the cardiac lineage. It does so through the inhibition of Wnt/β-catenin signaling but the underlying mechanism is still unclear.

Expression of Snx30 in Xenopus coincides with this critical period of cardiac specification and knockdown of Snx30 results in cardiac malformations as well as other defects in mesoderm- and endoderm-derived tissue. In addition, data from both Xenopus and HEK293T cell culture show that knockdown of Snx30 increases Wnt/β-catenin signaling.

This work provides the basis for future studies on Snx11 and Snx30. Interestingly, Snx11 and Snx30 seem to act as fine-tuners of signaling pathways. These proteins could potentially become interesting therapeutic targets due to their specificity and relatively subtle impact when knocked-down. As such, interference with their function could be useful to re-balance a cellular disequilibrium while minimizing side effects.

Key words: Sorting nexin, protein trafficking, embryogenesis, cardiogenesis, somitogenesis, Wnt/β-catenin, actin

Table of Contents

L'identification du jury ii

Résumé français iii

English Summary v

Acknowledgements xiv

Chapter 1: The cellular biology of protein trafficking 1

1.1 – Endocytosis 2

1.2 – Clathrin-mediated endocytosis 5

1.3 – Clathrin-independent endocytosis 9

1.4 – The endosomal system 13

1.5 – Receptor degradation and recycling 18

1.6 – Sorting nexins 21

1.7 – The PX domain 23

1.8 – Phosphatidylinositol phosphates 27

1.9 – SNX-BARs 30

1.10 – PX-only Sorting Nexins 33

1.11 – SNX-other 35

1.12 – RABs 36

1.13 – The cytoskeleton 38

1.14 – Vesicular transport of proteins 41

1.15 – Actin and membrane dynamics 46

1.16 – Embryogenesis 49

1.17 – Cardiogenesis 54

1.18 – Wnt signaling 63

1.18.1 – Endocytosis and Wnt/β-catenin signalling 68

1.19 – Somitogenesis 72

1.20 – Model organism: Xenopus laevis 75

1.21 – Disorders related to endosomes and sorting nexins 77

1.22 – Wnt/β-catenin signaling and disease 78

Chapter 2: Journal article #1 (submitted to the Journal of Biological Chemistry) 80

Chapter 3: Journal article #2 (submitted to Traffic) 122

Chapter 4: Conclusion 158

Characterization of two new sorting nexins 158

SNX30 and Wnt/β-catenin signaling 160

The dual functions of SNX11 164

References 166

Abbreviations

AAA: ATPases associated with various cellular activities

ANTH: AP180 amino-terminal homology

APC: Adenomatosis polyposis coli

APCDD: APC downregulated

BAR: Bin/Amphyphysin/Rvs

BMP: Bone morphogenetic protein

CHC: Clathrin heavy chain

CIE: Clathrin-independent endocytosis

CI-M6PR: Cation-independent mannose-6-phosphate receptor

CLC: Clathrin light chain

CME: Clathrin-mediated endocytosis

DAG: Diacylglycerol

DKK: Dickkopf-related protein

DOR: Delta opioid receptor

DSL: Delta, Serrate and LAG-2

EE: Early endosome

EEA1: Early endosome antigen-1

EGF: Epidermal growth factor

EGFR: Epidermal growth factor receptor

EMT: Epithelial to mesenchymal transition

ENT-1: Enterophilin-1

ENTH: Epsin N-terminal homology

EPS15: EGFR pathway substrate 15

ER: Endoplasmic reticulum

ERC: Endosomal recycling compartment

ERT: Enzyme replacement therapy

ESC: Embryonic stem cell

ESCRT: Endosomal sorting complexes required for transport

F-BAR: Fes/CIP4 homology BAR

FCHO: FCH domain only

FGF: Fibroblast growth factor

FHF: First heart field

FZ: Frizzled

GAP: GTPase-activating protein

GATA4: GATA-binding protein 4

GEEC: GPI-enriched early endosomal compartment

GEF: Guanine exchange factor

GFP: Green fluorescent protein

GPI: Glycosylphosphatidylinositol

GRK: G protein-coupled receptor kinase

GSK3: Glycogen synthase 3

HES: Hairy and enhancer of split

HPF: Hours post-fertilization

HRS: Hepatocyte growth factor-regulated tyrosine kinase substrate

HSC70: Heat shock cognate 70

I-BAR: Inverse BAR

IL2R: Interleukin 2 receptor

ILV: Intralumenal vesicle

JNK: Jun-N-terminal kinase

LBPA: Lysobiphosphatidic acid

LE: Late endosome

LEF: Lymphoid enhancer-binding factor

LRP5/6: Low-density lipoprotein receptor-related protein

LSD: Lysosomal storage disorder

MDCK: Madin Darby canine kidney

MESP: Mesoderm posterior

MHC1: Major histocompatibility class 1

MTOC: Microtubule-organizing center

MUSK: Muscle skeletal tyrosine kinase

MVB: Multivesicular body

NKX2-5: NK2 transcription factor related, locus 5

NOXO1: NOX organizing 1 protein

PCP: Planar cell polarity

PDAC: Pancreatic ductal adenocarcinoma

PDB: Protein database

PH: Pleckstrin homology

PHOX: Phagocyte NADPH oxidase

PI: Phosphatidylinositol

PIBM: PI-binding module

PIP: Phosphatidylinositol phosphate

PI(3)K: Phosphatidylinositol 3-kinase

PKA: Protein kinase A

PKC: Protein kinase C

PSM: Presomitic mesoderm

PTK: Protein tyrosine kinase

PX: PHOX-homology

PXe: Extended PX

RAB11FIP: Rab11 family interacting protein

ROR: Tyrosine kinase-like orphan receptor

RSPO: R-spondin

RYK: Receptor tyrosine kinase

SFRP: Secreted frizzled-related protein

SHF: Second heart field

SNX: Sorting nexin

SO: Spemann organizer

TCF: T cell factor

TGN: *trans*-Golgi network

Toca: Transducer of Cdc42-dependent actin assembly

VPS: Vacuole protein sorting

WAIF: Wnt-activated inhibitory factor

WIF: Wnt inhibitory factor

Acknowledgements

I would like to personally thank Gregor Andelfinger for his openness to new ideas, enthusiasm and contagious work ethic. This would have not been possible without him and I am forever grateful. I would also like to thank all members of the Andelfinger lab for their help, support and encouragement during my PhD training. Thank you to Sylvain Chemtob and members of his laboratory for valuable insight and expertise.

Many thanks to Christian Beauséjour for his insight and council.

Thank you to members of my pre-doctoral exam committee and to members of my thesis jury.

Finally, I would like to thank my parents and Marie-Claude for their support and encouragements.

Chapter 1: The cellular biology of protein trafficking

Living cells are in constant flux. As part of a living organism, cells must process signals coming from the extracellular milieu, and carry out an appropriate cellular response. During both of these essential steps (signal processing and cellular response) intracellular trafficking is fundamental. The necessity of intracellular trafficking is explained by the fact that molecules cannot travel far by free diffusion and signaling effectors must be properly localized to interact with their targets. Intracellular trafficking is thus involved in virtually all aspects of cellular biology since proteins must be located at their site of action to properly perform their task. Endosomal protein sorting is a form of intracellular trafficking that regulates the transportation of membrane-associated proteins across different intracellular compartments. This form of traffic occurs in the following sequence of processes: formation and fission of a transport vesicle from a donor membrane, transportation of this vesicle between compartments, and finally docking and fission of the vesicle with the acceptor membrane. However, prior to these processes, a decision is made as to which cargo will be selected and what will be its destination. This aspect of protein trafficking is termed endosomal protein sorting.

The main components that contribute to intracellular trafficking (endocytosis, the endosomal system and the processes of intracellular trafficking) will be discussed in the next sections with examples to illustrate how they function. Throughout these sections, it is important to consider that the results that stem from isolated cellular processes are in fact part of a holistic, interconnected system that is the living organism. As such, I will attempt to integrate data from molecular and cellular biology into developmental biology.

1.1 – Endocytosis

The entry of material into a eukaryotic cell occurs mostly through a process called endocytosis, an essential stage in many signaling pathways as it removes receptors from the cell surface. This limits the magnitude of signaling from extracellular sources and allows signaling to proceed from inside the cell. Endocytosis can also control ligand availability, as is the case for the membrane-bound DSL (Delta, Serrate and LAG-2) family of ligands, which activate the Notch family of receptors of adjacent cells [1]. Once internalized, material can travel throughout boundary-forming lipid membranes collectively known as the endosomal network, which includes compartments such as the early and late endosomes, the lysosome and the *trans*-Golgi network. Transportation of cargo throughout this dynamic network is a highly regulated process that requires the coordinated action of specialized trafficking proteins.

Many mechanisms of endocytosis exist and they have been divided into two major categories: clathrin-mediated endocytosis (CME) and clathrin-independent endocytosis (CIE) (Figure 1) [2]. Both these types of endocytosis are utilized to displace signaling receptors from the plasma membrane to an intracellular compartment. Endocytosis is also exploited by toxins, viruses and bacteria for penetration into the cell but this thesis will focus on the endocytosis and trafficking of receptors [3].

Endocytosis of a particular receptor can result in different outcomes depending on the endocytic route used. For example, internalization of the epidermal growth factor receptor (EGFR) with CME induces its recycling back to the plasma membrane [4, 5]. In contrast, if EGFR is internalized via CIE, the receptor is sent to the lysosome for degradation [4, 5]. In

addition, CME and CIE do not always produce the same effect. In Wnt/β-catenin signaling through the Frizzled receptor and LRP5/6 co-receptor, CME leads degradation of LRP5/6 while CIE leads to its recycling [6]. Therefore, the type of endocytosis alone does not determine the fate of internalized material mechanisms but rather contributes to signaling outcome, along with other factors such as the cellular context, the identity of internalized material and the trafficking machinery implicated in the process. The fate of internalized material and thus the sustainment, amplification or attenuation of signaling is intimately linked to endocytosis and subsequent sorting mechanisms. The next paragraphs provide a brief review of CME and CIE.

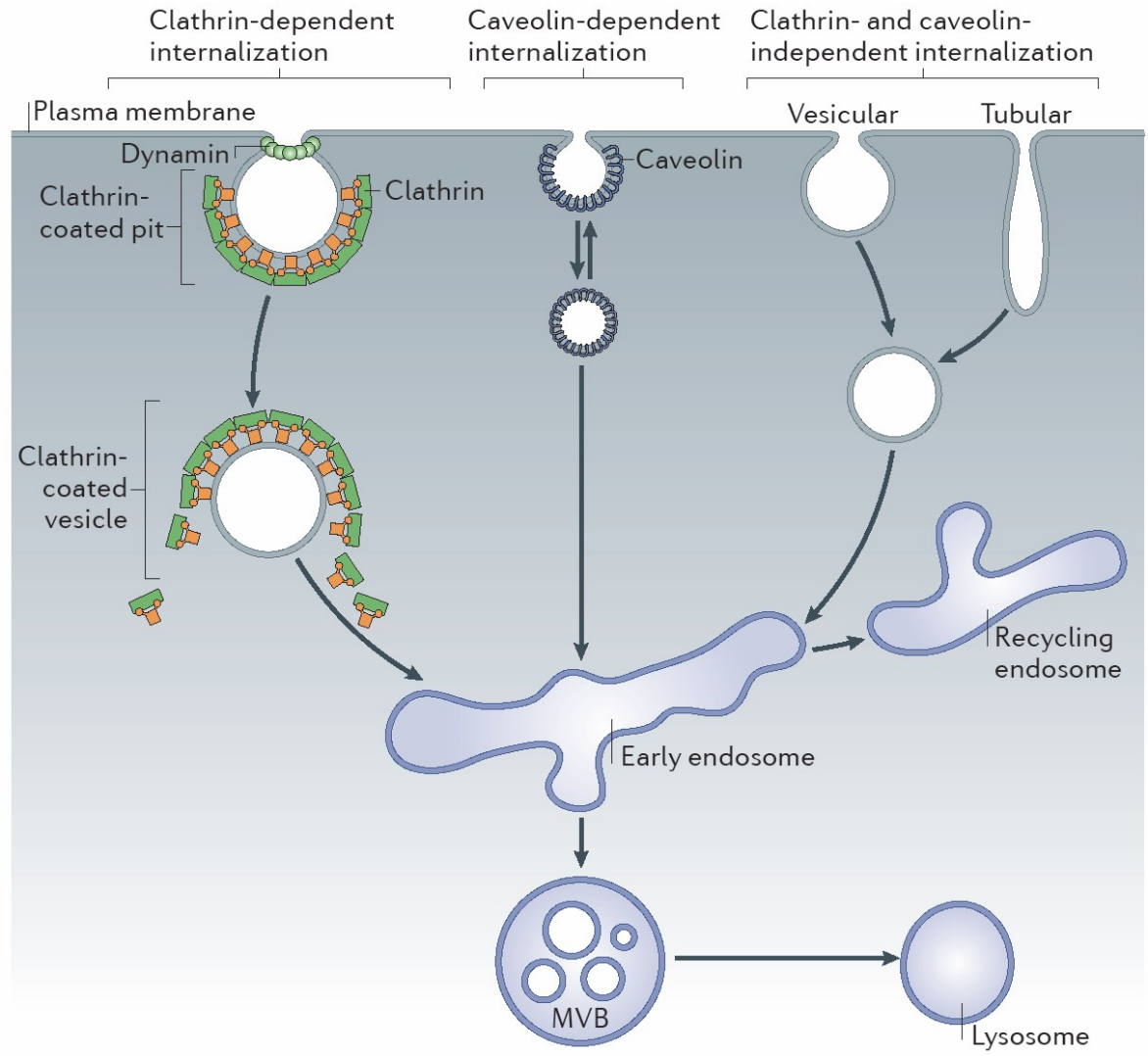

Figure 1. The different modes of endocytosis. Cells can internalize plasma membrane and receptors through a number of different routes. Clathrin-mediated and caveolin-mediated routes both require dynamin. The first destination in all routes is the early endosome, where protein sorting occurs, which directs cargo either back to the plasma membrane via the recycling endosome or into other compartments (multivesicular bodies (MVBs) or lysosomes) for degradation. [7]

1.2 – Clathrin-mediated endocytosis

The most studied and understood mechanism for the uptake of macromolecules is clathrin-mediated endocytosis. Clathrin is a protein that oligomerizes on the cytoplasmic side of the plasma membrane and assembles with other proteins to deform the plasma membrane, which becomes gradually invaginated, forming a clathrin-coated pit (CCP) (Figure 2). This CCP eventually buds off as a clathrin-coated vesicle, which is quickly uncoated before proceeding to their next intracellular destination. The whole process of clathrin-mediated endocytosis has been divided into five stages: nucleation, cargo selection, clathrin coat assembly, vesicle scission and uncoating [7].

1.2.1 – Nucleation

The first stage in CME is membrane invagination, triggered by the formation of a nucleation module, which is comprised of FCH domain only (FCHO) proteins, EGFR pathway substrate 15 (EPS15) and intersectins [8-10]. This nucleation module assembles at a specific site on the plasma membrane, transiently enriched with $PI(4,5)P_2$ [11]. During nucleation, the detection and induction of membrane deformations play important roles in the progression of endocytosis. For instance, the F-BAR domain of FCHO proteins and Snx9 bind to very low curvatures, generating further membrane bending [9, 10, 12].

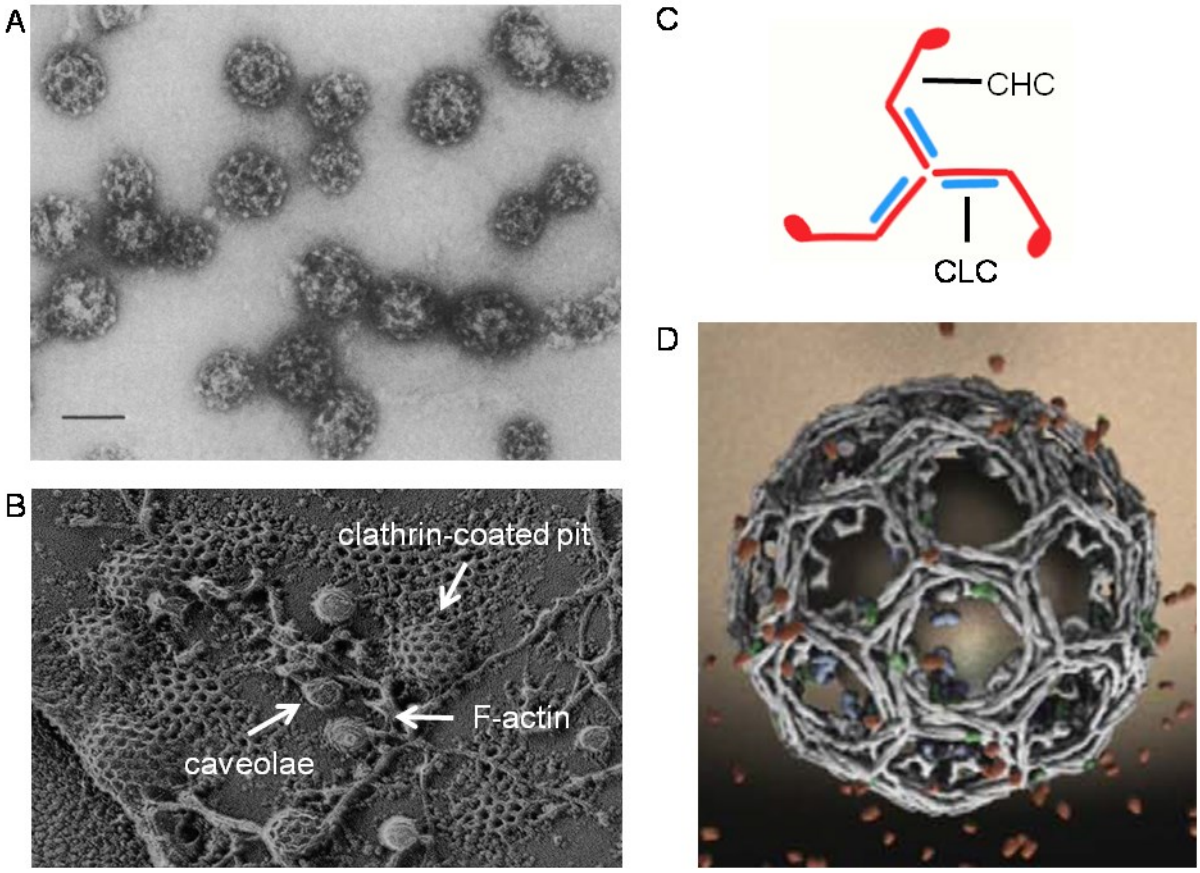

Figure 2. Clathrin. A) First identification of clathrin by Barbara Pearse in 1976 [13]. Shown here is an electron micrograph of bovine adrenal medulla fraction containing large clathrin coated vesicles (CCV) (X67,500). B) Quick-freeze deep-etch micrography of the inner plasma membrane surface of A431 cells showing the typical clathrin lattice of growing pits [14]. Caveolae are also seen surrounded by F-actin filaments. C) An illustration of the clathrin triskelia (CHC: clathrin heavy chain; CLC: clathrin light chain). D) A model of a clathrin-coated vesicle is depicted showing assembled clathrin triskelia [15].

1.2.2 – Cargo selection

Once the nucleation module is assembled at the plasma membrane, the AP2 adaptor complex joins the module and together, they mediate cargo selection [9]. AP2 acts as a major hub of interactions as it can directly and simultaneously bind to $PI(4,5)P_2$ and to motifs in the cytoplasmic tails of transmembrane receptors [16, 17]. Indirectly, AP2 can also bind to cargo via accessory adaptor proteins. For example, during Wnt/β-catenin signaling, internalization of the Frizzled receptor depends upon the recruitment of and binding to Dishevelled, which interacts with AP2 [18]. Other proteins of the endocytosis machinery also contribute to cargo selection, such as proteins with the AP180 amino-terminal homology (ANTH) and Epsin N-terminal homology (ENTH) domains, which are membrane-binding and membrane-bending domains, respectively [19, 20].

1.2.3 – Clathrin coat assembly

Once the cargo is selected, clathrin triskelia (Figure 2C) are recruited to the site of the nucleation module and adaptor proteins. Clathrin triskelia consist of three clathrin heavy chains and three clathrin light chains that form a polyhedral lattice around the forming vesicle. As invagination of the clathrin-coated pit progresses, adaptor proteins and curvature effectors move to the edge of the forming vesicle, where they continue to promote the formation of the growing pit [21, 22].

1.2.4 – Vesicle scission

Near the end of CCP formation, a small portion remains attached to the plasma membrane, which must be clipped off. This is largely dependent on the large GTPase called dynamin. By assembling into a spiral around the neck of the clathrin-coated pit, dynamin mediates membrane fission and the release of clathrin-coated vesicles (Figure 3) [23]. Recent studies have also shown that BAR domain-containing proteins like sorting nexin-9 (Snx9) and actin polymerization also contribute to vesicle fission [24-26].

1.2.5 – Uncoating

Once the vesicle has detached from the plasma membrane, ATPase heat shock cognate 70 (HSC70) and auxilin disassemble the clathrin coat from its lattice arrangement back to triskelia [27, 28]. This allows the detached and uncoated vesicle to travel through the cytoplasm and fuse with the acceptor membrane of its destination, the early endosome.

Clathrin coated vesicles are also sometimes formed during vesicle formation from intracellular compartments. The stages of vesicle formation in these cases are very similar, except that some modules are interchangeable; for example, AP1 or AP3 may be substituted for AP2 during vesicle formation from endosomes and the *trans*-Golgi network (TGN) [29].

1.3 – Clathrin-independent endocytosis

Several forms of clathrin-independent endocytosis exist and these mediate primarily the intake of fluid and membrane. Clathrin-independent endocytosis accounts for about 70% of fluid uptake [30] and 60-85% of membrane uptake [31, 32]. In addition, clathrin-independent endocytosis is implicated in plasma membrane repair, cellular spreading, cellular polarization, and modulation of intercellular signaling.

1.3.1 – Caveolae

Caveolae are submicroscopic plasma membrane pits (Figure 1B) that sense and respond to plasma membrane stresses, remodel the extracellular environment, and contribute to signaling pathways as a mode of endocytosis [33]. Caveolae are irregularly distributed across tissues and individual cells, and unlike clathrin-coated pits, they have no obvious coat. For example, they are practically undetectable in kidney cells while they can represent up to 50% of plasma membrane surface on endothelial cells and adipocytes [34, 35]. The main membrane components of caveolae are the oligomeric caveolins, which drive caveolae formation with the help of cavins [33, 36]. Cholesterol and phosphatidylserine also seems to be important membrane components for caveolae formation since they are abundant in areas that are rich in caveolae and their depletion disrupts caveolae formation [37, 38]. Due to the presence of these lipids, caveolae are sometimes called lipid-rafts. Although whether and how caveolae undergo endocytosis has been a subject of controversy for many years, a

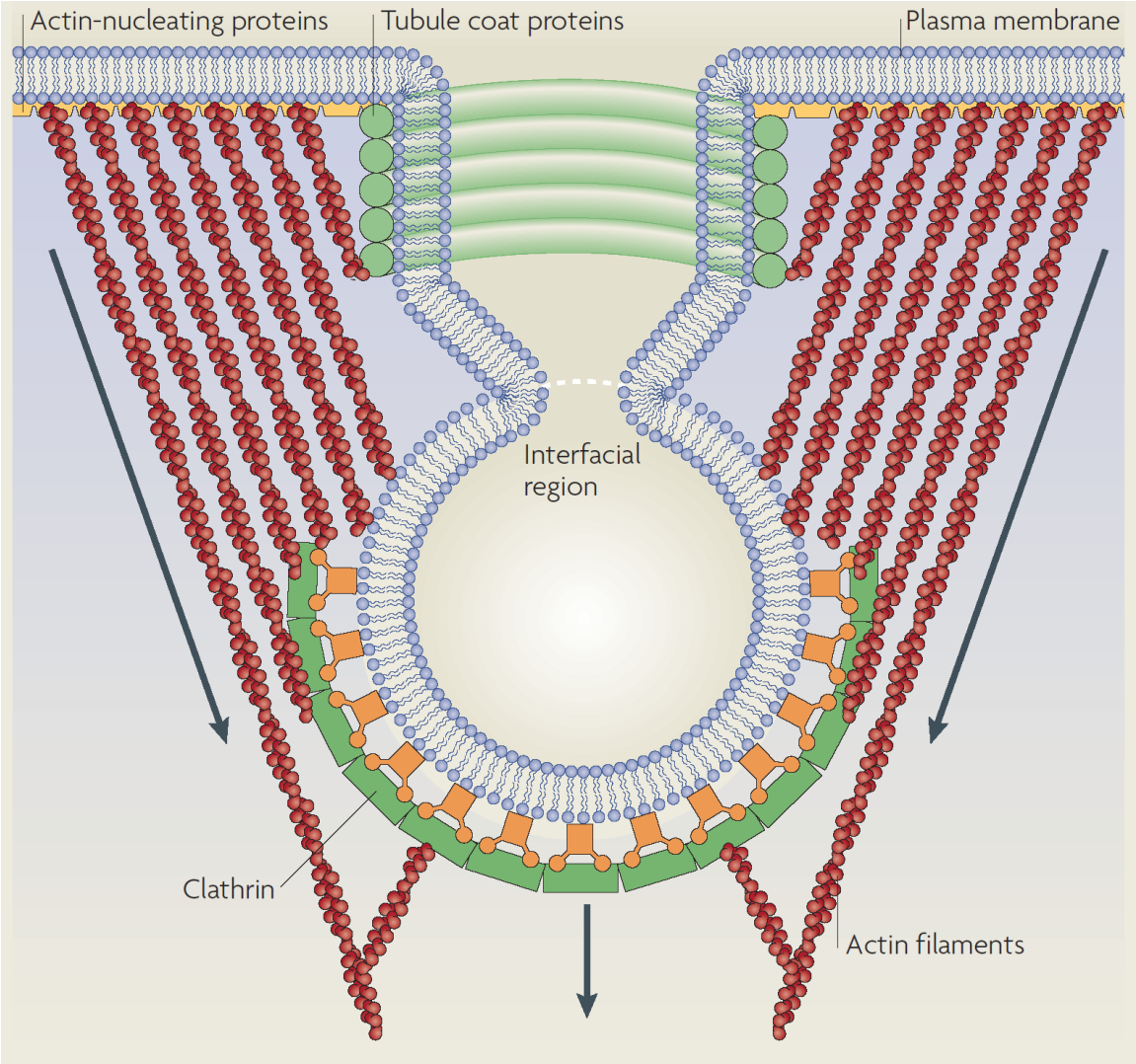

Figure 3. Membrane scission of a clathrin-coated vesicle. Contributing factors in the scission of endocytic carriers include the pinching action of dynamin as well as the force brought about by actin polymerization. Tubule coat proteins like Snx9 also contribute to membrane deformation and activation of dynamin. [39]

consensus has emerged that caveolae bud from the plasma membrane in a dynamin-dependent manner. In general, internalization of caveolae leads to their fusion with the early endosome, from where their components can recycle back to the surface [40].

As one of their biological functions, caveolae can flatten in response to stretching of the plasma membrane, thereby preventing damage or cell lysis. This has been shown in several cell types, including cardiomyocytes [41]. It is thus possible that caveolae and their components play important roles in mechanosensitive responses as both caveolins and cavins are released into the plasma membrane and cytoplasm, respectively, during flattening of caeolae [42]. Caveolae and caveolins have also been implicated in many signaling pathways, such as eNOS, Wnt/β-catenin and PAR-1 signaling, as well as in the regulation of lipids [33, 43, 44].

1.3.2 – RhoA, Cdc42, Arf6

In general, small GTPases like Cdc42, Arf6 and RhoA are used to differentiate between the endocytic routes employed by glycosylphosphatidylinositol-(GPI) anchored proteins, the major histocompatibility class 1 (MHCI) molecules and the interleukin 2 receptor (IL2R), respectively [45-47]. Other markers like flotillins are also involved in carrier formation and can be used to identify specific clathrin-independent routes [36]. These endocytic routes also make use of actin and actin-associated proteins [48, 49], as well as Snx9 [50, 51]. Importantly, clathrin-independent endocytosis is under differential regulation by signaling pathways and cell type [52]. While RhoA-dependent endocytosis requires dynamin and endocytosis via Cdc42 is

dynamin-independent, both routes are reported to be dependent on lipid rafts for vesicle formation [36, 45, 53]. Also protein toxins such as *Clostridium botulinum* C2 toxin make use of RhoA-mediated endocytosis [54, 55], but this is not exclusive since clathrin-dependent endocytosis can also take up a fraction of the C2 toxin [54].

The largest fraction of fluid uptake is mediated by Cdc42-dependent endocytosis [30, 53] but this pathway is also involved in the uptake of GPI-anchored proteins, and has therefore been called the GPI-enriched early endosomal compartment (GEEC) pathway [53]. The raft-associated proteins flotillin 1 and flotillin 2 play a role in both dynamin-dependent [56, 57] and -independent endocytosis [58]. Basolateral uptake of GPI-anchored proteins was found to be dependent on flotillin 2 and dynamin [56], whereas the flotillin 1-dependent uptake of GPI-linked proteins and cholera toxin B was reported to be dynamin-independent [58].

As previously mentioned, the endocytic route employed by a particular signaling molecule can have varying effects. An example of this is the endocytosis of LRP6, which is internalized in caveolar vesicles that move to early endosomes in a Rab5-dependent process, in response to Wnt3A [59]. The same study also showed that LRP6 is recycled back to the plasma membrane 4 hr after stimulation in a Rab11-dependent manner but could not exclude the possibility that a small portion of internalized LRP6 was transported to the lysosome or proteasome for degradation [59]. Interestingly, the same group later found that stimulation of LRP6 with the Wnt antagonist, Dkk1, resulted in clathrin-mediated LRP6 endocytosis, and the subsequent downregulation of this pathway [60].

This example demonstrates the intimate relationship that exists between specific signaling pathways and their underlying trafficking mechanisms. They also help appreciate the diversity

of responses a cell can have to an extra-cellular signal as any given endocytic pathway cannot be the sole determinant of signaling pathway outcome. Many factors need to be taken into account, including the cell-type, the extracellular signal, the receptor(s) involved, the endocytic route employed and the overall cellular context at that moment in time. The contributing factors ultimately act together to engender a cellular outcome.

1.4 – The endosomal system

Eukaryotic cells evolved a way to perform specialized reactions within isolated and tailored micro-environments, called endosomes. Endosomes are intracellular compartments that can receive and produce fleets of transport vesicles shuttling proteins and lipids (Figure 4). Although this membranous network is very dynamic, some compartments stand out as specialized stations, occupied by specific resident proteins and lipids, where specialized functions are performed. Accordingly, the various compartments that make up the endosomal network have been labeled as early endosomes, recycling endosomes, multivesicular bodies (MVB), lysosomes, and the TGN. This simplified model is made up of a recycling pathway for plasma membrane components and their ligands, a degradative pathway for breakdown of macromolecules, and an intermediary pathway where intracellular signaling can occur and where selected components from the recycling pathway can be transported to the degradative system and vice versa. Early endosomes (EEs) are the main

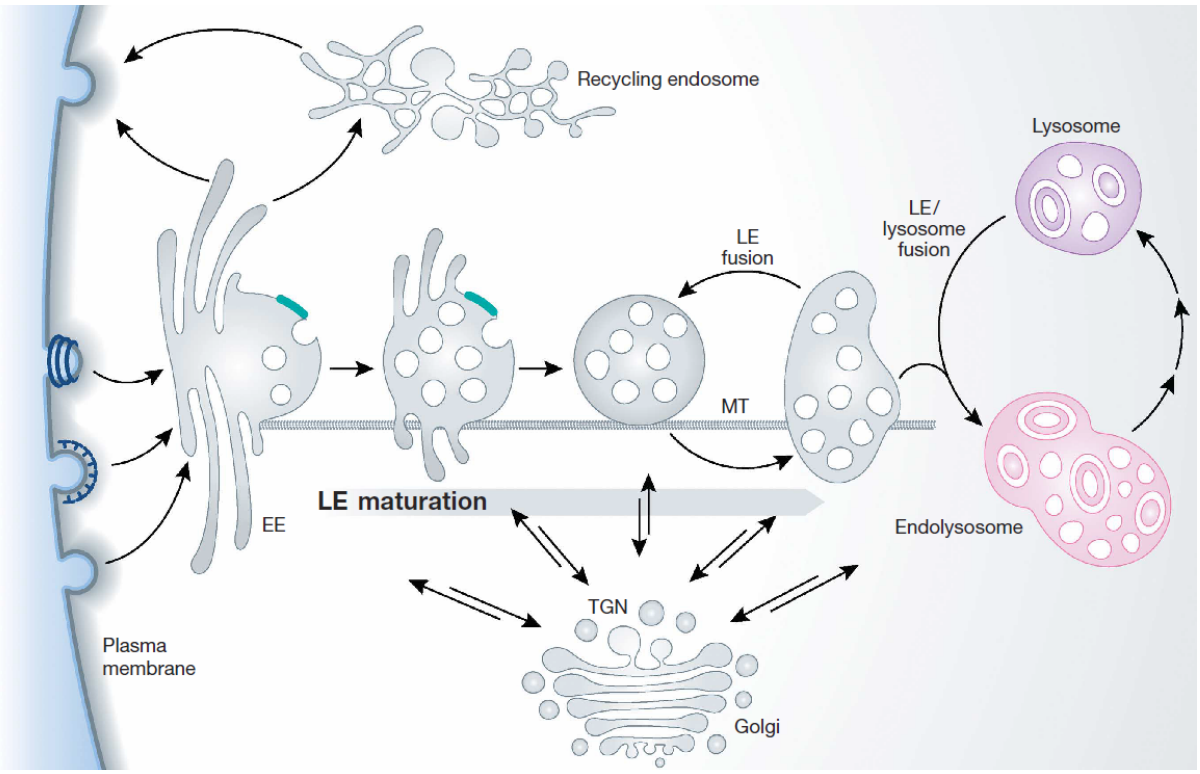

Figure 4. The major intracellular compartments that make up the endosomal network. Internalized cargo (by CME and CIE) first arrives in the early endosome (EE) and makes its way sequentially through the endosomal network. Trafficking proteins sort incoming cargo towards their next destination, following one of two main paths, degradation or recycling. Cargo destined for degradation is sorted to the multivesicular body/late endosome (LE) which travel along microtubules (MT), eventually fusing with the lysosome where catalytic enzymes breakdown proteins into elemental components to be reused by the cell. The endolysosome that is formed matures into a classical dense lysosome. Cargo can also be recycled back to the plasma membrane from any of these endosomal compartments directly to the plasma membrane or via the TGN or recycling

endosome. Throughout the endosomal network, retrograde and anterograde transport shuttles proteins and lipids to and from the *trans*-Golgi network (TGN), respectively. [61]

sorting stations where cargo and fluid internalized from different endocytic pathways converge [62]. As cargo progresses past early endosomes, it makes its way to multivesicular bodies. MVBs are also a transient stopover for lysosomal components travelling from the *trans*-Golgi network (TGN) to the lysosomes. Lysosomes house hydrolases that break down proteins found in this compartment. The TGN is a major sorting station for newly synthesized proteins and lipids that have undergone serial post-translational modifications by first passing through the Golgi apparatus. Throughout the endosomal network, cargo can be shuttled to recycling endosomes and transported to the plasma membrane. Finally, the cytoplasm must also be included as it is a source for essential elements of the trafficking machinery.

How EEs arise is not completely understood, however a significant amount of membrane and volume originates from endocytic vesicles (via CME and CIE) [61]. The fate of proteins and lipids that end up in EEs is determined through sorting mechanisms. Receptors, like EGFR, are often internalized and continue to signal even when located in EEs [63]. The peripherally located EEs contain regions with tubular extensions as well as a few intralumenal vesicles (Figure 4) [64]. These morphological differences are a showcase of the dichotomy of EEs: tubular extensions of EEs are usually involved in recycling while proteins targeted for degradation cluster within multi-vesicular domains [65].

A key resident of EEs is the Rab GTPase Rab5. Rab GTPases constitute the largest family of small GTP-binding proteins and are implicated in many trafficking processes. Much of the

biochemical attributes of EEs are acquired through the action of Rab5 and its effectors, which include phosphatidylinositol 3-kinase (PI(3)K) (VPS34/p150), early endosomal antigen-1 (EEA1), and Rabenosyn-5 [66]. PI(3)K generates PI(3)P which is typically enriched in the membranes of EEs [66, 67] and required for trafficking from this compartment as it recruits PI(3)P-binding proteins [68]. When present on the surface of endosomal membranes, PI(3)P acts as a molecular tag recognized by proteins such as EEA1 [69, 70], Rabenosyn-5 [71] and PX domain-containing proteins like sorting nexins [72]. Accordingly, EEA1 is one of the most commonly used molecular markers for EEs due to its precise localization to this compartment through its binding to both PI(3)P and Rab5. EEA1 enables membrane fusions of incoming vesicles in coordination with members of the SNARE family [73, 74]. The FYVE domain present in EEA1 is responsible for binding PI(3)P and is also present in Rabenosyn-5 [71]. Although the role of Rabenosyn-5 is still unclear, it may mediate the recycling of cargo back to the plasma membrane by its interactions with EHD1 and Rab5 [75]. In addition, sorting nexins localized to EEs play essential roles in sorting cargo to different endosomal destinations and will be discussed later [72, 76, 77].

Multivesicular bodies, also known as multivesicular endosomes or late endosomes as defined by the time it takes for internalized tracers to reach these compartments, are distinguished from other organelles by their large number of intralumenal vesicles (ILV) [78]. This characteristic offers many options to the cell by providing a means to store material in vesicles that can be delivered to lysosomes, released by exocytosis, or stored for future use. Although many proteins passing through this endosome are en route to the lysosome, some proteins do exit the degradation pathway through “back-fusion” of intralumenal vesicles with the MVB limiting membrane [79]. Unfortunately, markers of MVBs are few, which is perhaps

due to the fact that these endosomes serve as trafficking hubs for proteins en route to other destinations and because the machinery involved in MVBs formation is only transiently associated to the MVB membrane. The lysosomal membrane proteins LAMP1 and LAMP2 can be found on MVB membranes but only in the presence of the cation-independent mannose-6-phosphate receptor (CI-M6PR), since this latter protein is absent from lysosomal membranes [65]. In addition, Rab5, Rab7, Rab9, Rab27 and Rab35 are sometimes associated with MVBs [80, 81]. Intralumenal vesicles are occupied by tetraspanins and lysobisphosphatidic acid (LBPA), which can be used as additional markers [82, 83].

Lysosomes are defined by their acidic pH, mediated by v-ATPase, and the presence of hydrolases. These hydrolytic enzymes originate from the *trans*-Golgi Network and are first transported to MVBs before being ferried to lysosomes. TGN-to-MVB transport of hydrolase receptors is the primary function of the CI-M6PR [84]. On the surface of lysosomes are structural proteins, such as LAMP1/2, ion channels, as well as trafficking and fusion machinery proteins, like Rabs and SNAREs [85].

The Golgi apparatus is a central hub for sorting and transporting proteins and lipids that travel within the secretory and degradative pathways [86]. It also houses the machinery required for the post-translational modification of proteins, which are then sorted in the *trans*-Golgi network. The Golgi system is easily distinguishable by the shape of its structure, typically organized as stacks of flattened cisternae with dilated rims (Figure 4) [87]. This dynamic network receives cargo from the plasma membrane and endosomes, and directs transport of material coming from the endoplasmic reticulum (ER) en route to the secretory pathways [86].

1.5 – Receptor degradation and recycling

As cells synthesize new proteins according to their needs, proteins that are damaged, misfolded or simply no longer needed are degraded and their amino acids are reused. As such, a fine balance exists between protein synthesis, degradation and recycling. A deficiency in degradation mechanisms would be significant and could lead to catastrophic proteotoxicity within the restricted intracellular space [88, 89]. On the other hand, since degradation is irreversible, tight regulation is required to avoid reckless destruction. When possible, proteins that are still required and functional can be recycled for reuse. Rudolf Schoenheimer conducted early experiments on protein turnover in the late 1930s. In a single mass spectrometry experiment, he analyzed the fate of stable isotope-labeled amino acids that had been fed to mice, which allowed determination of the turnover rate of thousands of individual proteins [90]. For a long time, the lysosomal compartment was considered the main site of protein degradation, through the action of resident proteases. However, this view was challenged when most cellular proteins remained insensitive to alkalinization of the lysosomes. In later years, the ubiquitin-proteasome degradation system was discovered and replaced lysosomes as the major catalyst of protein degradation [91, 92].

Central to this model is the small molecule ubiquitin, which is covalently attached to lysine residues of proteins targeted for degradation, through interaction with an E3 ligase protein that recruits an E2-enzyme charged with ubiquitin [93]. Typically, proteins targeted to the proteasome are tagged with a chain of multiple ubiquitin molecules (polyubiquitination) while those destined for lysosomes are tagged with a single ubiquitin molecule (monoubiquitination). Proteasomal degradation is performed by ATP-dependent proteases, the most well-known

member being the 26S proteasome. ATP-dependent proteases are multi-subunit protein-wrecking machines that share the common architecture of a barrel-shaped compartmental peptidase capped by a hexameric AAA + unfoldase (ATPases associated with various cellular activities) [94]. A monoubiquitination modification induces the sorting of proteins into the internal vesicles of EEs [95]. A MVB then detaches from early endosomes and travels along microtubules to eventually fuse with lysosomes [95]. Although less common, multiple monoubiquitinations and in some cases K63-linked polyubiquitin chains have also been shown to provide a signal for MVB targeting [96, 97]. Monoubiquitination is recognized by a series of complexes called the endosomal sorting complexes required for transport (ESCRT), which then mediate the trafficking of these proteins to the lysosome [98].

In mammals, the ESCRT machinery consists of more than 20 proteins, grouped into three complexes (ESCRT-I, -II, and –III) and other associated proteins such as the ATPase vacuolar protein sorting 4 (Vps4) [99]. ESCRT is mostly known for its role in MVB formation but it is also involved in other membrane fission processes, such as the terminal stages of cytokinesis and separation of enveloped viruses from the plasma membrane [99]. In yeast, four ESCRT complexes have been identified and are numbered according to the order in which they act in the ESCRT pathway (ESCRT-0, -I, -II and -III). Studies from mammalian cells also support this model of sequential assembly and disassembly for ESCRT protein dynamics [99]. Near the end of MVB biogenesis (and other membrane fission processes), two membranes that remain connected by a thin neck are severed, a process attributed to ESCRT [99]. In mammals, ESCRT-I is recruited to sites of MVB formation by the adaptor protein Hrs [100]. This and other interactions bring about the sequential recruitment of ESCRT-II and –III, and the progression of MVB biogenesis [99].

Besides their roles in protein degradation, proteins found in mature MVBs can also be re-routed back to the plasma membrane or temporarily isolated from the cytoplasm. This is dependent on ESCRT-0, which promotes recycling of certain proteins, such as the β_2-adrenergic receptor and the epithelial Na^+ channel [101, 102]. Another interesting example of MVBs function, is the sequestration of cytosolic glycogen synthase kinase 3 (GSK3) into ILVs during Wnt/β-catenin signaling, which will be discussed further [103].

Sorting of receptors for recycling to the plasma membrane is achieved through extensive tubulation of the EE membranes [104]. Tubulation is an elongation of endosomal membranes where cargo accumulates and eventually buds off inside a vesicle carrier en route to an endoplasmic recycling compartment (ERC) or directly back to the plasma membrane. Accordingly, recycling directly to the plasma membrane is termed “fast recycling” while recycling via the ERC is called “slow recycling”. For example, slow recycling of the transferrin receptor takes between 30-60 minutes, while its fast recycling takes about 10 minutes [105]. Mediating these pathways are sorting proteins like Rab4, which targets receptors directly back to the plasma membrane (fast recycling), and Rab11, which regulates slow recycling [106, 107]. However, the use of these Rabs as endosomal markers should be done with caution since Rab4 has also been detected on membranes of the ERC [108].

In addition to the ESCRT machinery, other protein families, such as the sorting nexins and the small Rab GTPases, are required for sorting internalized proteins towards various endosomal destinations. These large families of proteins also contribute to protein trafficking and are thus intimately linked to protein degradation, recycling and sequestration.

1.6 – Sorting nexins

The first description of a mammalian sorting nexin (Snx) was published in 1996, with the identification of SNX1 in a yeast two-hybrid screen using the core tyrosine kinase domain of EGFR [109]. Mammalian Snx1 was found to contain a region homologous to a previously identified yeast protein, Mvp1p, a multicopy suppressor of Vps1p mutants deficient in carboxypeptidase Y receptor trafficking [110]. Co-localization of Mvp1p with Vps1p to Golgi membranes pointed to a potential role in membrane trafficking [110]. The relevance of the interaction between EGFR and Snx1 was uncovered by demonstrating that Snx1 could bind to the lysosomal targeting code on EGFR and contribute to its transportation to lysosomes as overexpression of Snx1 increased the rate of both constitutive and ligand-induced EGFR degradation [109]. This function was later confirmed by others and was also shown to involve the hepatocyte growth factor-regulated tyrosine kinase substrate (Hrs) [111] and enterophilin-1 (Ent-1) [112]. Hrs is an ubiquitin-binding protein that sorts ubiquitylated proteins like the transferrin receptor into clathrin-coated microdomains of early endosomes, thereby targeting them to the late endosome and lysosome, and preventing recycling to the cell surface [100]. Ent-1 is an intestinal protein involved in enterocyte differentiation and the overexpression of Ent-1 reduces cell surface expression of EGFR, an effect increased by co-expression of Snx1. Shortly after the discovery of Snx1, Haft *et al.* (1998) introduced three new sorting nexins (Snx2, Snx3 and Snx4), which along with Snx1 as well as others proteins previously identified in *Caenorhabditis elegans* and *Saccharomyces cerevisiae* all shared a common conserved domain, the SNX-PX domain [113]. Today, mammalian sorting nexins count 33 members, all characterized by the presence of the sorting nexin PX (SNX-PX) domain (Figure 5) [72, 76, 77].

The roles of many sorting nexins have been investigated and members of this protein family are now recognized as important factors for endosomal protein sorting.

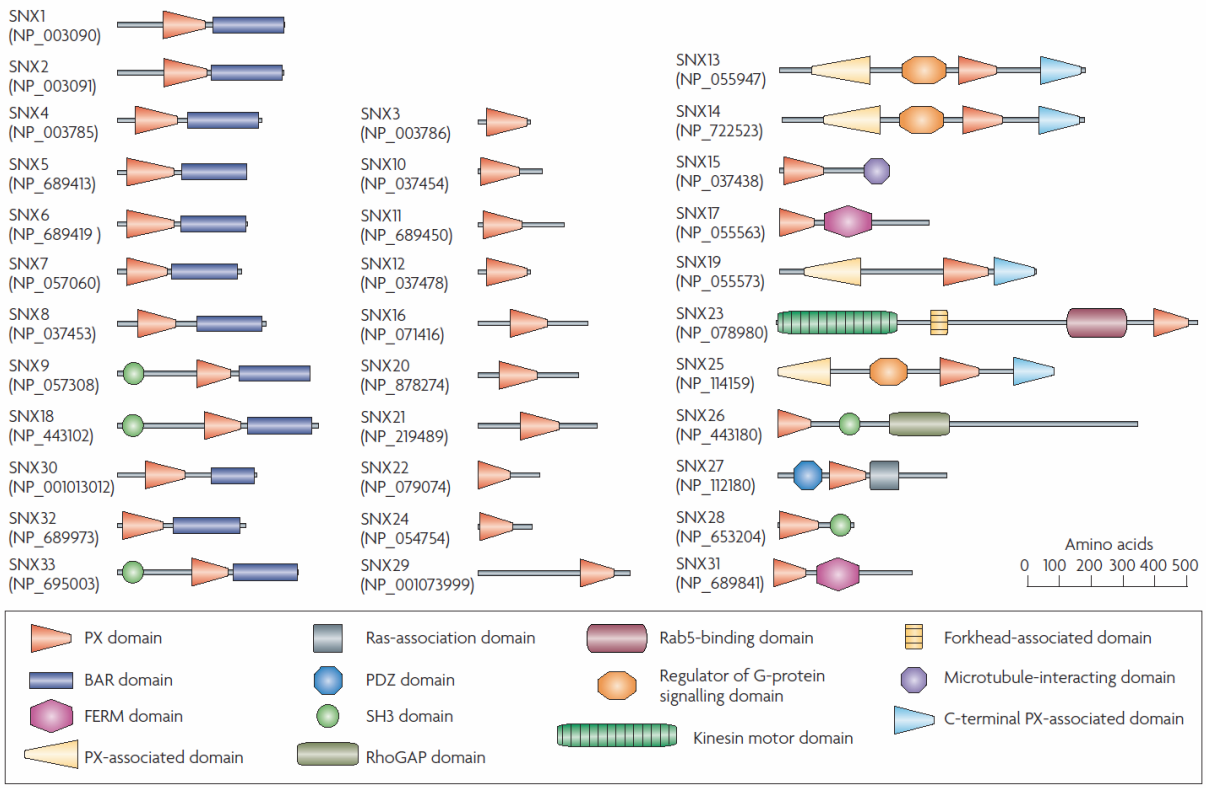

Figure 5. The domain structure of mammalian sorting nexins. All sorting nexins (33 members) contain a SNX-PX domain. The presence (or absence) of other conserved domains is used to divide the sorting nexins into three subfamilies: the SNX^{BAR} contain a C-terminal BAR domain (left), the SNX^{PX} contain simply an isolated SNX-PX domain (middle), and the SNX^{other} contain another recognized domain, in addition to the SNX-PX domain (right) [114]

1.7 – The PX domain

The PHOX-homology domain (PX domain), as its name implies, is homologous to the PHOX domain, named according to the protein complex where it was initially identified: the phagocyte NADPH oxidase (PHOX). The PHOX motif (110 aa) is present in subunits $p40^{phox}$ and $p47^{phox}$ of the NADPH oxidase complex of neutrophils [115]. $p40^{phox}$ and $p47^{phox}$ reside in quiescent neutrophils, in association with a third subunit, $p67^{phox}$. This tertiary complex regulates the oxidative activity of flavocytochrome b_{558}, composed of the catalytic heterodimer $gp91^{phox}$-$p22^{phox}$, which is kept inactive in quiescent cells. In these dormant cells, $p47^{phox}$ has an auto-inhibitory conformation that hides its SH3 and PHOX domains due to intramolecular interactions [116, 117]. When immune mediators activate the neutrophil, $p47^{phox}$ becomes phosphorylated and exposes its SH3 domain to interact with $p22^{phox}$. In addition, the PHOX domain is also released, which allows the protein to interact with PIPs. The role of $p47^{phox}$ is thus essential for the recruitment the membrane of the $p47^{phox}$-$p67^{phox}$-$p40^{phox}$ complex and for its interaction with flavocytochrome b_{558}. This way, the assembly of the phagocyte oxidase complex at the membrane allows the production of reactive oxygen species that destroy invading microorganisms. Other homologs of $p47^{phox}$ et $p67^{phox}$ have since been identified, such as the NOX organizing 1 protein (NOXO1), which contains a PHOX domain that is required for the recruitment of proteins at the plasma membrane [118-120].

In yeast, PX domain-containing proteins are implicated in processes of vesicular transport, cellular signaling, budding control and polarization [77, 121]. The evolutionary conservation of the PX domain is strongest in proteins involved in vesicular transport such as Mvp1p, Vps5p/Grd2p, Grd19p/Snx3, and Vam7p. Mvp1p, Vps5p and Grd19p are required for the

retrograde transport from the pre-vacuolar endosome/late endosome to the “late” Golgi (similar to the *trans*-Golgi in mammals) [122-125]. Snx4, Snx41 and Snx42 are other SNX-PX domain-containing proteins, which are implicated in recycling receptors from the sorting endosome (post-Golgi endosome) to the “late” Golgi [126].

In mammals, many proteins contain the PX domain, including PI3 kinases, CISK and FISH, but the majority of these proteins fall under the class of sorting nexins. Studies in yeast have shown that the PX domain is capable of interacting with PIPs, primarily PI(3)P, but also with other phosphorylated derivatives, such as $PI(3,4)P_2$, $PI(3,5)P_2$ and $PI(4,5)P_2$, interactions that should not be disregarded [77, 127-132]. A total of 27 crystal structures of the mammalian PX domain are accessible on the protein database (PDB), stemming from 14 different proteins but only two structures have been resolved in complex with PI(3)P : $p40^{phox}$ (PDB : 1H6H) and SNX9 (PDB: 2RAK). The interaction of the PX domain with PI(3)P is an electrostatic bond between the 3-phosphate of PI(3)P and a specific and conserved arginine of the PX domain. The consensus sequence of the interaction of the PX domain with PI(3)P is $R[Y/F]X_{23-30}KX_{13-23}R$ (Figure 6) [77].

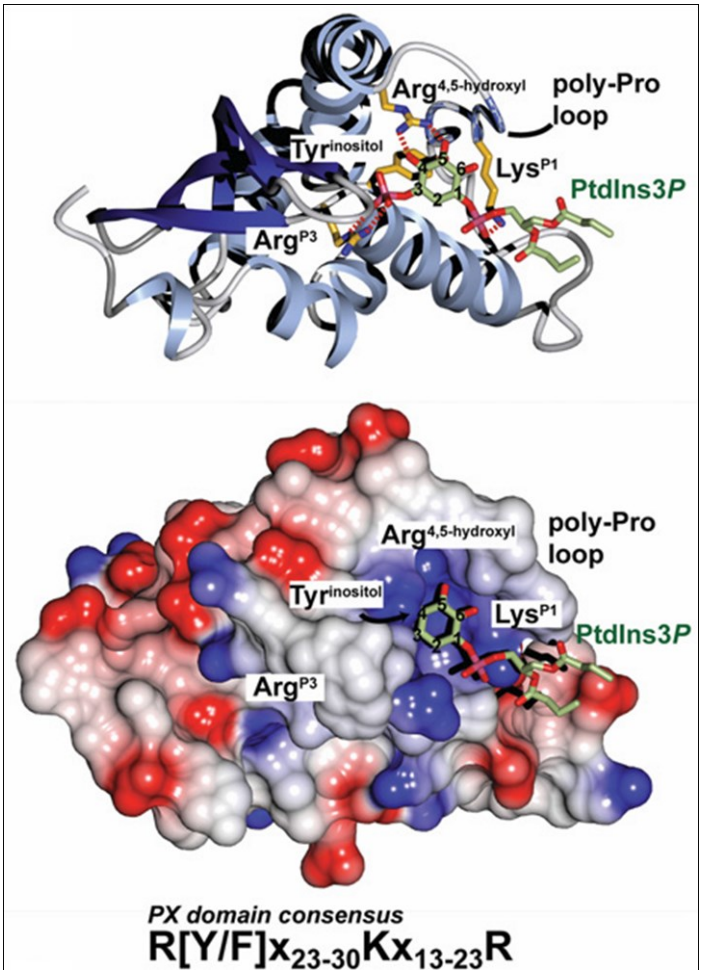

Figure 6. The interaction between the PX domain and phosphatidylinositol-3-phosphate. Ribbon and surface structures of a representative PX domain from p40^{phox} are shown in complex with PI(3)P. Surface structure color codes indicate hydrophobicity, from blue (most hydrophilic) to red (most hydrophobic). Key PX-PI(3)P interactions: the arginine side chain electrostatic association with the 3-phosphate (Arg^{P3}), stacking of the inositol ring with the tyrosine (or phenylalanine) side chain immediately downstream from the conserved arginine residue (Tyr^{inositol}), contact of a lysine side chain with the 1-

phosphate (Lys^{P1}), and hydrogen bonds of the 4- and 5-hydroxy groups to a second arginine side chain ($Arg^{4,5\text{-hydroxyl}}$). [77]

The affinity of different PX domains to phospholipids is determined by two approaches: by analyzing the binding to liposomes and by "dot blots" or "PIP-strips". The approach by PIP-strips is technically less challenging than artificially-producing liposomes, which requires delicate manipulations due to the instability of PIPs. In PIP-strips, pure phosphorylated derivatives of phosphatidylinositol are applied on nitrocellulose membranes after which proteins are incubated and then their affinities are detected by chemiluminescence. The liposome method involves the generation of liposomes composed with up to 50% of the tested phospholipid in an environment of varying proportions of phosphatidylserine, phosphatidylethanolamine or phosphatidylcholine, required for stability. Even if the PIP-strip method is easier to perform, the liposome method is considered closer to physiological conditions since it introduces a structural aspect of the protein-PIP interaction that cannot be replicated in 2-dimensional tests like PIP-strips. In fact, comparisons between both methods can produce different results for the same protein [76, 133]. Using PIP-strips, the PX domain of Snx1 had specific affinity with $PI(3,4,5)P_3$ and weaker affinity to $PI(3,5)P_2$ [76, 134]. However, when using the liposome method, Snx1 had comparable affinities with both PI(3)P et $PI(3,5)P_2$ [76]. The interaction of Snx1 with PI(3)P instead of $PI(3,4,5)P_3$ seems more physiologically plausible since the increase of $PI(3,4,5)P_3$ by a constitutively active PI3K did not increase the association of Snx1 to the membrane where $PI(3,4,5)P_3$ was enriched [76]. These observations demonstrate the importance to use multiple methods of analysis to determine the lipid affinities of unknown proteins.

1.8 – Phosphatidylinositol phosphates

Phosphatidylinositol is used as a scaffold that can be phosphorylated at the 3-, 4- and/or 5-positions to generate phosphatidylinositol phosphates (Figure 5A). Despite their low abundance (less than 10% of total cellular phospholipids), PIPs serve as both structural and regulatory molecules in response to stimulation of certain cell surface receptors and control endosomal biology by regulating the correct timing and location of vesicular trafficking events [135, 136]. Through organelle-specific phosphatidylinositol kinases and PIP phosphatases, PIPs can undergo rapid phosphorylation/dephosphorylation cycles that lead to distinct and transient subcellular distributions of individual PI species. These species are recognized by PIP-binding modules (PIBMs), which include the FYVE, pleckstrin homology (PH), ENTH, ANTH and PX domains. The expression of proteins with these PIBMs tagged with green fluorescent protein (GFP) has permitted the construction of a map of intracellular PIP distribution (Figure 3B).

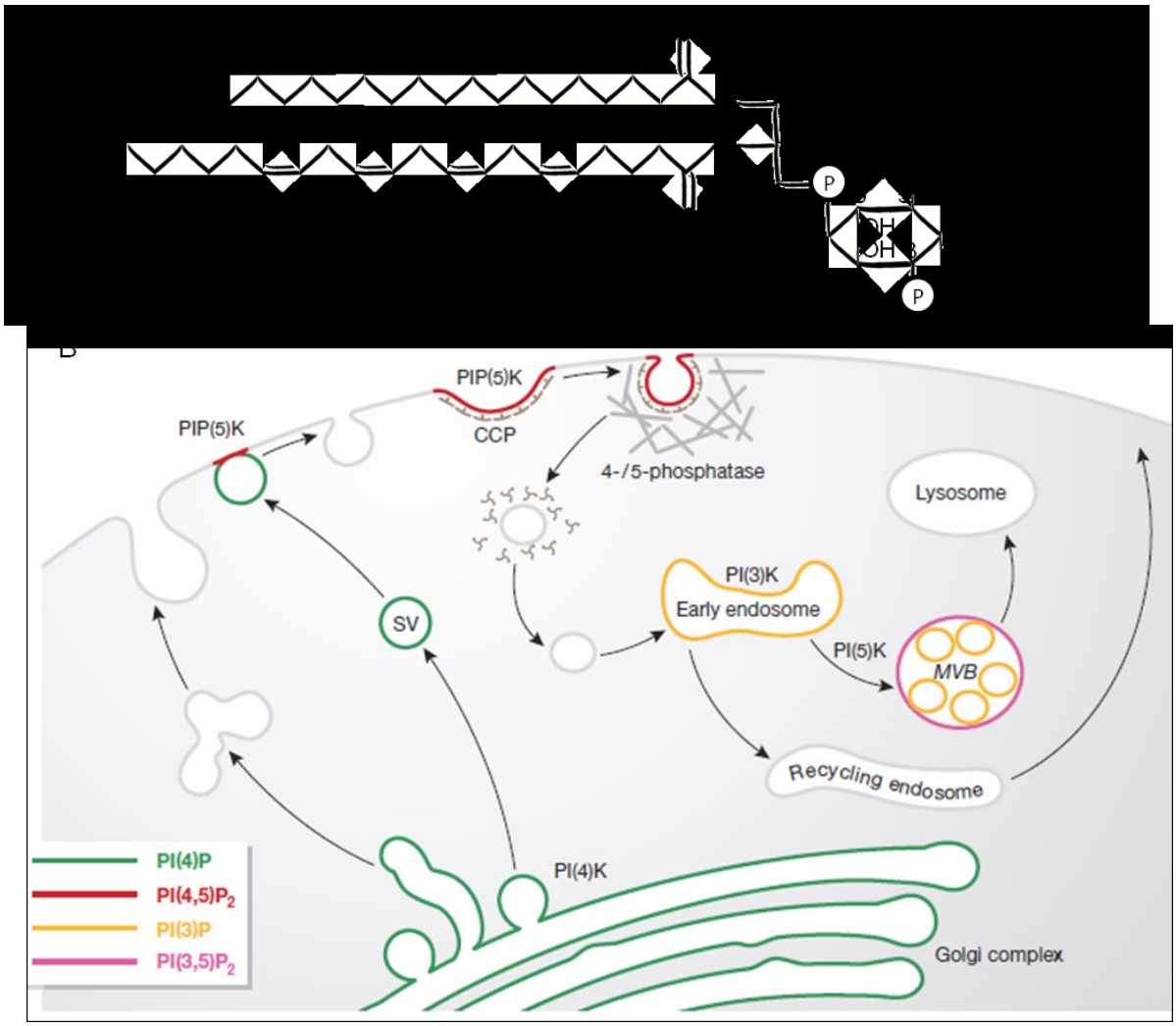

Figure 7. Phosphatidylinositol phosphates and their intracellular distribution. A) Phosphatidylinositol is an amphiphile lipid that can be phosphorylated on positions 3, 4 and 5 of the polar inositol headgroup. Depicted here is phosphatidylinositol-3-phosphate (PI(3)P), phosphorylated on position 3 of inositol. Other species could be generated through the action of kinases and/or phosphatases at positions 3, 4, and 5. B) Subcellular distribution of PIs and their metabolizing enzymes in exo- and endocytic membrane traffic. SV: secretory vesicle; CCP: clathrin-coated pit, MVB: multivesicular body [137].

Phosphatidylinositol and PI(4)P are considered as the main precursors of PIPs. However, PI(4)P has been shown to interact with cytoskeletal proteins, namely talin, suggesting a functional role [138]. PI(4)P is also enriched on the membranes of the Golgi complex, while concentrations of $PI(4,5)P_2$ are kept low, which is likely due to the presence of PI(4)K and $PI(4,5)P_2$ phosphatase [136]. $PI(4,5)P_2$ is mainly found on the inner side of the plasma membrane [139, 140]. It is required for the invagination of clathrin-coated pits after which levels of $PI(4,5)P_2$ drop due to 5-phosphatase activity [141]. $PI(4,5)P_2$ is also required during the first steps of phagocytosis but is quickly converted to $PI(3,4,5)P_3$ by type I PI(3)K [136].

PI(3)P is mainly found on membranes of early endosomes, on intralumenal vesicles of MVBs and at the plasma membrane when it is generated during signaling processes [142]. PI(3)P is also required in Golgi-to-vacuole transport in yeast [143]. During phagocytosis, PI(3)P is generated by type III PI(3)K (Vps34) and is required for phagosomal maturation [144]. Conversion of PI(3)P to $PI(3,5)P_2$ occurs at MVBs and is required for protein sorting at these endosomes [136]. During the exocytic cycle, PI(4)P is generated in secretory granules [145]. PI(4)P and $PI(4,5)P_2$ are also found in the Golgi complex, where PI(4)P promotes transport from the Golgi and $PI(4,5)P_2$ is important for maintaining the architecture of Golgi membranes [146].

Generation of PIPs is also required during transportation processes along cytoskeletal routes. For example, enrichment of $PI(4,5)P_2$ in nascent vesicles is required for actin comet tail assembly that mediates propulsion and movement [147]. Microtubule-based motility may also be regulated by regional PIPs as the motor protein kinesin was shown to interact with $PI(4,5)P_2$ [148]. Most phosphatidylinositol kinases and phosphatases are cytosolic and their targeting to specific regions of lipid membranes is not fully understood. It may involve small GTPases that

either recruit or activate phosphatidylinositol-modifying enzymes, such as Rab5, which activates PI(3)K at the early endosome [66, 136].

The interaction between the PX domain and PI(3)P (and other PIPs) is in general a weak interaction and the recruitment of sorting nexins to membranes is achieved by the contribution of other domains and molecular interactions, a concept termed “coincidence detection” [149]. For sorting nexins of the SNX^{BAR} subfamily, this additional contribution is brought about by the BAR domain.

1.9 – SNX-BARs

In addition to the PX domain, some sorting nexins also contain a BAR domain, referred to as SNX-BARs. The BAR (Bin/amphyphysin/Rvs) domain is an amphipathic motif exposing both a hydrophobic and hydrophilic surface. In an aqueous solution, this protein domain forms monodimers and heterodimers that form a six-helix bundle curved in a banana-shape, which bonds with the curved surface of lipid membranes [150-153]. Fifteen structures of the BAR domain have been produced, prompting the division of this domain into two sub-groups: the F-BAR (Fes/CIP4 homology-BAR) and the I-BAR (Inverse-BAR) [151, 154]. The association between the F-BAR dimer at the N-terminus of Toca (Transducer of Cdc42-dependent actin assembly) and lipid membranes demonstrated how this motif could associate with membranes and shape them into cylindrical tubules [155]. By integrating the atomic models of F-BAR

dimers [153] with cryo-EM reconstructions of membrane tubules, Frost *et al*. (2008) were able to show how cationic residues on the concave surface of the F-BAR motif engage the lipid bilayer and allow the rigid dimer to impose its shape onto the underlying membrane [155]. Proteins that contain the BAR domain play essential roles in the formation of tubules, which preludes vesicle budding. Tubules are localized and elongated deformations found in many endosomes.

Most of our understanding into the role of sorting nexins comes from retromer studies. The retromer is an evolutionarily conserved pentaheteromeric protein complex that is essential for the late endosome-to-TGN retrograde transport of the CI-M6PR receptor in mammals and vacuolar protein-sorting receptor-10 (Vps10p) in yeast [156]. The mammalian CI-MPR is a type I transmembrane receptor that recognizes the mannose-6-phosphate tag present on hydrolytic enzymes at the TGN and delivers these digestive enzymes to late endosomes before making its way back to the TGN [70]. The efficient retrieval of these receptors from the late endosome to the TGN is accomplished by retromer and is crucial to maintain efficient sorting and forward transport of hydrolytic enzymes to the lysosome in mammals [68, 157] or vacuole in yeast [73, 122]. Furthermore, the fundamental mechanisms for this retrograde pathway are evolutionarily conserved from lower to higher eukaryotes.

The retromer complex functions as a cytoplasmic vesicle coat that can be divided into two distinct sub complexes: a cargo recognition complex and a sorting nexin dimer. In yeast, the cargo recognition complex of retromer is composed of Vps35p, Vps26p and Vps29p, while the sorting nexin dimer is composed of Vps5p, Vps17p [158]. Vps35p associates with membranes through its interaction with Vps26p, while Vps29p stabilizes Vps35p and interacts with the second sub complex (Vps5p and Vps17p) [67, 73, 74, 159]. Vps5p and Vps17p are SNX-BARs

that associate with highly curved membranes and PI-enriched regions of lipid membranes [122, 160]. The yeast retromer therefore localizes to specific regions of vacuolar membranes to retrieve Vps10p and mediate tubule/vesicle formation. In mammals, the cargo recognition complex is composed of Vps26-Vps29-Vps35 [158]. However, the exact components of the sorting nexin dimer are less clear but is likely made up of a combination of Snx1 or Snx2 (Vps5 orthologs) and Snx5 or Snx6 (Vps17 orthologs) [158].

In addition to SNX1, other sorting nexins also have CI-M6PR-independent functions. For example, SNX5 has been shown to mediate both internalization and recycling of a G-protein-coupled receptor, the D_1 dopamine receptor (D_1R) [161]. SNX5 coexists at the plasma membrane with D_1R and GRK4 (G-protein-coupled receptor kinase 4), where SNX5 interacts with the C-terminal of the D_1R and forms a functionally cohesive complex for selective receptor stimulation and efficient signal propagation, amplification and termination. In this role, SNX5 likely functions as a scaffold that is not only essential for endocytosis but also for receptor recycling. Accordingly, in the absence of SNX5, phosphorylation by GRK4 remains unhindered and impairs D_1R endocytosis and delays recycling, leading to failure of cAMP production on agonist stimulation [161]. This findings supports the idea that SNXs are promiscuous proteins that can associate with various other trafficking components to direct endosomal sorting of a wide variety of receptors.

1.10 – PX-only Sorting Nexins

In some sorting nexins, the only conserved protein domain identified to date is a N-terminal PX domain. Many of these SNXs have C-terminal regions that likely play important functional roles. Such is the case for SNX11, where a novel extended PX (PXe) domain was recently discovered by crystal structure analysis [162]. Evolutionarily, Snx11 is most closely related to Snx10, which was first shown to be important for endosome homeostasis since overexpression of Snx10 resulted in the formation of abnormally large vacuole [163]. Later studies showed that Snx10 plays a role during osteoclast formation as it is strongly up-regulated during RANKL-induced osteoclast differentiation *in vitro* and strongly expressed in osteoclasts *in vivo* [164]. In accordance, a mutation in an evolutionarily conserved residue of the PX domain of Snx10 (R51Q) was found to induce malignant osteopetrosis of infancy [165]. Osteoclasts with this mutation abnormally displayed large endosomal vacuoles and impaired resorptive function, a major factor in osteopetrosis.

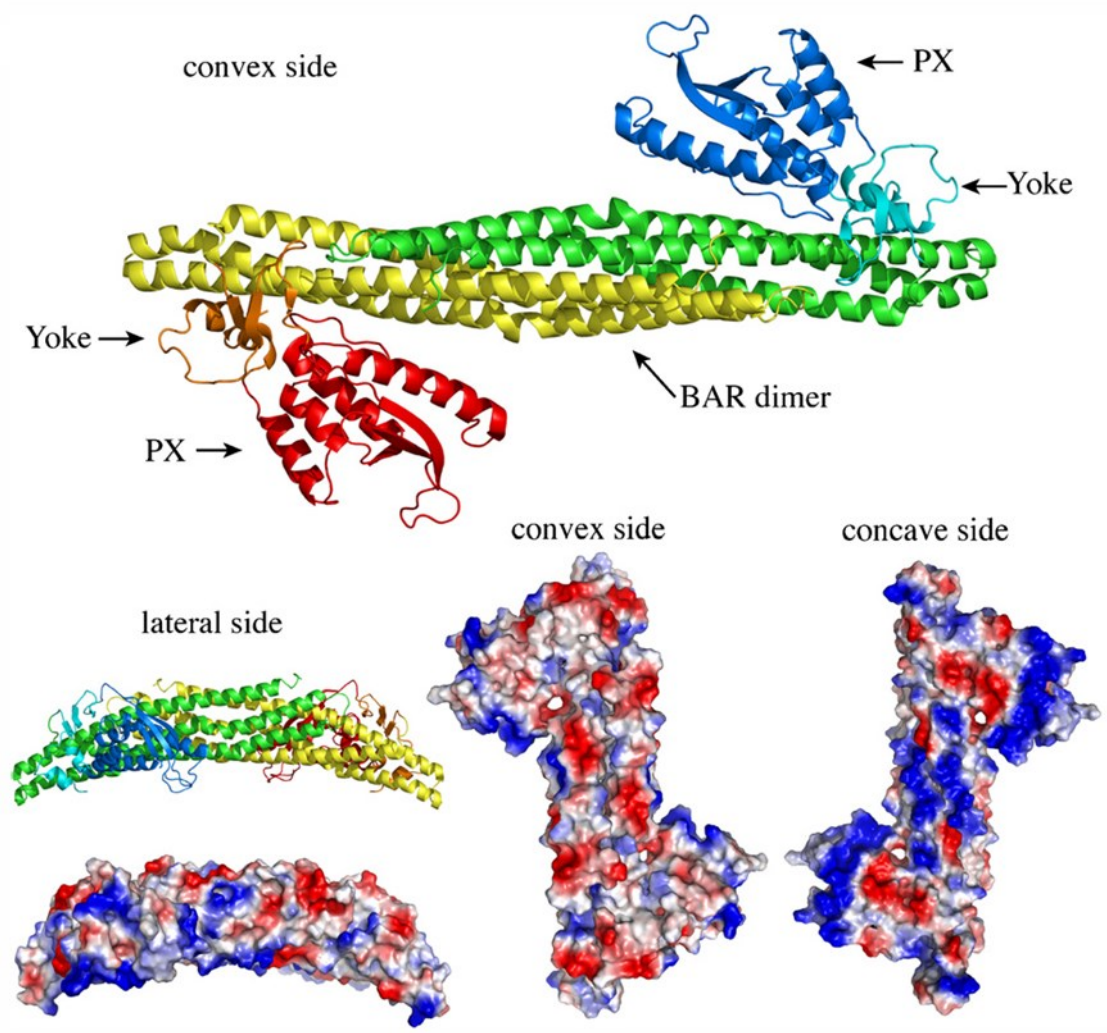

Figure 8. BAR dimers. A) Ribbon and space-fill models of the SNX9 BAR-PX dimer are shown. The two SNX9 proteins are depicted in red/orange/yellow and green/cyan/blue (PX domain: red/blue; BAR domain: yellow/green; yolk domain, which links the PX domain to the BAR domain: orange/cyan). Space-fill models showing the electrostatic distribution, red (acidic, negative residues), blue (positive, basic residues). [50]

Finally, SNX10 was shown to regulate the intracellular trafficking of V-ATPase, a multi-subunit complex required for ciliogenesis, acidification of osteoclasts and bone resorption [166]. Interestingly, Snx11 was found to antagonize Snx10-dependent vacuolation *in vitro* possibly through competitive binding with a common partner but its function remains poorly described [162].

1.11 – SNX-other

Sorting nexins can also mediate receptor recycling. For example, fast recycling of the β2 adrenergic receptor (β2AR), a seven-transmembrane signaling receptor, is a process that requires SNX27 [167, 168]. Here, VPS29 concentrates at β2AR-positive membrane tubulations. Previous to this finding, β2AR recycling was known to occur by the concentration of the receptor into endosomal tubulations, and this was dependent on a C-terminal PDZ ligand, [169]. However, initial ligand-induced endocytosis did not require retromer components. Instead, depletion of VPS35 or VPS29 significantly reduced β2AR recycling and resulted in endosomes devoid of β2AR tubules. This effect was similar to disrupting the receptor's C-terminal PDZ ligand. Further investigation identified Rab4A as another essential component of β2AR recycling, as well as PDZ domain-containing SNX27, which acts as a cargo adaptor to retromer. In fact, SNX27 was shown to bind directly to the WASH complex, which in turn enabled its association with retromer components [168]. This indicates that retromer

components can mediate receptor trafficking at different endosomal compartments, by associating with various adaptor proteins.

1.12 – RABs

As previously mentioned, other important players in regulating membrane identity and vesicle traffic are the small Rab GTPases. Rab GTPases cycle between the GTP-bound state (active), catalyzed by guanine exchange factors (GEFs), and the GDP-bound state (inactive), driven by the combined action of the intrinsic GTPase activity of the Rab protein and catalyzed by GTPase-activating proteins (GAPs) [159]. In humans, over 60 members of the Rab family have been identified, which localize to distinct endosomal membranes [157]. Their association with membranes occurs through the post-translational addition of hydrophobic geranylgeranyl groups, which facilitates the attachment to target membranes and indirectly brings about interactions with coat components, motors and SNAREs. In turn, binding of Rabs to relevant membranes and to their respective effector proteins contributes to endosomal trafficking processes such as vesicle budding, vesicle uncoating, vesicle motility and vesicle fusion [157].

During vesicle budding, sorting of cargo into specific transport vesicles requires its association with cytosolic coat complexes. For example, Rab9 localizes at the multivesicular body and, like retromer, is required for retrograde transport of the CI-M6PR from this compartment to the *trans*-Golgi network [170, 171]. Once cargo is included into a transport

vesicle, coat complexes must be shed to allow membrane fusion with the acceptor membrane. For instance, Rab5, which is present on clathrin-coated vesicles, helps AP2 uncoating by promoting dephosphorylation and increasing $PI(4,5)P_2$ turnover [172]. In addition to actin microfilaments and microtubules, vesicle motility along these molecular cables is dependent on the kinetic force provided by various motor proteins like myosins, kinesins and dyneins. As such, certain Rab GTPases assist in proofreading the interactions between motor proteins and transport vesicles. Such is the case of Rab27a, which connects myosin Va to vesicle-like melanosomes shuttling towards the cell periphery [173]. Another example is a resident of endocytic recycling vesicles, Rab11a. Through its interaction with the Rab11 family interacting protein 2 (RAB11FIP2), Rab11a links recycling vesicles to myosin Vb [174]. As transport vesicles reach their destination, they must dock and fuse with the acceptor membrane. Here again, Rab GTPases are involved in this final step of endosomal trafficking. Evidence for this first came from studying a mutation of the yeast Rab GTPase Sec4, which causes accumulation of TGN-derived vesicles [175]. Later studies revealed that Rab GTPases contribute to vesicle fusion by recruiting elongated tethering complexes that form long distance connections between the vesicle and the acceptor membrane [157].

Another essential component of protein trafficking is the cytoskeleton, which provides the framework that guides vesicular transport and mechanical force required for reshaping the cell.

1.13 – The cytoskeleton

The cytoskeleton is a dynamic intracellular scaffolding system that contributes to morphology and plasticity, migration, signal transduction and intracellular trafficking. During these processes, cytoskeletal elements generate the force required for membrane deformations, create structural scaffolds and act as tracks for motor proteins. Microtubules, intermediate filaments and actin microfilaments are the three filamentous structures that make up the cytoskeleton, regulated through the fine balance between assembly and disassembly. Although a brief overview of each component will be given, the main focus will be on actin dynamics.

Microtubules are hollow tubes formed from the association of multiple alpha/beta tubulin heterodimers, which radiate from the microtubule-organizing center (MTOC) located at the centrosome in the cytoplasm [176]. Structures like the mitotic spindle of dividing cells and the core of cilia and flagella are dependent on microtubules. Microtubules are also important for structuring cell shape, maintaining organelle localization and serving as tracks for the movement of vesicles and other cytoplasmic particles [177]. As such, both anterograde (away from cell body) and retrograde (toward cell body) movements are mediated by microtubules [177]. To generate the force needed for transportation of particles, cells rely on motor proteins that travel along cytoskeletal tracks, using ATP for chemical energy [178]. Molecular motors travelling on microtubules are kinesins and dyneins.

Intermediate filaments (IFs) are named like this because their diameter (10nm) falls between that of microtubules (24nm) and actin microfilaments (8nm). IFs comprise a

heterogeneous group of structures encoded by many genes (at least 50 IF genes in humans), such as keratins, plectins, lamins, and desmins [179].

Actin microfilaments are the main driving force in cellular shape changes, which are required for processes such as cellular migration, signaling and cytokinesis [180]. Actin is an evolutionarily conserved protein found in all eukaryotic cells and it is also closely related to prokaryotic actin-like proteins, suggesting ancient evolutionary origins. Actin is an ATP-binding protein that can be found in monomeric soluble form, globular-actin (G-actin), or assembled into filamentous actin (F-actin) (Figure 6). When bound to ATP, actin monomers can be incorporated into microfilaments and shortly after, undergo ATP hydrolysis due to their ATPase activity. As the microfilament grows, actin-ATP subunits cap the growing end to prevent disassembly and promote growth. Actin microfilaments grow from their barbed (plus) end while the opposing end, where actin-ADP subunits tend to leave, is referred to as the pointed (minus) end. Since self-assembly is kinetically unfavourable, factors called actin nucleators facilitate actin polymerization.

The ARP2/3 complex is the most characterized actin nucleator, which is comprised of seven polypeptides including ARP2 and ARP3 plus five additional subunits, ARPC1-ARPC5 [180]. The ARP2/3 complex can nucleate filaments *de novo* and organize them into branched networks. Nascent filaments elongate at their barbed end and are capped by ARP2/3 at their pointed end. Assembly can be initiated by nucleating new filaments from monomers or by generating free barbed ends that act as templates for polymerization by uncapping or severing existing filaments. However, the activity of actin nucleation by the ARP2/3 complex alone is inefficient and requires filament binding, phosphorylation as well as the involvement of nucleation-promoting factors (NPFs). Most NPFs contain a WCA domain,

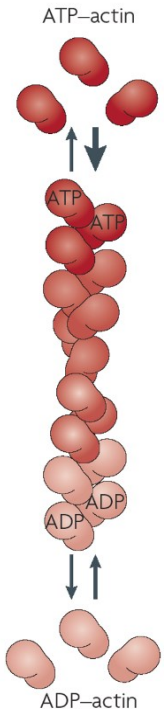

Figure 9. Actin. G-actin is a 42 kDa monomeric ATP-binding protein than can undergo cycles of self-assembly into filamentous actin (F-actin). ATP hydrolysis creates the ADP-bound form and subsequent depolymerization of the actin filament. Growth of the actin filament occurs primarily at the barbed end with the addition of ATP-actin and is capped by factors such as the ARP2/3 complex at its pointed end (ADP-actin) [181].

which is the minimal sequence element required for activation of ARP2/3-mediated actin nucleation, found in proteins such as the Wiskott-Aldrich syndrome protein (WASP) superfamily and the formins.

1.14 – Vesicular transport of proteins

Intracellular traffic of proteins (cargo) between two compartments is conducted by coated transport vesicles (carriers) that bud from one membrane and fuse with another. Selectively packaged in these carriers are the cargo as well as machinery proteins required for proper targeting. The three types of vesicular carriers that have been most extensively studied are clathrin-coated vesicles (endocytosis and late secretory pathway), COPII-coated vesicles (export proteins from the endoplasmic reticulum), and COPI-coated vesicles (within the Golgi apparatus and Golgi-ER traffic) [182]. Despite the different structural components and compartment specificities of endosomal coat complexes, some of the mechanisms of vesicle coat formation are similar and often initiated by the GEF-dependent activation of a small GTPases. During coat formation of clathrin- and COPII-coated vesicles, adaptor complexes are first recruited to the membrane followed by the coat complexes, which begin to polymerize [182]. These adaptors include the small GTPases of the Arf1/Sar1 family that regulate their assembly [183]. In the case of COPI, the adaptor and coat complexes exist as a single heptameric complex that is recruited to the membrane as a whole [184]. Transient binding of coat complexes to short peptide sequences present on cargo also contributes to cargo selection [185].

Retromer, which assembles at sites of protein sorting, interacts with cargo via the cargo recognition complex protein VPS35 and a conserved sorting motif [FW]L[MV] present on the cargo protein [186]. However, studies of retromer in *C. elegans* and yeast have shown that alternative sorting motifs or mechanisms of cargo recruitment also exist. Such is the case in *C. elegans*, where retromer mediates the retrograde trafficking of CED-1, a protein that lacks

the previously stated sorting motif [187]. Alternative mechanisms of cargo recognition were shown in a study on the yeast protein Grd19/Snx3 (PX-only), which acts as a cargo adaptor for retromer. Grd19 mediates the retrograde transport of the iron transporter Fet3p-Ftr1p by binding to retromer and to a sorting motif in the cytoplasmic tail of Ftr1p [188]. Finally, Snx1 (SNX-BAR) can associate directly with certain cargo proteins (GPCRs) and mediate their trafficking independently of retromer [189]. Such evidence highlights the diversification of retromer function in higher organisms.

The role of SNX-BARs in the progression of budding is to induce membrane tubulation, which is an elongation of the donor membrane. As previously mentioned, SNX-BARs homodimers and heterodimers can sense and/or induce membrane curvature. How this is accomplished is still unknown, but the mechanism is believed to be similar to that of the N-BARs [152, 190, 191]. For a protein to induce membrane curvature, the difference in the energy of binding to curved versus flat membranes must be greater than the energy required for membrane deformation. If the difference in binding energies is insufficient for deformation, a protein may still favour binding to preexisting curved membranes and this is referred to as curvature sensing. The proteins endophilin and amphyphysin have often been used for studying the curvature sensing/inducing properties of the BAR domain. These proteins contain an amphipathic helix N-terminal to the BAR domain, which, when inserted into the cytosolic leaflet of the bilayer, creates a difference in tension. This difference drives curvature, which is then stabilized by the BAR dimer [152, 190, 191]. It is believed that SNX-BARs function in a similar way. The progression of membrane curvature eventually leads to the formation of an elongated tubule, which is explained by the tip-to-tip and lateral contacts made between BAR domains that result in the formation of higher ordered helical arrays. This stabilizes the

formation of high curvature membrane tubules and turns local membrane deformation into global deformation [192].

As the protein coat continues to assemble, other cellular machineries, such as the actin cytoskeleton (discussed later), assist in membrane re-sculpturing required for bud formation [182]. Scission at the neck of the bud then ensues through the actions of the coat proteins and GTPase activity [193, 194]. Interestingly, clathrin-coated vesicles also play a role in retrograde trafficking, including retromer biology [192]. Isolated CCVs were shown to contain VPS35 as well as Snx1, Snx2, Snx5 and Snx6 [195]. This association may be due to direct binding of retromer to clathrin as many SNX-BARs contain an inverted clathrin-binding box within the PX domain [196].

Lastly, to allow fusion with the target compartment, the coat depolymerizes under the effect of GTP hydrolysis mediated by GAPs or by GAP activity within the coat complex [7, 197]. During retromer-mediated transport, clathrin depolymerization seems to involve RME-8, a DNA-J domain protein [198, 199]. DNA-J domain proteins also include auxilin, which are known to promote uncoating of CCVs at both the plasma membrane and TGN [28]. RME-8 colocalizes and directly associates with Snx1 on early endosomes [198]. In addition, interference with RME-8 disrupts trafficking of known retromer cargos, such as CI-M6PR. As such, through its interaction with RME-8, retromer recruits regulators of clathrin dynamics at sites of retrograde trafficking. Transportation of vesicles to their final destination occurs either by diffusion or by motor-mediated transport along a microtubule or actin cytoskeletal tracks [200]. All three types of molecular motors (kinesins, dyneins and myosins) have been implicated in this process [201-203]. As the transport vesicle reaches its destination compartment, proteins and protein complexes tether the vesicle to its target membrane. Members of the Rab and Ras GTPase

families both play critical roles in determining the specificity of vesicle targeting [204, 205]. Fusion of the vesicle with its target membrane is dependent on a family of proteins called SNAREs (soluble N-ethylmaleimide-sensitive factor attachment protein receptor). Present on both the transport vesicle and target membrane, the two proteins associate to form a complex and drive the fusion of two lipid bilayers [206, 207].

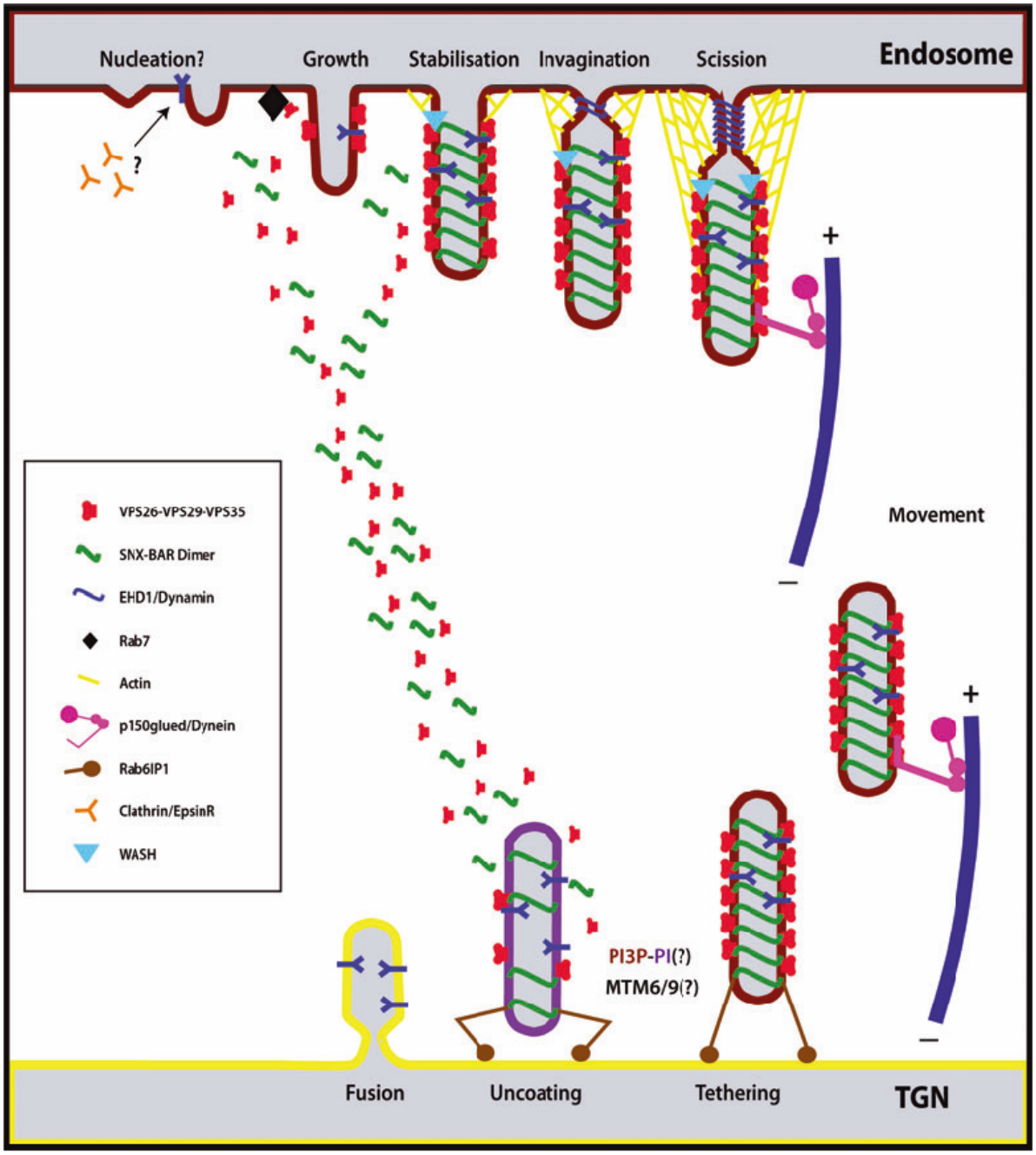

Figure 10. The process of retromer-mediated vesicular transport. For the retromer, membrane tubulation is driven by specific combinations of SNX1/SNX2 and SNX5/SNX6, which is coupled with cargo sorting through the association of the cargo recognition

complex (VPS26-VPS29-VPS35) with cytosolic tails of cargo (e.g. CI-MPR). Vesicle scission proceeds by an unknown mechanism but likely requires dynamin-like proteins of the EHD family and force generated by microtubule motors and/or actin polymerization. Uncoating of the vesicle carrier occurs possibly through the action of myotubularins, prior to SNARE-mediated fusion. However, the precise role of clathrin in nucleation is still unclear. [192]

1.15 – Actin and membrane dynamics

Mounting data now strongly suggests an implication for actin polymerization in membrane trafficking. In yeast, the formation of actin microfilaments is a definitive prerequisite for clathrin-mediated endocytosis [180]. This was shown by observing co-localization between endocytic and actin assembly proteins, and from a series of screens for endocytic mutants, which identified mutations in actin-binding protein genes [180]. These results were later confirmed with live imaging, which demonstrated coordinated assembly and disassembly of endocytic and actin-associated proteins at actin patches [208]. In yeast, the initial curvature of the membrane is generated by clathrin and endocytic proteins, such as the BAR domain-containing SYP1 [180]. At this point, SYP1 prevents actin assembly possibly by inhibiting WASP/ARP2/3-mediated actin polymerization [209]. As invagination progresses, the induced membrane curvature is sensed by other BAR domain-containing proteins like BZZ1, which is recruited

along with other endocytic proteins and actin polymerization-promoting proteins like ARP2/3 [210]. Actin assembly then proceeds to force further invagination of the nascent pit and eventually the actin network drives the inward flow of the newly formed vesicle.

In mammalian cells, actin polymerization is required for processes such as phagocytosis, macropinocytosis, caveolin-mediated endocytosis, and CME [180]. As in yeast, many endocytic adaptors used during CME can interact with actin assembly proteins. These include HIP1R, which inhibits actin assembly at endocytic sites and binds to clathrin, F-actin and cortactin [211]. During the formation of clathrin-coated pits, actin polymerization has been reported to occur at cortical sites in a temporally regulated manner [212]. There are also BAR domain containing proteins such as Snx9/Snx18, which can associate with dynamin and WASP proteins while positively regulating WASP/ARP2/3-mediated actin assembly [51]. Snx9 has a C-terminal PX-BAR domain and an additional N-terminal SH3 domain. Snx9 forms BAR homodimers, uniting the PX-BAR domains to form a single "superdomain" for membrane sculpting [213]. The SH3 domain of Snx9 binds to class I polyproline sequences, which are found in dynamin and the actin regulators WASP and N-WASP [214, 215]. In accordance, both dynamin 1 and dynamin 2 bind effectively to Snx9 *in vitro* and *in vivo* [12, 216]. Binding of Snx9 to the actin regulators WASP and AP-2 have also been described [217, 218]. Additionally, Snx9's function during this process is greatly enhanced by the presence of $PI(4,5)P_2$, which induces Snx9 oligomerization and increases its effect on the GTPase activity of dynamin [213, 216]. Taken together, these studies support a mechanism whereby Snx9 is recruited to clathrin-coated pits, through interactions with AP-2, clathrin and highly curved membrane surface enriched in $PI(4,5)P_2$ [213]. Dynamin and Snx9 likely act together to narrow down the neck of a clathrin-coated pit to a point at which a sudden pushing force may be required to

separate the vesicle from the membrane. Such a force might be mediated by local actin polymerization and would be associated with a shift in Snx9 function, from recruitment an assembly of dynamin to binding and activation of N-WASP [213]. Additional data supporting this hypothesis comes from studies showing the synergistic effect of Snx9 and phospholipids ($PI(3,4)P_2$, $PI(3,5)P_2$, $PI(4,5)P_2$, $PI(3,4,5)P_3$) in activating N-WASP [51, 219]. Also, when Snx9 lacking the SH3 domain is overexpressed in cells, it leads to the production of long membrane tubules, likely due to inefficient recruitment and activation of the scission machinery [215, 220, 221].

Now that I have highlighted the importance of intracellular trafficking on cell signaling, the challenge remains to integrate *in vitro* biomolecular data into an *in vivo* context. Cell culture studies do not take into account the plethora of factors and physical constraints that influence individual cells within a living organism. Nevertheless, this is the ultimate goal, to better understand the role of each gene *in vivo*. The next section will delve into embryogenesis and the many stages and signaling pathways involved during development. The focus of this thesis will be mainly on cardiogenesis and somitogenesis.

1.16 – Embryogenesis

"It is not birth, marriage, or death, but gastrulation, which is truly the most important time in your life." Lewis Wolpert (1986)

The period between fertilization and birth is called embryogenesis, a time when we build ourselves from a single cell. This process of progressive change is exquisitely regulated by maternally transmitted signals, as well as transcriptional, translational and post-translational regulation from the embryo, which coordinate cell divisions, fate specification and movements. The development of the embryo produces an explosion of cellular diversity, which solicits increasingly complex and specific cellular signaling. Therefore, the intracellular trafficking mechanisms associated with these signaling pathways must be in place to prevent any erroneous signaling, which the delicate embryo cannot afford. Hence, by better understanding embryogenesis and the processes of cellular differentiation, the cause of many congenital defects may be identified and new avenues for regenerative medicine, diagnosis and therapies may be discovered.

Embryogenesis leads to the elaboration of sophisticated body architecture, including the formation of the three major axes, namely the anteroposterior (AP), dorsoventral (DV) and left-right (LR) embryonic axes, with an internal collection of organs of varied morphology and function. Embryogenesis also encompasses the specification of the germ layers, the patterning and diversification of cell fates along the embryonic axes. For simplification, *Xenopus*

embryogenesis will be the main focus although certain aspects of embryogenesis in other model organisms will also be discussed when needed.

Gastrulation is the first major morphogenetic change to occur in vertebrates. This process transforms a mass of morphologically similar cells (blastula) into three distinct germ layers. The ectoderm, the outermost layer of the embryo, gives rise to the peripheral and central nervous system, tooth enamel and the epidermis. The mesoderm is the middle layer and develops into cardiac, smooth and skeletal muscle, as well as red blood cells and the tubule cells of the kidney. Finally, the endoderm forms the inner layer of the gastrula and develops into the epithelial lining of multiple systems, including the intestine, the lungs, the pancreas, and the endocrine glands and organs (Figure 11).

Gastrulation follows a set of evolutionarily conserved movements: emboly/internalization, epiboly, convergence and extension. Emboly, or internalization, is the defining gastrulation movement, which transports the prospective mesodermal and endodermal cells move inward through an opening called the blastopore, also known as the primitive streak in the mouse and chick, and beneath the future ectoderm. This generates the three germ layers of the embryo and establishes the AP, DV and LR body axes.

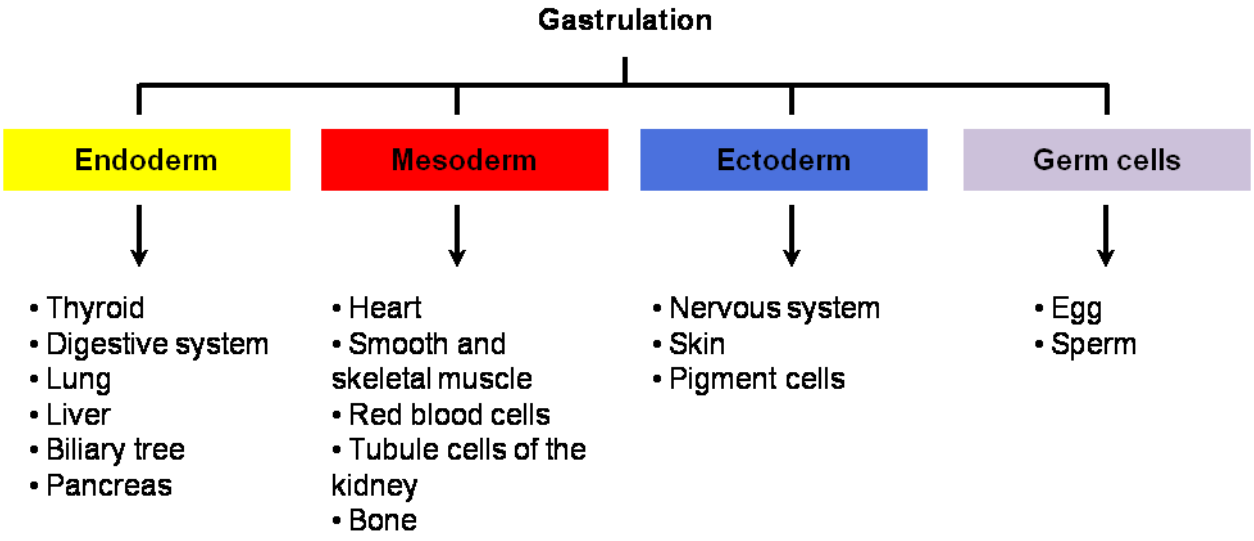

Figure 11. Germ layers and their descendants. Gastrulation leads to the formation of the three germ layers: endoderm, mesoderm and ectoderm. These cell populations give rise to distinct organs and systems (shown below each germ line). Germ cells are also produced during gastrulation.

Cells migrating inward along the archenteron generate a tube that will eventually form the digestive tract and the cells that line this tract form the endoderm. During emboly, cells migrating inward undergo an epithelial to mesenchymal transition (EMT), which allows them to move more freely within the developing embryo [222]. This entails the disassembly of epithelial junctions, downregulation of cell adhesion molecules, and remodeling of the cytoskeleton [223]. Asymmetrical delivery and removal of these cytoskeletal and adhesion components is accomplished by polarized membrane transport and endocytosis, which drive these changes [224]. Once inside the gastrula, involuted tissue breaks away from and migrates under the

internal side of the blastocoel roof [225]. This tissue continues to migrate deep into the embryo, as individual but synchronized cells. As the nascent germ layers begin to thin and spread, the embryo starts epiboly. Cells become narrow and flat by radial intercalation, which results in the expansion of a thin sheet of cells and the elongation of the embryo. Near the end of gastrulation, the embryo undergoes the last step of gastrulation, convergent extension (CE), which elongates the embryo from head to tail, narrowing dorso-ventrally. CE is achieved by planar intercalation of cells between their anterior and posterior neighbours. As such, cells along the lateral mesoderm converge to the embryonic midline and simultaneously extend [226].

The formation of the three germ layers is molecularly orchestrated and begins with maternal signals originating from the vegetal half of the embryo. The pre-gastrula embryo can be divided into three prospective germ layers with the vegetal half forming the prospective endoderm, the equatorial region forming the prospective mesoderm and the animal region forming the prospective ectoderm. Maternal VegT is a T-box transcription factor that is expressed vegetally and which activates TGF-β and nodal signaling, to induce the mesoderm and endoderm [227]. The dorsal side of the embryo is regulated differently from the ventral region with the Wnt pathway being the primary determinant. Through the dorsal activation of Wnt signaling, high levels of *Xnr1* and *Xnr2* (*Xenopus* nodal-related genes) help to establish the posterior and anterior domains of mesoderm [227]. As such, the prospective mesoderm can also be divided into domains with unique molecular signatures. For example, while posterior paraxial mesoderm gives rise to somites, head mesoderm develops into the branchial arches.

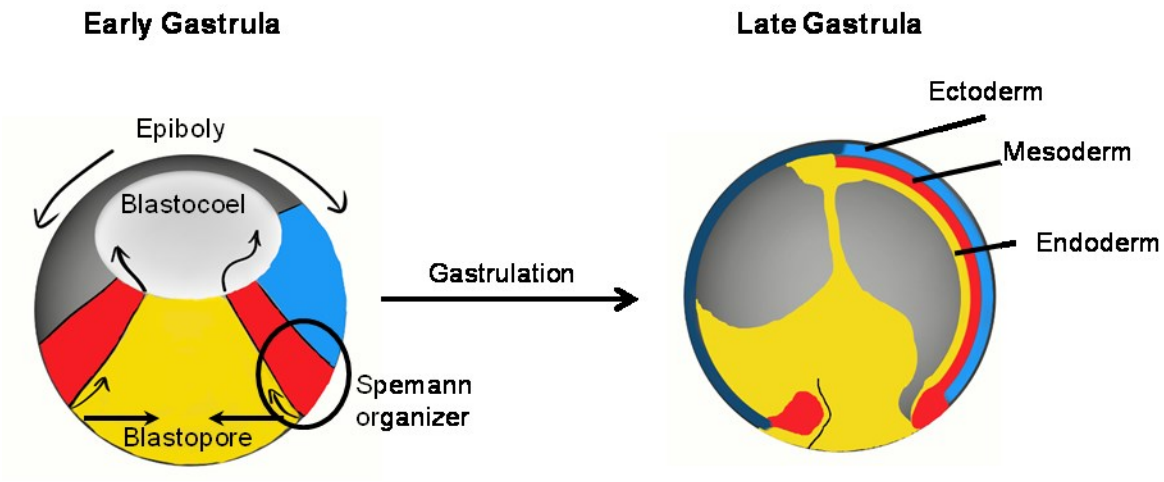

Figure 12. Fate maps and gastrulation movements in *Xenopus laevis.* Left: early gastrula cross section with animal/anterior up and dorsal to the right. Prospective endoderm is the most vegetal (yellow), while mesodermal precursors (red) form a broad band between endodermal and animally located ectodermal precursors. Dorsal enrichment of β-catenin establishes the Spemann organizer, which then coordinates gastrulation movements (arrows). Right: late gastrula cross section depicting the three germ layers: ectoderm (blue), mesoderm (red) and endoderm (yellow).

Regulating a vast majority of the changes observed during gastrulation is the Spemann organizer (SO), which is located around the initial site of cellular ingression (Figure 12). Signals originating from the SO, namely the two factors, fibroblast growth factor (FGF) and Snail, drive EMT. However these two factors are mutually repressive and maintain the balance of ectodermal progenitors in the epiblast and mesendoderm progenitors that ingress during

gastrulation [228]. As gastrulation progresses, a small population of mesoderm cells become fated to the cardiac lineage.

1.17 – Cardiogenesis

In vertebrates, the heart is one of the first organs to fully develop, providing the growing embryo with a constant distribution of oxygen and nutrients. For more detailed information on cardiogenesis and the recent advances in the subject, please refer to these excellent reviews [229-231]. Vertebrate cardiogenesis is evolutionarily conserved and many similarities exist between mammalian and amphibian heart development. However, compared to a mammalian heart, the heart of an amphibian bears significant anatomic differences, the most striking being its three chambers versus four in mammals (Figure 13). The heart of amphibians is made up of two partially septated atria and a single, non-septated but highly trabeculated ventricle. The spiral outflow tract in the amphibian heart is equipped with two valves in series, which direct blood flow to the pulmocutaneous or systemic arteries based on the relative resistance in these vascular beds [232, 233]. Despite these differences, mammalian and amphibian cardiogenesis is practically identical during the early phases and only begin to diverge after the heart tube stage and the early stages of looping. By studying cardiogenesis in *Xenopus laevis*, we may further our knowledge of human heart development.

At the onset of vertebrate gastrulation, prospective heart cells originate as two bilateral patches of specified mesoderm on the dorsal side of the embryo (Figure 14A) [234]. During

gastrulation movements, these cardiac progenitors migrate dorso-anteriorly as two populations of cells and then ventrally to fuse at the ventral midline during neurulation (Figure 14A) [234].

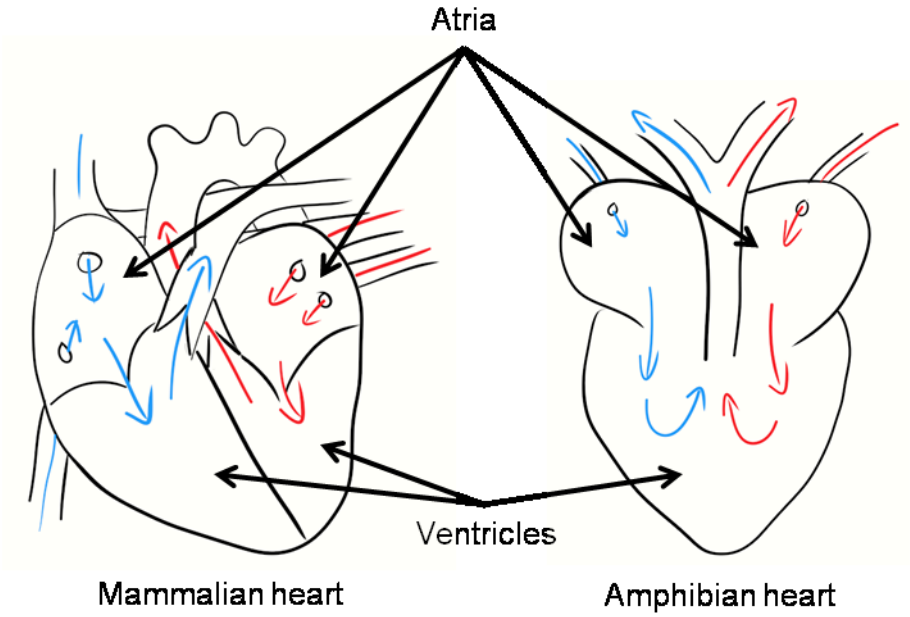

Figure 13. Inside the mammalian and amphibian hearts. Here are simplified illustrations of mammalian and amphibian hearts. Morphological differences and similarities are shown, most noticeable is the fact that unlike a human heart, which has four chambers (2 atria, 2 ventricles), the amphibian heart has only three (2 atria, 1 ventricle). As only one ventricle pumps blood through the body, a mixture of blood, both Oxygen-rich (red) and –poor (blue), leaves the heart. Interestingly, studies have shown that some form of sorting does occurs between O_2-rich and –poor erythrocytes [232, 233].

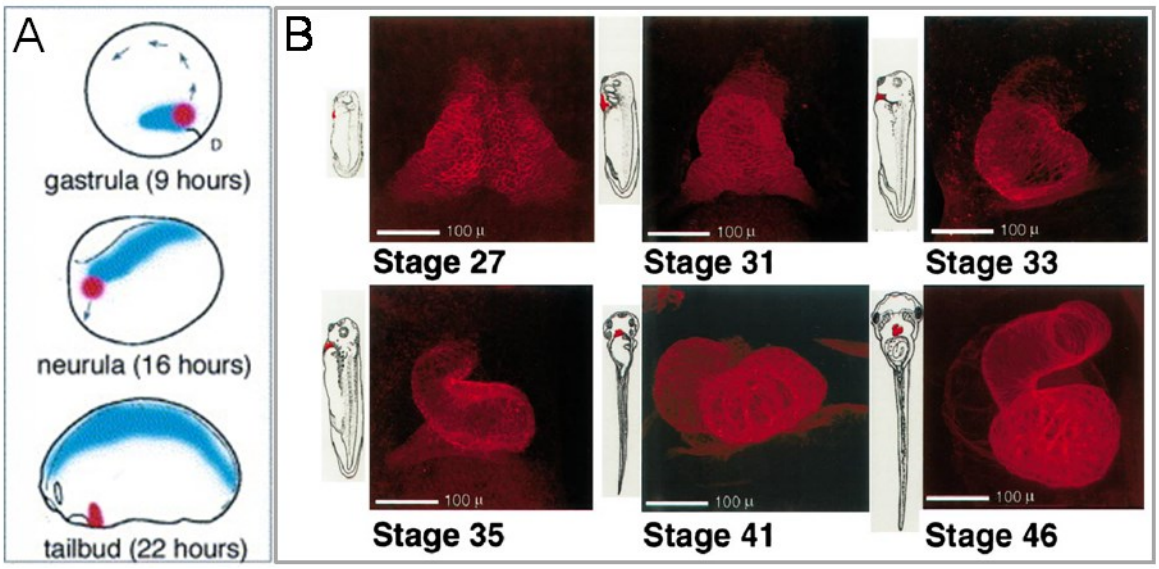

Figure 14. Cardiogenesis in *Xenopus laevis*. A) Prospective heart cells (red) are found on the prospective dorsal side (D) of the early gastrula mesoderm, adjacent to the axial somitic mesoderm (blue). By the end of gastrulation, these cardiac progenitors have migrated to the dorsoanterior end of the embryo. The bilateral patches eventually fuse at the ventral midline during the end of neurulation (Stage 21) [235]. B) Ventral view of *Xenopus laevis* embryos immunostained with anti-fibrillin. These images show the morphological changes that occur during cardiogenesis: primitive heart tube (stage 27), formation of the linear heart tube (stage 31), completion of the linear heart tube (stage 33), spiral looping of the heart tube (stage 35), the onset of chamber formation (stage 41), completion of the three-chambered heart (stage 46) [232].

Once the two populations of cardiac progenitor cells merge at the ventral midline they begin to form the cardiac muscle. This group cells form the majority of the myocardium and are

divided into two distinct cell populations called the first (FHF) and second heart (SHF) fields (Figure 15) [230, 236]. The two distinct heart fields can first be detected at the cardiac crescent stage. FHF cells are the first to differentiate while cells of the SHF migrate later to join the differentiated FHF cells [230]. The FHF occupies an anterior lateral position and may provide a scaffold upon which the SHF forms. In general, cells from the FHF contribute to the left ventricle while SHF cells contribute to the outflow tract and the right ventricle, as well as to both atria [237]. These cells eventually form a primitive myocardium that begins its lifelong contractions as it continues to develop into a multichambered organ (Figure 14B) [230]. Both the FHF and SHF differ with respect to the onset of terminal differentiation but retrospective clonal analyzes indicates these two cell populations derive from one common cardiac progenitor cell population (CPC) [238, 239].

In the final stages of heart development, the cardiac tube undergoes a leftward bend, creating the outflow tract, which is followed by the formation of the atrioventricular valve that separates the atria from the ventricle (Figure 14B) [230]. Finally, the atrium divides into two asymmetrical chambers, the right atrium being the larger of the two, and trabeculae form within the wall of the ventricular myocardium [230].

On a molecular basis, one of the earliest markers of cardiac progenitors is the transcription factors Mesp1 (mesoderm posterior 1), which lies on top of the cardiovascular lineage, upstream of other important markers for cardiac progenitors, such as Isl1 [240]. Expression of Mesp1 is required for the migration of cells towards the anterior region of the embryo [241]. This gene is transiently expressed in nascent mesoderm and descendants of these cells colonize the whole myocardium, including both heart fields [229]. Myocardial transcription factors, such as Nkx2-5 (NK2 transcription factor related, locus 5) and Gata4 (GATA-binding

protein 4), are first detected in the cardiac crescent, where myocardial differentiation begins [229]. Nkx2-5 and Gata4 depend on positive signaling from BMPs (bone morphogenetic proteins) and FGFs (fibroblast growth factors), while an inhibitory effect on differentiation is exerted by Wnt signaling [242]. While SHF cells are easily identified by many molecular markers, including genes like Fgf8, Fgf10, Isl1, and Tbx1, there is a lack of molecular markers for the FHF [229]. Nevertheless, a small set of genes have been proposed, namely Nkx2-5, Hand1 and Tbx5, and may be associated with FHF cells due to their mutant phenotypes, which display mainly left ventricular defects [229].

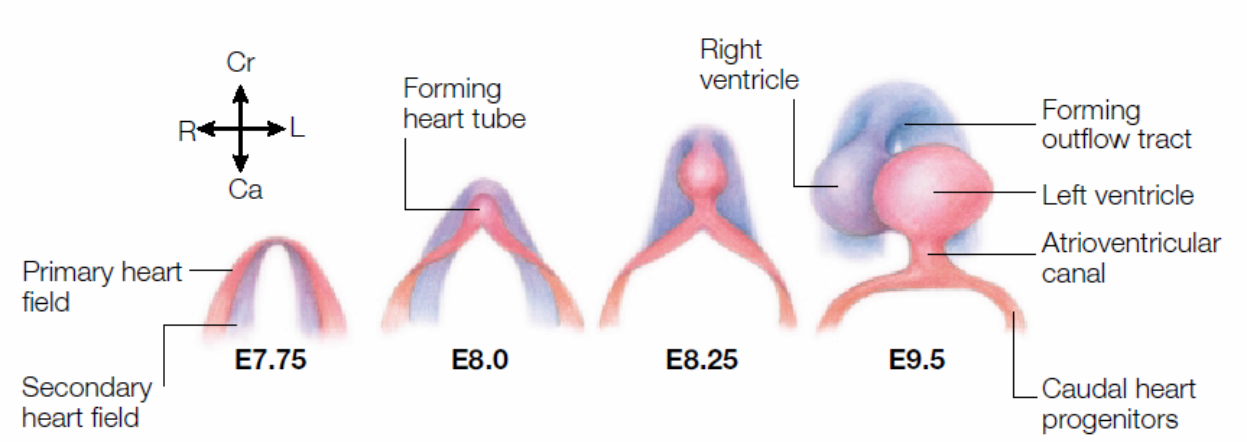

Figure 15. First and second heart fields during mouse cardiogenesis. Here are shown the relative positions and movements of the first and second heart fields, relative to each other. The body axes are indicated. Ca, caudal; Cr, cranial; L, left; R, right. [243]

During heart development, cardiac progenitor cells undergo multiple phases of specification and proliferation. Early cardiogenesis is marked by signaling from both the bone

morphogenetic protein and Wnt signaling pathways, which play pivotal roles [244]. While BMP signaling promotes cardiac specification, Wnt/β-catenin signaling can have either a positive or negative effect on the progression of cardiogenesis [244, 245]. Early work in *Drosophila* suggested that Wnt/β-catenin signaling plays a general positive role on cardiogenesis [246]. However, later studies reported conflicting results on the role of Wnt/β-catenin signaling during cardiogenesis. On the one hand, inhibition of Wnt/β-catenin signaling in chick and *Xenopus* embryos promoted heart development while its activation in anterior mesoderm suppressed cardiac differentiation [247, 248]. Also, data obtained from mouse studies showed that endoderm specific knockout of β-catenin results in the formation of multiple, ectopic hearts [249]. On the other hand, cell culture-based experiments showed that inhibition of Wnt/β-catenin signaling in P19 teratocarcinoma stem cells decreased expression of cardiac specific genes [250].

These apparently contradictory results have now been resolved into a new model that suggests a biphasic effect (agonistic or antagonistic) of Wnt signaling on cardiogenesis depending on the developmental timing (Figure 16). This was elegantly shown in heat shock inducible transgenic zebrafish embryos where application of Wnt8, a Wnt agonist, before gastrulation produces more cardiomyocytes, whereas application of Wnt8 after gastrulation results in less cardiomyocytes [251]. Correspondingly, a reverse effect could be achieved by the timed delivery of the Wnt inhibitor Dkk1. In mouse embryonic stem cells (ESCs), expression of some canonical Wnt ligands starts slightly earlier than the expression of cardiac genes, and inhibition of these ligands at early time points inhibits cardiac differentiation and reduces the contractile area within embryoid bodies [251, 252].

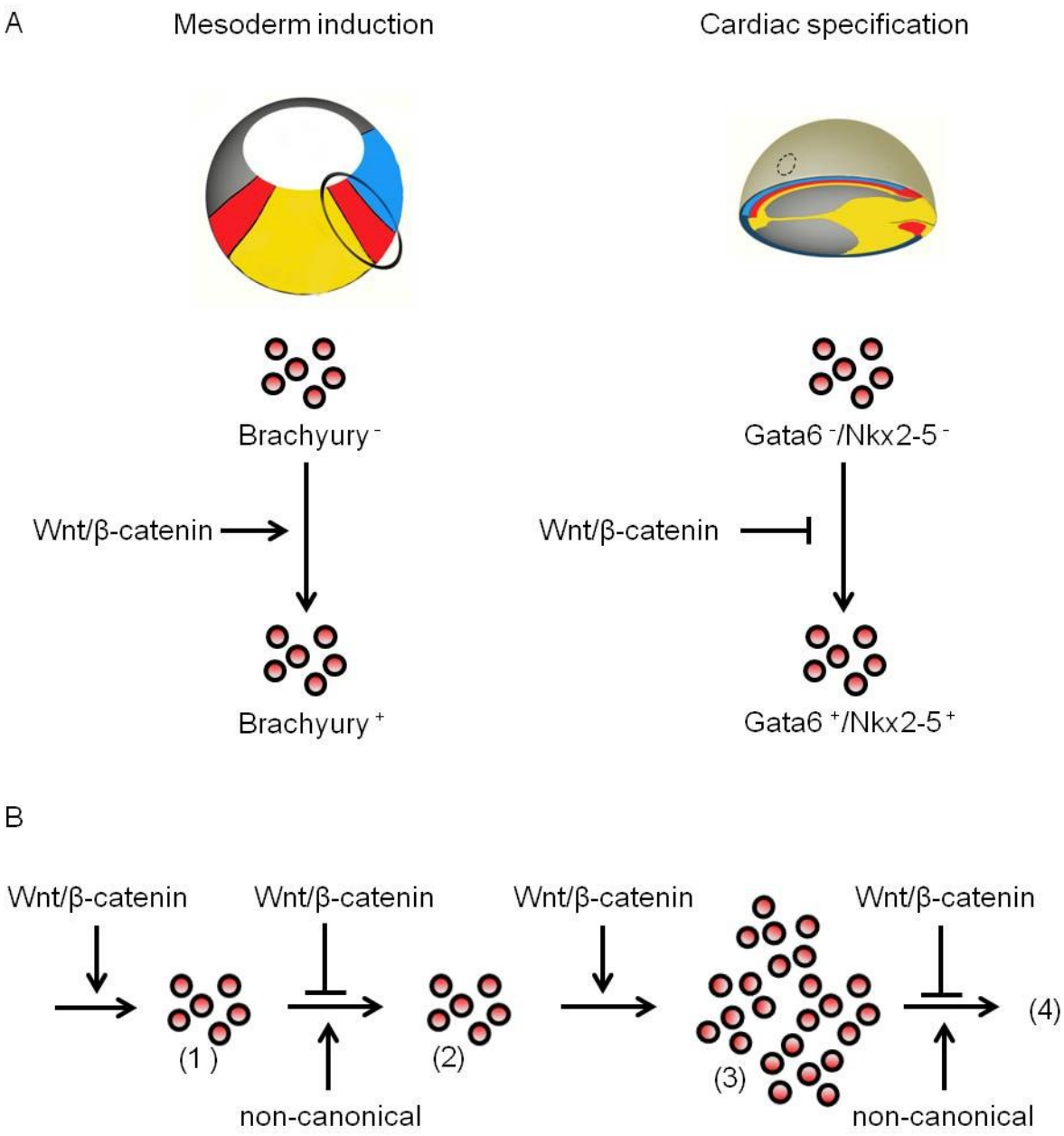

Figure 16. Wnt/β-catenin regulation and cardiac specification. A) Wnt is a determining factor during cardiogenesis. Wnt/β-catenin signaling promotes specification of cells to mesoderm and the concomitant expression of Brachyury (left panel, pre-gastrula). Following mesoderm formation, inhibition of Wnt/β-catenin is required for commitment

to the cardiac lineage and expression of early cardiac markers Gata6 and Nkx2-5 (right panel, gastrula). The general area corresponding to pre-cardiac mesoderm is circled (left panel). Once specified, cardiac progenitors migrate anteriorly as two lateral populations. The dotted lines (right panel) shows this lateral location. Mesoderm: red; endoderm: yellow; ectoderm: light blue; epidermis: dark blue. B) The multiple phases of Wnt signaling during early cardiac development. The actions of canonical and non-canonical Wnt signaling are shown for the progression of each stage: (1) Mesoderm formation, (2) Specification, (3) Proliferation, (4) Terminal differentiation.

As a prerequisite for the formation of cardiac progenitor cells, the mesoderm germ layer must be induced in the early embryo and this process is dependent upon Wnt/β-catenin signaling (Figure 16A – left panel) [253-257]. In accordance, the canonical Wnt ligands Wnt3 and Wnt8a are expressed in the early gastrula-stage embryo and are also required during differentiation of mouse ESCs into multipotent mesoderm cells [254, 258]. A known marker for newly formed mesoderm cells is the T-box transcription factor Brachyury (Bry), which is required for posterior mesoderm formation and likely a direct target of Wnt/β-catenin signaling [256, 257]. In addition to the prerequisite of expressing Bry, mesoderm progenitors that are Flk-1^{+}/Mesp1^{+} will follow the cardiac lineage, while those are Flk1^{+}/Mesp1^{-} are fated for the hematopoietic cell lineage [259].

As prospective cardiac progenitors mature and acquire a mesoderm signature, Wnt/β-catenin signaling suddenly becomes a negative factor in their progression through cardiogenesis [244]. Evidence supporting this idea first came from studying Notch signaling,

which can redirect differentiating mouse embryonic stem cells fated for the hematopoietic lineage toward the cardiogenic lineage [260]. Here, Notch activation resulted in an upregulation of molecules inhibiting Wnt/β-catenin signaling, namely secreted Frizzled-related protein-1 (Sfrp1) and Sfrp4, and the addition of Wnt3a (canonical) but not Wnt5a (non-canonical) completely abolished the effect of Notch. In another study, it was found that overexpression of a stable variant of β-catenin in Isl1-positive cardiac progenitor cells caused a downregulation of several important cardiac genes [261]. Supporting these data were the findings that Wnt/β-catenin signaling negatively regulates Gata6 (early cardiac transcription factor), and that the Wnt inhibitor Dkk1 can improve the differentiation of Mesp1-induced cardiomyogenesis [254, 262].

Contrary to Wnt/β-catenin signaling, non-canonical Wnt signaling contributes to cardiogenesis in mesoderm cells (Figure 16B). Supporting evidence comes mostly from studies of Wnt11 and Wnt5a, which induce contractile tissue formation and is upregulated in $Bry^{+}/Flk1^{+}$ cardiogenic progenitors, respectively [251, 260, 263-265]. In addition, Notch signaling or Mesp1 activation seem to upregulate non-canonical Wnt ligands during cardiogenesis [266, 267].

Even with these results, we still cannot draw a clear picture of heart development. Although the importance of Wnt/β-catenin signaling has been demonstrated, the molecular components and mechanisms that regulate the activation and inhibition of this signaling pathway across each step of cardiogenesis are still poorly understood. Initiation of this pathway occurs when Wnt is secreted protein, which ends up stabilizing the transcriptional co-activator β-catenin. Between these key proteins lie many transducing factors, which determine whether the Wnt signal is received and acknowledged by the cell. Therefore, to fully comprehend the implication

of Wnt/β-catenin signaling during cardiogenesis, we must better understand the mechanisms that regulate this major signaling pathway.

1.18 – Wnt signaling

The Wnt family of secreted glycoproteins is a large family of evolutionarily conserved morphogens; essential for a wide array of developmental and physiological processes, they are involved in embryonic axis formation, segmentation, organogenesis, as well as stem cell proliferation [268-275]. Furthermore, Wnt pathways are closely linked to disease, such as tumorigenesis [276, 277], bone disease [278] and neurodegenerative diseases [279].

As Wnt signaling is activated, a Wnt molecule, originating from a close or distant cell, binds to a cell-surface receptor, which initiates a cascade of events leading to transcriptional changes. In the classical (canonical) model, Wnt signaling requires binding of Wnt to both a receptor (Frizzled (Fz), Fz1-10 in humans) and a co-receptor (low-density lipoprotein receptor-related protein (LRP), LRP5/6) [280, 281]. Frizzled receptors are seven-transmembrane proteins that bind with high affinity to Wnt ligands while LRP5/6 are single-pass transmembrane proteins that bind poorly to Wnt but help stabilize the Fz-Wnt-Lrp complex and contribute to downstream signaling [282]. Other less described co-receptors implicated in Wnt signaling include the Tyrosine kinase-like orphan receptor (ROR) [283], protein Tyrosine kinase 7 (PTK7) [284], receptor Tyrosine kinase (RYK) [285], muscle skeletal receptor Tyrosine kinase (MUSK) [286] and proteoglycan families [287]. Secreted receptor-binding agonists of Wnt signaling

include 19 known Wnts, the R-spondin (RSPO) family and Norrin [288]. Known antagonists of Wnt signaling are either secreted as soluble molecules or expressed at the cell surface as transmembrane inhibitors. Inhibition can be achieved by competitive binding of antagonists to receptors and co-receptors, by binding of secreted inhibitors to secreted Wnts, by preventing the maturation of receptors or by interfering with receptor interactions and internalization [288]. Secreted inhibitors include Cerberus, the Dickopf-related proteins (Dkk), secreted Frizzled-related protein, SOST, Wnt inhibitory factor (WIF), and Wise/SOST [288]. Transmembrane inhibitors identified to date include Shisa, Wnt-activated inhibitory factor 1 (Waif1/5T4), adenomatosis polyposis coli down-regulated 1 (APCDD1), and Tiki1 [288].

Activation of Wnt signaling can produce different results; it can stabilize the cytoplasmic protein β-catenin (canonical Wnt signaling) or produce a β-catenin-independent response (non-canonical Wnt signaling). Using this classification, Wnt1, Wnt3a, Wnt8 and Wnt8b are recognized as canonical Wnt signaling agonists whereas Wnt4 and Wnt5a take part in the non-canonical pathway [289]. However, this classification is a highly subjective oversimplification since several Wnts can activate both the canonical or non-canonical pathways, depending on the cellular context and the receptors present at the cell-surface. In addition, new research has revealed that considerable crosstalk occurs between β-catenin-dependent and –independent signaling pathways [289]. There are at least 15 different Wnt receptors and co-receptors, and their specific combination with a specific Wnt determines the downstream pathway. For example, Wnt5a, which was initially classified as a non-canonical Wnt activator, has been shown to activate the Ca^{2+} signaling pathway when specific Frizzled receptors are present, namely Fz2, Fz3, Fz4, Fz5, and Fz6 [290-292]. Yet, Wnt5a can also activate the canonical Wnt pathway if it encounters both Fz4 and LRP5 [293]. Despite this simplified classification

and due to the scope of this work, canonical and non-canonical Wnt nomenclature will still be used to refer to instances of β-catenin-dependent and –independent signaling, respectively.

Canonical Wnt signaling (Wnt/β-catenin) revolves around a cytoplasmic protein, β-catenin (Figure 17). Newly synthesized β-catenin is found at adherens junctions, immobilized by E-cadherin. There it can indirectly modulate the actin cytoskeleton through its interaction with α-catenin. During inactive Wnt/β-catenin signaling, levels of cytoplasmic β-catenin (from excess synthesis or released from adherens junctions) are kept low due to phosphorylation of β-catenin by the "destruction complex" [289]. This complex includes glycogen synthase kinase 3, adenomatosis polyposis coli (APC), Axin, the E3-ubiquitin ligase β-TrCP and casein kinase Iα [294]. Phosphorylation of β-catenin depends on kinases in the destruction complex and serves as a signal that targets β-catenin for proteasomal degradation [289]. The interaction of Wnt with Frizzled and LRP5/6 activates Wnt/β-catenin signaling by causing the disassembly of the β-catenin destruction complex. In turn, β-catenin accumulates in the cytoplasm and eventually translocates to the nucleus where it acts as a transcriptional co-activator, associating with the transcription factors TCF (T cell factor) and LEF (lymphoid enhancer-binding factor) [295-297]. The disassembly of the β-catenin destruction complex is not completely understood but involves the recruitment of two scaffolding proteins, Dishevelled and Axin, to the intracellular domains of Frizzled and LRP5/6, which inhibits the phosphorylation of β-catenin [294]. Other mechanisms that promote the stabilization/accumulation of β-catenin have recently been discovered and will be discussed in the "Endocytosis and Wnt/β-catenin signaling" section.

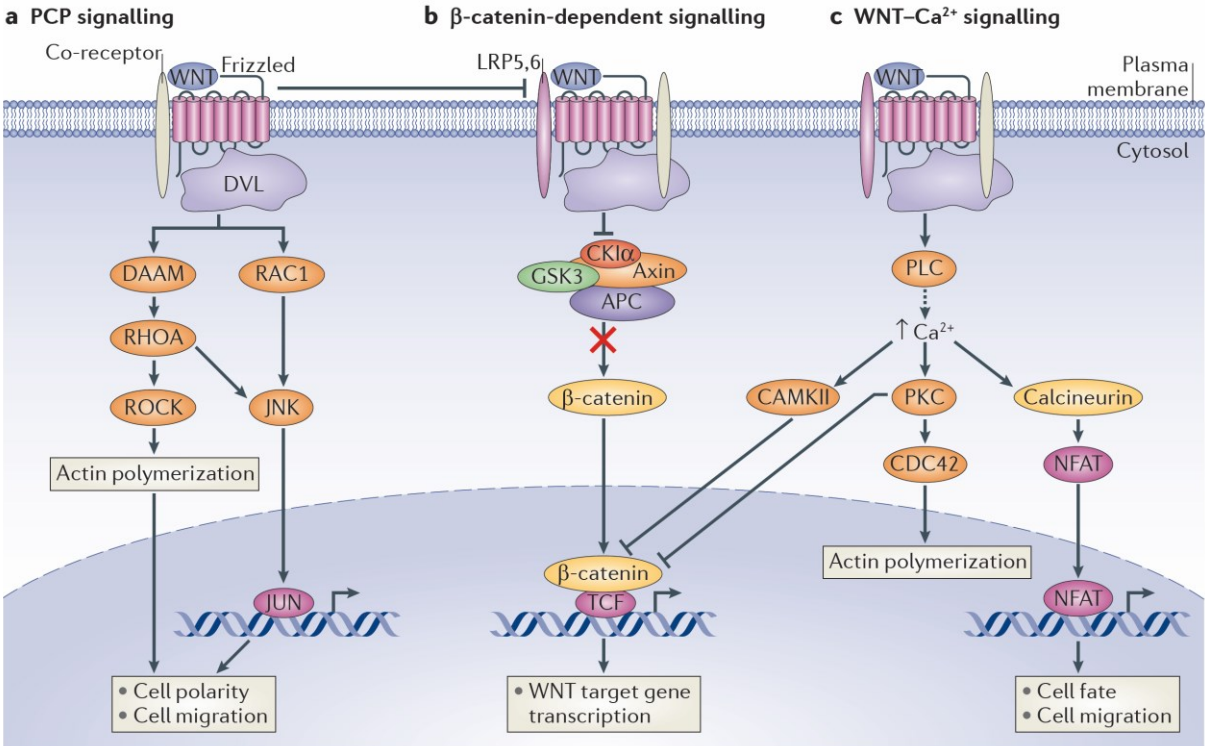

Figure 17. The different pathways of Wnt signaling. A) Planar cell polarity (PCP) signaling activates of the small GTPases RHOA and RAC1, which in turn activate RHO kinase (ROCK) and JUN-N-terminal kinase (JNK), respectively, leading to cytoskeletal rearrangements, namely actin polymerization and microtubule stabilization. Cellular activities influenced by this pathway include the regulation of cell polarity, cell motility and morphogenetic movements. B) In the absence of a Wnt ligand (from excess synthesis or released from adherens junctions), levels of cytoplasmic β-catenin are kept low due phosphorylation by the destruction complex (GSK3-APC-Axin-CKIα) and subsequent ubiquitination/proteasomal degradation. When Wnt receptors/co-receptors are activated by Wnt, a Fz-LRP-Wnt complex is formed, which inhibits the destruction complex. LRP signalosomes are formed, sequestering certain components of the

destruction complex, such as GSK3 to MVBs, allowing β-catenin to accumulate in the cytoplasm. β-catenin then translocates to the nucleus where it associates with the LEF/TCF transcription factors to activate transcription of target genes. C) The Wnt-Ca^{2+} pathway activates Ca^{2+}- and calmodulin-dependent kinase II (CAMKII), protein kinase C (PKC) and calcineurin. In turn, Calcineurin activates nuclear factor of activated T cells (NFAT), which regulates the transcription of genes involved in cell fate determination and cell migration. Both the PCP and Ca^{2+} pathways inhibit Wnt/β-catenin signaling at various degrees. [289]

Non-canonical (β-catenin-independent) Wnt signaling encompasses pathways that do not use β-catenin but instead employ different signaling cascades to elicit a transcriptional response. These include the planar cell polarity (PCP) signaling, the Ca^{2+} pathway, and the Wnt5A-ROR signaling (Figure 17).

PCP signaling involves a cascade of activated molecules initiated by the activation of Frizzled receptors, the small GTPases RAC1 and RHOA, and RHO kinase (ROCK) and Jun-N-terminal kinase (JNK) [289]. The downstream output of the PCP pathway leads to cytoskeletal remodeling and changes in cell polarity via small GTPases and/or transcriptional activation of JNK-dependent transcription factors, for example the activating transcription factor 2 (ATF2) [287, 298]. The PCP pathway is prominently involved in regulating cell polarity in morphogenetic processes, such as cell movement during gastrulation, neural tube closure and the orientation of stereocilia in the inner ear [287, 298].

Another possible consequence of activating Wnt signaling is the transient increase in concentrations of inositol 1,4,5-triphosphate (IP3), 1,2 diacylglycerol (DAG), and Calcium (Ca^{2+}) [299]. IP3 diffuses through the cytosol and interacts with calcium channels on the membrane of endoplasmic reticulum, releasing Ca^{2+} ions and resulting in the activation of calcium calmodulin dependent protein kinase II (CaMKII) [290]. DAG also travels through the cytosol and activates protein kinase C (PKC), and the combined action of CaMKII and PKC activates various regulatory proteins (NFκB and CREB), which translocate to the nucleus as transcription factors [299, 300].

Aside from its association with Frizzled receptors, Wnt5a can also bind another transmembrane protein, the receptor tyrosine kinase Ror1/2, and mediate non-canonical signal transduction [299]. Wnt5a/Ror signaling also activates the calcium pathway, which has important implications in the neural tube formation, axonal pathfinding of the mammalian brain, testes development, and heart and bone formation [299, 301].

1.18.1 – Endocytosis and Wnt/β-catenin signalling

Endocytosis is an essential step in Wnt/β-catenin signaling but the mechanism regulating this and the following steps are only beginning to be understood. The first evidence for the role of endocytic trafficking in regulating Wnt signalling came from work in *Drosophila*. During the early stages of embryogenesis, signals like Wnt, act as short (distance three cell diameters)

and long range (distance over twenty cell diameters) signaling molecules, secreted in the form of soluble morphogens. In the *Drosophila* embryonic epidermis and the wing imaginal disc, Wg (*Drosophila* homolog of Wnt) can be detected in cytoplasmic puncta within Wg-responsive cells and interference with endocytosis abolishes this intracellular localization of Wg [302, 303]. In these endocytosis-defective cells, Wg accumulates on the extracellular surface, suggesting that Wg is normally internalized through the endocytic pathway. In addition, by providing a degradation route, endocytosis seems to regulate the distribution of Wg in the extracellular medium and restricts the range Wg signaling [304]. When endocytosis and subsequent lysosomal degradation are compromised in embryonic epidermis, excess Wg levels cause increased signalling and misspecification of epidermal cell fate. In accordance, Wg, arrow (*Drosophila* homolog of LRP) and DFz2 (*Drosophila* Frizzled 2) are trafficked to the lysosome in the wing imaginal disc of wild-type animals [305]. In this context endocytosis seems to play a negative role on Wnt signaling. However, later studies have revealed a positive role of endocytosis in activating Wnt/β-catenin signaling, as clathrin, dynamin and Rab5 were each shown to be required for activation of this pathway in *Drosophila* and mouse L cells [306, 307].

Recent work has begun to shed a light on the mechanism behind endocytosis of the Wnt/Fz/LRP complex. This process follows a series of events including phosphorylation and trafficking of the complex to the appropriate endosomal compartment. After Wnt stimulation, CK1γ phosphorylates the LRP6 intracellular domain in a Dvl-dependent manner, which then recruits the negative regulator Axin [308-311]. Phosphorylation of LRP6 occurs at multiple conserved sites, notably at PPSXS motifs, where both Serine (or Threonine) residues are phosphorylated [282]. In addition to phosphorylation by the non-proline kinase CK1γ, phosphorylation of LRP6 is also carried out by proline-directed kinases GSK3, Protein kinase

A (PKA), Pftk members, and G protein-coupled receptor kinase (Grk5/6) [282]. Recent studies have shown that 15 minutes after Wnt stimulation, protein aggregates called LRP6 signalosomes are formed at and under the plasma membrane [311]. LRP6 signalosomes are made up of phospho-LRP6, Frizzled, Dvl, Axin and GSK3, and partially co-localize with caveolin, suggesting that caveolae-dependent endocytosis is at play in this context [311]. Once GSK3 is recruited to the cytoplasmic side of LRP6 signalosomes, it propagates Wnt signaling by phosphorylating LRP6 and other substrates such as Dvl, APC, Axin and β-catenin [312]. However, GSK3 activity must then be inhibited in order for β-catenin to accumulate in the cytoplasm. Therefore, GSK3 has paradoxical positive and negative effects in early and mid Wnt/β-catenin signaling [313]. To prevent phosphorylation of β-catenin by GSK3, GSK3-containing LRP6 signalosomes are sequestrated into multivesicular bodies, a process which leads to β-catenin stabilization (Figure 18) [103]. This isolates GSK3 from all cytoplasmic proteins and prevents GSK3-mediated phosphorylation of its substrates, including β-catenin. By avoiding phosphorylation by GSK3, β-catenin accumulates in the cytoplasm and translocates to the nucleus. Sequestration of the LRP6 signalosomes into MVBs depends upon at least two components of the ESCRT machinery, namely Hrs and Vps4 but other factors are also likely involved [103]. However, the inclusion of the ESCRT machinery in this process confirms the requirement for MVB formation as these proteins are essential in MVB formation. These recent advances have shed light onto the mechanism of Wnt/β-catenin signaling activation but many questions remain. For example, how are LRP6 signalosomes sorted at the early endosome and routed towards the MVBs? Answers to this and other questions will likely have important impacts on our understanding of Wnt signaling and Wnt-related illnesses.

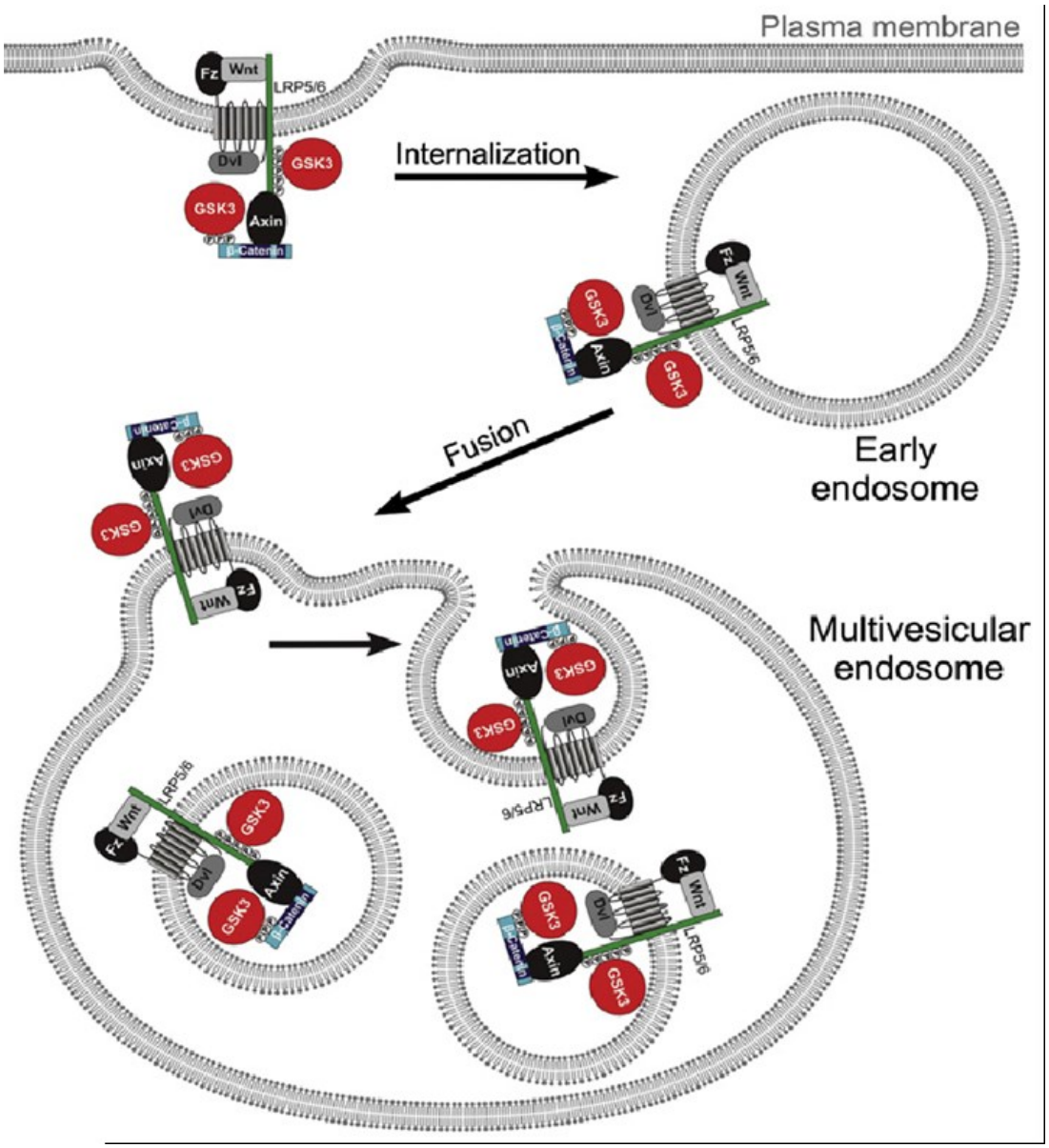

Figure 18. Model of Wnt-dependent sequestration of LRP6 signalosomes into multivesicular bodies during canonical Wnt signaling. Binding of GSK3 (red) to the Wnt receptor complex (including phosphor-LRP6, phosphor β-catenin, Dvl, Axin, and APC) sequesters GSK3 inside the intralumenal vesicles of MVBs. [103]

To continue on aspects of embryogenesis relevant to this work, we will now cover a post-gastrulation process called somitogenesis.

1.19 – Somitogenesis

The vertebrate body plan is segmented, a feature most clearly seen in the skeleton. Early during development (after gastrulation), the formation of epithelial blocks of mesoderm begins, a process called somitogenesis [314, 315]. Each somite gives rise to various mesoderm descendants: the ventral part of the somite, the sclerotome, gives rise to cartilage and bone of the vertebrae and ribs, whereas the dorsal side of the somite, the dermomyotome, contributes to the overlying dermis of the back and to the skeletal muscles of the body and limbs [316]. In amniotes like chicken and human, the somitic lineage is part of the paraxial (or presomitic) mesoderm (PSM) while in lower vertebrates such as fish and frog, it is part of the dorsal mesoderm [314]. During somitogenesis, somites progressively segments into bilaterally symmetrical epithelial somites, in an anterior to posterior direction (Figure 19). As somites emerge from the anterior end of the PSM, proliferating cells in the primitive streak replenish the posterior PSM [314]. Soon after their formation, somites subdivide into the sclerotome, and dermomyotome.

Somitogenesis is controlled by a molecular periodicity acting in PSM cells, which has been termed the “segmentation clock” [314]. Although this segmentation clock and the major signaling pathways involved are evolutionarily conserved, some characteristics are species-

specific, such as the periodicity and final number of somites. For example, the rhythm of somite production in zebrafish is around 30 minutes while in mammals it can take up to several hours (4-5 hours in humans) [317]. This periodicity of gene expression in vertebrates was first illustrated by the rhythmic expression of the *HES1* (hairy and enhancer of split-related 1) mRNA in the chick embryo PSM [318]. The transcriptional oscillations of *c-hairy* occurred with the same periodicity as the somitogenesis process and were the basis upon which the clock model was built. Subsequently, studies in fish, frog and mouse identified several other genes (the vast majority belonging to the Notch, Wnt and FGF signaling pathways), which exhibit the same periodicity and indicate an evolutionarily conserved mechanism in vertebrates [318-323] .

Notch signaling is required for synchronization of the oscillations among neighbouring cells [317]. Among the downstream targets of Notch signaling are *HES1* as well as the notch ligand *Delta*. In zebrafish, mutations in Notch signaling suppress the cyclic gene expression pattern, which is rather replaced by a salt-and-pepper expression pattern [324, 325]. In these mutants, the first somites segment normally, suggesting that oscillations are set initially. However, owing to the lack of Notch-dependent coupling, segmentation progressively drifts out of synchrony, resulting in segmentation failure. The current models holds that oscillations in expression are generated and maintained through negative feedback loops driven by unstable negative regulators of this pathway, such as *Her1* and *Her7* (zebrafish homologues of *HES1*) [326, 327]. In other words, activation of Notch results in the expression of both *Delta* and *Her1*. As Delta ensures the transmission of Notch signaling to adjacent cells, *Her1-Her7* simultaneously inhibits additional expression of both itself and *Delta*. Therefore, *Her1-Her7* ensure that Notch signaling only last for a short period of time. Of note, the *Her1-Her7* oscillator also requires the *Her13.2* partner, which is downstream of FGF signaling [314].

In amniotes like the mouse, a similar mechanism of synchronism exists but involves additional genes. Here, FGF and Notch signaling induce expression of Notch inhibitors (like *Lfng* (lunatic fringe) and the *HES* genes) and Notch ligand, which ensure the transmission of Notch signaling to adjacent cells as well as the activation of a negative feedback loop, similar to the Her-based loop in zebrafish [314]. However, Wnt signaling is also involved in synchronizing the clock cycle in the mouse. Interestingly, Wnt signaling oscillates in opposite phase to the cyclic genes products of Notch and FGF signaling. Downstream Wnt targets include the several negative feedback inhibitors of the pathway, such as *Dkk1* [323]. The complex epistatic relationships and multiple crosstalks between the Notch, FGF and Wnt signaling pathways makes it challenging to determine their respective contributions to the molecular circuitry responsible for generating the oscillations, i.e. “the segmentation clock pacemaker”. Future work will be needed to produce a working model of these relationships and will most.

As much as the signaling pathways involved in somitogenesis and cardiogenesis are important for the changes in gene expression and cellular identity, the underlying mechanisms that regulate each signaling pathway, such as receptor trafficking, are also essential. However, this aspect of cellular signaling adds an additional layer of complexity to an already complex model. The unification of cell culture and developmental studies will require precise characterization of gene function on both levels. Therefore, simple and well-characterized models are essential in helping further our understanding of complex developmental processes. One such model organism is the African clawed frog, *Xenopus laevis*.

1.20 – Model organism: Xenopus laevis

Historically, *X. laevis* embryos, were used for studying early embryogenesis whereas later events of were not examined due to technical limitations. *X. laevis* was favoured as a model organism for early embryogenesis because of the ease at which microinjections of mRNAs in specific cleavage-stage cells could be done for both gain and loss-of-function experiments. The steps of *X. laevis* embryogenesis are well-characterized and share many genetic and anatomic similarities with other vertebrates, including humans. Today, studies using *X. laevis* have yielded many insights into how vertebrate development is controlled from heart and liver organogenesis to the development of the skeleton and central nervous system. In particular, cardiac defects can be extensively analyzed in living embryos since early embryogenesis can proceed in the absence of a functional circulation system, a process that takes approximately 3.5 days and is complete at 80 hours post-fertilization (hpf) (Stage 42). Work by Nieuwkoop and Faber (1994) describing each stage of development, from the first cell division to the formation of adult morphology has helped immensely in providing a standard by which to stage-characterize Xenopus embryos. A single female can be induced to lay thousands of eggs year-round, which quickly develop externally in an aqueous solution. Embryos are relatively large and exhibit a remarkable ability to recover from microsurgery. In addition, Xenbase (www.xenbase.org) is a useful and community-oriented online resource where information on *Xenopus* developmental biology, genetics and experimental procedures can be obtained.

The eggs laid by a female are fertilized using sperm extracted from the male testis, which must be dissected due to their internal localization. The zygote develops through multiple cell divisions and eventually generates a large mass of cells, called the blastula, at 4 to 5 hours

post fertilization (Stage 7-8). Gastrulation commences quickly after (Stage 10, 9 hpf), and the blastopore become discernible. This circular opening eventually closes shut at around 16 hpf (Stage 14), which marks the end of gastrulation, and the beginning of neurulation. The neural plate becomes progressively more prominent on the dorsal side of the embryo. From stage 14 to 26 (30 hpf), the embryo undergoes extensive cell rearrangements and starts to show many recognizable features of a tadpole (ex: head, body and tail). The transformation of the embryo from a spherical to an elongated shape is the result of convergent extension along the anterior-posterior body axis. During this process, mediolateral intercalation of cells in the neural plate and underlying mesoderm simultaneously squeezes the blastopore shut and closes the neural tube. Following neural tube closure, organs such as the brain, heart and eyes start to develop. At stage 42 (80 hpf), most major organs have developed and are now functional.

A common tool for studying gene function in *X. laevis* is by morpholino-induced gene knockdown. Morpholinos oligos (MO) are short chains of about 25 antisense morpholino subunits offered commercially by GeneTools, LLC. Each morpholino subunit is comprised of a nucleic acid base, a morpholine ring and a non-ionic phosphorodiamidate intersubunit linkage. By binding with high affinity to mRNA, they block translation initiation through a steric blocking mechanism. Unlike RNA, morpholinos do not degrade and are therefore functional inside the embryo until multiple cell divisions lowers their concentration within each cell and renders them ineffective. Through the use of microinjections, specific amounts of MO can be injected into a fertilized zygote or into specific cells of which the descendants are known.

Despite these advantages, certain limitations do exist when studying Xenopus development. For example, micro-injections do not persist in the embryo for more than a few days, making it unrealistic to manipulate gene functions in later stages of development.

Therefore, exploiting the characteristics of multiple models (both *in vivo* and *in vitro*) may be most beneficial in understanding the role of any gene. Through the study of developmental process in *Xenopus laevis* and of their associated signaling pathways in cell culture models, we will better understand the underlying mechanisms that regulate the many steps of embryogenesis. In turn, this understanding may lead to improved detection and treatment of human diseases.

1.21 – Disorders related to endosomes and sorting nexins

Since protein degradation is such an important aspect of cellular biology, it is not surprising to find that dysregulation in this process can have deleterious effects. Inheritable lysosomal storage diseases are an example of this and have been classified according to the stored substance (ex: sphingolipidoses, mucopolysaccharidoses, mucolipidoses, glycoprotein and glycogen synthase storage diseases) [328]. Under pathological conditions, these substances are enzyme substrates that accumulate inside the cell, which is manifest most commonly by neurodegeneration [329]. Among the lysosomal storage diseases, a few have been approved for enzyme replacement therapy (ERT) but obstacles to this therapy remain, including immune reactions against the infused enzyme, mistargeting of enzymes to organelles other than lysosomes, and intractable tissues. Mutations in various sorting nexins have also been linked to disease. Snx10 is involved in osteoclast formation and resorption activity and has been associated with osteopetrosis [164, 165]. Snx31 has been identified as a new gene possibly

linked to melanoma [330]. Finally, in addition to its role in Wnt secretion (which is likely relevant in Wnt-associated diseases), Snx3 could be involved in erythropoiesis and disorders of iron metabolism due to its regulation on transferrin receptor trafficking [331]

1.22 – Wnt/β-catenin signaling and disease

The link between Wnt/β-catenin signaling and cancer has been known since the discovery of the gene *int-1* as a mammary oncogene in mice [332, 333]. Additional support for this came from the finding that ~85% of colorectal cancers have an inactivated APC gene, leading to constitutive nuclear localization of β-catenin [334-336]. Often, dysregulation of Wnt/β-catenin signaling is observed in tumours and hematologic malignancies without any mutations in the coding regions of the respective genes. For example, epigenetic silencing of Wnt antagonists like the SFRPs has been shown in colon, breast, prostate and lung cancers [337-341]. Increased expression of Wnt ligands and dishevelled have also been described for many cancer types [342-345]. Even though elevated Wnt/β-catenin signaling may suggest poor prognosis for patients with cancer, this is not always the case. For example, in melanoma, high Wnt/β-catenin signaling is associated with lower proliferative index and correlates with a more favorable prognosis for patients [346-349]. This is explained by the fact that elevated β-catenin in melanoma promotes expression of MITF, which itself drives differentiation toward a melanocyte-like fate and reduces cell movements [350, 351]. Better prognosis is also associated with increased Wnt/β-catenin signaling in patients in at least some stages of

prostate, ovarian and colorectal cancers [352-354]. In some mouse models, activation of Wnt/β-catenin signaling appears to function as a tumour suppressor. For example, inhibition of Wnt in human mesenchymal stem cells leads to high-grade sarcoma formation in nude mice [355]. In some cancers, such as in mouse models of pancreatic ductal adenocarcinoma (PDAC), overexpression of constitutively active β-catenin can arrest transformation, resulting in the formation of a much more benign tumour type [356, 357]. In addition to cancer, Wnt signaling is implicated in neurological and autoimmune diseases, and inflammation [358]. Both schizophrenia and Alzheimer's disease have also been associated with aberrant Wnt/β-catenin signaling [359-361].

Interestingly, a mutation in the N-terminal region of Snx4 (upstream from the PX domain) was found in the primary tumour of lobular breast cancer (oestrogen-receptor-positive) [362]. This mutation, along with five other mutations, was also prevalent 9 years later after analysis of metastatic lobular breast cancer tumours. This is yet another important finding that suggests essential roles for SNX-BARs in regulating major signaling pathways involved in cellular proliferation and differentiation.

Chapter 2: Journal article #1 (submitted to the Journal of Biological Chemistry)

SNX11 associates with PtdIns(3)P and regulates actin-dependent and –independent trafficking

Michel Cameron[1], Séverine Leclerc[1], Iness Charfi[1], Kathleen Riopel[1], Tang Zhu[1], Mohammad Amrei[1], D. Woodrow Benson[2], Sylvain Chemtob[1], Graciela Pineyro[1], Gregor Andelfinger[1]

[1] From Génétique Cardiovasculaire, CHU Sainte-Justine, Departments of Pediatrics and Biochemistry, University of Montréal
[2] Children's Hospital of Wisconsin

*Running title: Functional characterization of SNX11

Keywords: sorting nexins, actin polymerization, receptor trafficking

Background: Sorting nexins (SNXs) without a BAR (Bin-Amphiphysin-Rvs) domain remain largely uncharacterized.

Results: SNX11 regulates somitogenesis, actin polymerization and PI3-kinase dependent receptor recycling.

Conclusion: SNX11 functions in actin-dependent and –independent processes.

Significance: A functional description of each sorting nexin will provide a better understanding of how endosomal sorting integrates into developmental processes.

ABSTRACT

Proteins of the sorting nexin family are involved in processes that regulate endosomal protein sorting of diverse cargo through their association with membranes and cargo-binding protein complexes that move along filamentous paths. After identification of Snx11 as a positional candidate gene for canine tricuspid valve malformation, we set out to functionally characterize SNX11 in vitro, in cell culture and Xenopus knockdowns. We found that SNX11 physically and functionally interacts with many of cytoskeletal proteins, including actin. SNX11 was widely expressed in adult mouse tissues. We show a functional role for SNX11 in actin nucleation, somite development and receptor trafficking. We propose SNX11 as a functional candidate for competitive interaction with other SNX family members.

The sorting nexin (SNX) family of proteins includes 33 members implicated in a wide variety of intracellular sorting and trafficking events (1-3). Their PHOX-homology (SNX-PX) domain associates with phosphatidylinositol-phosphates (PIPs), enriched in specific regions of endosomal membranes where sorting events occur (4). Three sorting nexin subfamilies were determine by domain architecture and include SNX that only contain an isolated SNX-PX domain (SNXPX), those containing a C-terminal BAR (Bin-Amphyphysin-Rvs) domain (SNXBAR), and SNXs that contain another recognized domains in addition to the SNX-PX domain (SNXPX-other), and (5). Early work on SNXs focused on their role in the retrograde transport of the cation-independent mannose-6-phosphate receptor (CI-M6PR), which maintains an active pool of hydrolase receptors in the trans-Golgi network (3,6). The mammalian pentaheteromeric retromer is composed of a SNX-BAR dimer and a cargo-recognition complex (VPS26-VPS29-VPS35). The BAR domain of SNX-BARs is a banana-shaped C-terminal domain that dimerizes and induces and/or senses membrane deformation such as tubulation (7). Following the identification of SNX11 as a positional candidate gene for canine tricuspid valve malformation, we set out to characterize this SNXPX, of which many members remains poorly characterized (8).

Two phylogenetic relatives of SNX11, namely SNX3 and SNX10, have recently been investigated. In the mouse, loss of SNX3 in leads to anemia due to defective recycling of the transferrin receptor (9) while earlier studies described a critical role for SNX3 in the secretion of the Wnt ligand (2,10). Homozygous recessive mutations of human SNX10 cause early-onset osteoporosis, corroborating previous findings in which SNX10 is required for osteoclast formation and resorption activity (11,12). These studies reveal the functional diversity that SNXPX can play across multiple signaling pathways.

The goal of this study was to clarify the function of SNX11 by in vivo and in vitro methods. We first investigated SNX11's expression profiles in mice and then analyzed the functional role during embryogenesis. We provide evidence that this ubiquitously expressed protein is involved in somitogenesis and interacts with proteins involved in actin organization. We also show that SNX11 can regulate recycling of the delta opioid receptor (DOR). The ability of SNX11 to simultaneously bind specific phospholipids and proteins suggests that it is an organizer of the coupling between membrane and cytoskeletal proteins in the mammalian cell.

EXPERIMENTAL PROCEDURES

Plasmid construction-RNA was extracted from newborn mouse hearts using Trizol according to manufacturer's instructions (Invitrogen) and cDNA were synthesized with oligodT primers and SuperScript Reverse Transcriptase (Invitrogen). The full-length murine SNX11 was amplified from cDNA by PCR and cloned into pCR2.1 vector (TA cloning kit; Invitrogen). Two clones with different restriction enzyme digest fingerprints were chosen for sequencing and further analysis. The isoforms were named SNX11a (long) and SNX11b (short) based on length.The sequences were cloned in pBluescript II sk(-)into HindIII and XbaI sites. The human pCMV-sport6-SNX11 was from Open Biosystems.

The full length isoform SNX11 A was amplified by PCR and cloned into pEGFP-N1 (XhoI and HindIII).

Bacterial expression plasmids were generated by insertion of respective full-length or truncated SNX11 fragment into pGEX-4-T1 or pET30a (Figure 3A).

shRNA-SNX11 was from Open Biosystems (confirm clone ID: RHS127684).

Cell culture, transfection and establishment of HEK293T_SNX11-GFP cell line-HEK293T cells were cultured at 37ºC in the presence of 5% CO2 in Dulbecco's modified Eagle medium (DMEM, Wisent) supplemented with 10% FBS, 100 u/mL penicillin and 100µg/mL streptomycin. Cells were seeded a day before in 12 wells plate at 100,000 cells par well. 1-2µg DNA (pEGFP-SNX11 A) and 16µg of polyethylenimine 1 mg/ml (PEI, Sigma) in basic DMEM without FBS and antibiotics were mixed and incubate for 15 minutes before transfected the cells. This mix was added to the cells and incubated for 4-5 hours at 37ºC in the presence of 5% CO2 before changing with completed DMEM. Establishment of the stable cell line, HEK293T_SNX11-GFP was done by selection for the transfected plasmid with 400µg/mL G418 (Wisent).

Murine cDNA and PCR- Total murine RNA was extracted with TRIzol reagent (Invitrogen) from dissected tissues. cDNA was synthesized with Superscript II reverse transcriptase (Life technologies). Murine Snx11 (F: CGTCAAGGTCTCCAGCATTTCC; R: CGCCCTGATCTTGGAAGAAAGC) and GAPDH (F: AAGATGGTGATGGGCTTCCCG; R: TGGCAAAGTGGAGATTGTTGCC) were amplified by PCR.

Antibodies-SNX11 was detected by immunochemistry with a goat anti-SNX11 antibody (Novus Biological). For its detection by western blotting and immunofluorescence, a rabbit polyclonal SNX11 antibody was produced with the following antigen sequenced CGWAQEERQSTSHLAKGDQ by Open Biosystems.

For EEA1, Mannose-6-phosphate, LAMP1, we used antibodies from Abcam. Golgi tracker, mitochondria tracker and ER tracker, AlexaFluor 594 and 488 were purchased from Molecular probes. The GST tagged proteins and Flag tagged proteins were respectively detected with a

monoclonal mouse anti-glutathione-S-transferase (Sigma) and a monoclonal mouse anti-flag M1(Sigma). A polyclonal anti-GFP (Santa-Cruz) was used to amplify the GFP detection in some immunofluorescence experiments.

Anti-ITM2A, -cathepsin L (ctsl) and -tubulin-α (sc-12462) were purchased from Santa Cruz Biotechnology, Inc., anti-Na+/K+ ATP1B1 was from Millipore upstate, anti-phalloidin was from Sigma (P1951), and LASP-1 was detected with a monoclonal mouse antibody (Chemicon International).

SDS-PAGE and Western blotting-The tissues from rat and mouse organs were homogenized in RIPA buffer (Tris-HCl 50 mM, pH 7.4, 1% Igepal CA-630, 0.25% Na-deoxycholate, 150 mM NaCl, 1 mM EDTA). After centrifugation, the supernatant was quantified with bicinchoninic acid and 25 µg/µl of proteins were solubilized in Laemmli buffer. Proteins were separated by sodium dodecyl sulfate polyacrylamide gel electrophoresis and transferred to nitrocellulose by standard methods. The blots were probes with an affinity purified anti-SNX11 antibody (dilute 1/400) and peroxydase conjugated anti-rabbit antibodies (Biorad) followed by Super signal West Femto (Thermo Scientific). The autoradiography was made with a hope Micromax X-ray film processor.

Immunohistology-Tissue from rat (kidney, heart, vasculature, skin, uterus, liver and lung) and human tissues were fixed in paraformaldehyde 4%, embedded in paraffin and cut in sections of 5 µm. Antigen retrieval was processed by incubating the slides in 0.01M sodium citrate for 20 min at 68ºC. Then, the Vectastain ABC kit (Vector laboratories) was used to stain SNX11 according to the manufacturer instructions. The goat polyclonal anti-SNX11 antibody (Novus biological) concentration was 2.5 µg/mL. The slides were counterstained with methyl green.

Immunofluorescence of SNX11 in HEK293T_SNX11-GFP cells-HEK293T_SNX11-GFP cells were grown on collagen-coated coverslip. Cells were starved at 37ºC/5% CO2, washed with PBS and fixed with methanol for 10 minutes at room temperature. Image-iTFX signal enhancer (Invitrogen) was added for 30 minutes before blocking in PBS/5%BSA. Cells were then incubated with anti-EEA1 (2.5 µg/mL), anti-LAMP1 (1 µg/mL), anti-Mannose-6-phosphate receptor (2 µg/mL), anti-ATP1B1, anti-cathepsin L (CTSL), anti-LASP1 (1 µg/mL), or anti-ITM2A (1µg/mL) antibodies in PBS/1%BSA for 1h at room temperature. After washing with PBS, the slides were incubated 1h at room temperature with AlexaFluor 594 secondary antibodies (2 µg/mL). Cells were also incubated with an anti-GFP antibody (1 µg/mL) for 1h at room temperature. After washes with PBS, the cells are incubated with an AlexaFluor 488 secondary antibody. The coverslip were mounted on slides with Prolong antifade reagent (Invitrogen).

For live staining of the Golgi apparatus and mitochondria, HEK293T_SNX11-GFP cells were starved during 4h at 37ºC/5% CO2 and incubated with Golgi- (0.25 µM), ER- (0.5 µM) and mito-trackers (0.5 µM) (Molecular Probes) for 15 min at 37ºC in the presence of 5% CO2 according to the manufacturer's instructions. Cells were then washed with PBS and fixed with paraformaldehyde 4% for 15 minutes.

Optiprep subcellular fractionation-Two 15-cm culture dishes of HEK293T_SNX11-GFP cells were starved with DMEM medium containing 100U/mL penicillin and 100mg/mL streptomycin (without FBS) for overnight. In the next day the cells reached to 100% confluent and were harvested in a 50-ml tube and centrifuged at 1500 rpm for 10 min. The cells were washed with cold PBS and suspended in 0.8ml Homogenization Buffer (0.25M Sucrose, 25mM KCl, 5mM MgCl2, 20mM Tris-HCl, pH7.4 and 1 x protease inhibitor cocktail complex). The cells were then

homogenized by 12 gently strokes to pass through a 25-gauge needle on ice. The post-nuclear supernatant (PNS) fraction was obtained by centrifugation of the homogenate at 700 x g at 4oC for 10 min.

An OptiPrep (Sigma) gradient was prepared in a 16 x 96mm Ultra-Clear Centrifuge Tube (Beckman), which contains 2ml of 2.5%, 3.5ml of 10%, 3.5ml of 20%, and 3.5ml of 30% OptiPrep. The prepared PNS fraction (about 0.9ml) was mixed with 2.1ml 50% OptiPrep to get 35% OptiPrep concentration and loaded on the bottom of the gradient OptiPrep tube. After ultracentrifugation at 130,000 x g at 4oC for 22 hours, the OptiPrep was separated into 12 fractions (each contains 1.3ml OptiPrep) from heavy to light density order.

To identify the subcellular fraction, each 20ul of the fractions were separated by an 8% SDS-PAGE (for EEA1) or 12% SDS-PAGE (for RAB9A) for immunoblot analysis. The early endosome fraction was identified with rabbit polyclonal EEA1 antibody (Santa Cruz), and the late endosome fraction was proved by mouse monoclonal RAB9A antibody (Santa Cruz), SNX11 was dectected with the rabbit antibody purchase from Open Biosystem.

Yeast two-hybrid screen-A yeast-two hybrid (Y2H) screen was performed according to instructions of the manufacturer (MatchMaker GAL4 Two-hybrid System 3, Clontech, Palo Alto, CA, USA). The newly cloned isoform of SNX11, SNX11 B, was cloned full-length as bait into pGBKT7 downstream of the sequence for the DNA-binding domain of GAL4 and transformed into AH109 competent yeast cells. A lack of protein toxicity or transcriptional activation in AH109 cells was assayed in culture and protein expression confirmed by western blot using an anti-c-Myc antibody. Transformed AH109 cells were mated with strain Y187 yeast pre-transformed with a Matchmaker 17 day mouse embryo library (Clontech). Diploid yeast were

assayed on SD/-Leu, SD/-Trp, and SD/-Leu/-Trp media for mating efficiency and selected for bait/prey interactions on SD/-Ade/-His/-Leu/-Trp/X-□-Gal media (high-stringency). Positive, blue colonies were scored for growth, confirmed by 2 replica plating on high stringency media, and selected for plasmid isolation in library-specific antibiotic broth. 360 activation domain/library inserts were amplified by PCR, run on agarose gels to eliminate clones containing multiple library plasmids, and fingerprinted by HaeIII digestion to eliminate duplicate clones. Selected PCR products were sequenced to determine interacting prey protein identity. A comprehensive table of prey clones identified in this screen is appended (Table 1).

GST pull-down-In order to confirm the interactions of SNX11 B with 10 prey clones of interest were re-transformed into DH5□ bacterial cells and their protein interaction with SNX11 B confirmed by GST pull-down assay (MagneGST, Promega).

Bacterial protein expression and purification-BL21-Gold (DE3) Competent Cells (Stratagene) were transformed with either GST or his-clones according to the manufacturer instructions. Bacteria were grown over-night at 37 ºC with agitation. A dilution 1/50 of this pre-culture was grown 2h in LB medium before the induction of target protein with 0.1 or 0.5 mM of Isopropyl ß-D-thiogalactopyranoside (IPTG) for 3h. The bacteria were harvest and centrifuge 10 min at 4000 rpm. The induction was confirmed in gel electrophoresis and staining with Coomassie blue for GST-tagged proteins and in western blotting with a his probe (Santa Cruz) for the his-tagged proteins (data not shown).

The GST-tagged proteins were purified with MagneGST Protein Purification System according to Promega instructions.

The His-tagged proteins were purified with the Ni-NTA column (Qiagen) according to the manufacturer instructions.

Lipid overlay assay-PIP strip (Echelon Biosciences Inc.) were blocked with 5% non-fat dry milk in TTBS (20 mM Tris-base, 150 mM NaCl, 0.1% tween 20) overnight at 4ºC. The PIP strips were incubated with the purified GST-protein for 1h at room temperature. After washes in TTBS, they were incubated with GST antibody (4.5 µg/mL). The PIP-strip were washed and incubated with a anti-mouse HRP conjugated antibody (40 ng/mL, Bio-Rad). The detection was processed with ECL plus (Perkin Elmer). The autoradiography was made with a hope Micromax X-ray film processor.

Morpholino knockdown of Xenopus SNX11-Female Xenopus laevis were primed with 50 IU of pregnant mare serum gonadotropin (PMSG) 2 to 4 days before injection of 500-800 IU human chorionic gonadotropin (hCG) on the evening before egg collection. Nine to 12 hours after injection, eggs were collected and transferred into a fresh petri dish with Marc's Modified Ringers (MMR, 0.1M NaCl, 2mM KCl, 1mM MgSO4, 2 mM CaCl2, 5 mM HEPES (pH 7.8), 0.1 mM EDTA). The eggs were fertilized in vitro with male frog testis and de-jellied by soaking them for 5-15 min in 2-3% L-Cysteine, pH8. Staging of embryos was performed according to Nieuwkoop and Faber (13). The eggs were injected with different concentration of morpholino.

Antisense morpholino oligonucleotides were designed by Gene Tools, LLC. The antisense morpholino was designed to the translation start. Morpholinos were injected into the dorsal animal blastomeres at the 1 and 2-cell stages. The injections were confirmed by monitoring fluorescence from labeled oligonucleotides. The morpholinos used were Snx11 utr- 5′-CTGAGCCGGGATTATCCTGAGACA-3'-fluorescein. The specificity of the morpholinos was

tested in western blot with the SNX11 antibody produced by Open Biosystems. Rescue injections were carried out with capped mRNA as previously described (14).

Actin polymerization-For this assay, we used the actin polymerization biochem kit (Cytoskeleton). The pyrene labeled muscle actin was resuspended with general actin buffer (5 mM Tris pH 8, 0.2 mM CaCl2) supplemented with 0.2 mM ATP and 1 mM DTT and left on ice for 1h to depolymerise actin oligomers. The residual nucleating centers were remove by centrifugation at 14,000 rpm at 4ºC for 30 min. The Arp2/3 was diluted to 0.3 mg/mL in G-buffer and kept on ice. The VCA domain protein was resuspended to 1 mg/mL by adding 500µl of milli-Q water. Just before use, the pyrene labeled actin was diluted to 0.1 mg/mL in ice-cold general actin buffer supplemented with 0.2 mM ATP and 1 mM DTT. According to the wells, 5 µl of VCA 1 mg/mL, 2 µl Arp2/3 complex 0.3 mg/mL, 200 µl polymerization buffer (5 mM Tris pH 7.5, 50 mM KCl, 2 mM MgCl2, 0.1 mM CaCl2, 1 mM EGTA, 0.5 mM DTT, 0.2mM ATP) and 1 µM his-tagged proteins (or 0.5 µM for his-SNX11A + 0.5 µM his-lasp1) were added. Actin polymerization was followed by the increase in fluorescence emission from 410 nm +/- 20 nm over 60 min period at room temperature (ecitation wavelength 355 +/- 20 nm) on an Envision microplate reader (Perkin Elmer)

DOR recycling-Recycling of internalized receptors to the plasma membrane was estimated using an ELISA-based method adapted from a previously published protocol (PMID: 18363847). HEK293T cells stably expressing Flag-DOR were seeded at a density of 200,000 cells/well and grown on 24-well polylysine-coated plates for 48 h. For SNX11 experiments, HEK293T cells were transfected 24 h after plating either with 8µg Flag-DOR or 4µg Flag-DOR and 6µg shRNA SNX11, which ensured similar membrane expression of Flag-DORs in both conditions. The experiment was carried out 48h post transfection. The day of the experiment,

one hour preceding induction with a single dose of DPDPE (1 μM; 30 min), protein synthesis was blocked with 10 μM cycloheximide that remained present throughout the duration of the assay. At the end of the internalization period, the agonist was removed by washing with DMEM at 37°C (3 × 1 min). Cells were then placed within the incubator to recover in an agonist-free medium (DMEM/HEPES/cycloheximide containing vehicle, cytochalasin (10μM), nocodazole (10μM), wortmannin (10nM) or BEZ235 (10nM)) for increasing periods of time. Experiments were stopped by addition of cold PBS, and cells were subsequently fixed for 15 min at 4°C in paraformaldehyde (3%) and nonspecific binding was blocked by incubation with PBS/BSA 1%/CaCl2 1 mM at room temperature (RT) for 30 min. Cells were subsequently incubated with anti-FLAG M1 antibody (1:1000; Sigma-Aldrich) for 1 h (RT), washed three times, and incubated with peroxidase-conjugated (HRP) anti-mouse antibody (1:8000; GE Healthcare) for 30 min. After extensive washing, 200 μl of the HRP substrate o-phenylenediamine dihydrochloride (SIGMA FAST OPD, Sigma-Aldrich) was added to each well. The reaction was allowed to proceed for 8 min and stopped using 50 μl of 3N HCl. Two-hundred microliters of the mix were then transferred to a 96-well plate for optical density (OD) evaluation at 492 nm in a microplate reader (Victor3; PerkinElmer). OD readings corresponded to the signal generated by receptors at the cell surface. The amount of surface receptors internalized following exposure to agonists was calculated by subtracting OD obtained in the presence of agonist from the one obtained in its absence. Results were expressed as percentage of receptors initially present at the membrane according to the following calculation: 100 × (ODBasal −ODStimulated)/(ODBasal) where ODBasal and ODStimulated correspond to the signal obtained in absence or presence of agonist respectively.The amount of internalized receptors that recycled back to the surface was expressed as percentage of receptors internalized following exposure to the agonist.

Mutation screening of SNX11-Patients with Ehlers-Danlos (ED) syndrome negative for disease-causing mutations in known ED genes were identified from a database at the Shriner's Hospital in Montreal, QC. Informed consent was obtained from the parents, legal guardians, or patients, respectively. The study was approved by the Institutional Review Boards at all participating institutions.

RESULTS

SNX11 homology, and murine and human expression-Sorting nexin 11 (2333 bp, gene accession: AF121861) encodes a protein (264aa, predicted molecular weight 30 kDa) with a single conserved N-terminal PX domain (aa 8-123) and two low complexity domains (aa 179-192 and 207-224) at the C-terminal end, as predicted by the Simple Modular Architecture Research Tool (SMART) (Figure 1A) (15,16). Compared to hSNX11, the predicted mouse (isoform a) and Xenopus proteins share 85% (PX domain: 99%) and 69% (PX domain: 95%) sequence identity, respectively. Although human and mouse sequence are very similar, Xenopus Snx11 is shorter in length (165aa) and lacks the C-terminal low complexity domains. Based on protein sequence alignment, the closest phylogenetic relative of human SNX11 is SNX10, which shares 83% sequence identity (PX domain: 86%) but also lacks the second low complexity domain (Figure 1A). Cloning of the murine full-length open reading frame from mouse heart cDNA revealed the presence of a shorter murine Snx11 isoform (isoform b) arising from the exonization of an Alu-repeat element. Isoform b is identical to ENSMUST00000127375 and predicted to be 197aa in length, identical with the long isoform (isoform a) up to aa180 (predicted molecular weight 22 kD) (Figure 1A).

SNX11 was widely expressed across adult tissue derived from all three germ layers with strongest expression in brain, skeletal muscle, spleen, lung and testis (Figure 1B). In accordance, immunohistochemical staining of SNX11 in adult human tissues revealed widespread expression, as shown by staining in the kidneys and cartilage (Figure 2A-E, M). Likewise, expression of SNX11 was also prevalent in diverse tissues as shown by staining in heart, vessels, skin, uterus, liver, and lungs (Figure 2F-L). In human kidneys, SNX11 was most strongly expressed in the podocytes, distal tubules and glomerular cells (Figure 2A-E). In rat heart, SNX11 was found in the fibrous skeleton and valvular tissue of the heart (Figure 2F, G). Moreover, the staining was more intense in the mitral tissue as compared to the tricuspid tissue (Figure 2G). In human cartilage, SNX11 was highly expressed in the chondrocytes of the superficial zone (Figure 2M).

SNX11 associates with PtdIns(3)P-To assess the lipid-binding properties of SNX11, we performed a lipid overlay assay using lipid blots (PIP-strips). Full length SNX11 (isoforms a and b) associated with PtdIns(3)P, but truncated versions of SNX11 were unable to associate with any phospholipid (Figure 3B), demonstrating that alone, the PX domain of SNX11 (aa14-132) is insufficient for PtdIns(3)P binding. Thus, the two C-terminal alpha-helices (coiled-coil domains) are required for lipid-binding, consistent with previous results of protein crystallography defining an extended PHOX-domain for SNX11 (17).

SNX11 localizes to the Golgi and late endosomes-To better understand the role of Snx11 and its interaction partners, we examined its intracellular localization. We transfected HEK293T cells with a GFP-tagged Snx11 construct (Snx11-GFP) and examined its expression profile by confocal microscopy. Snx11-GFP protein was mainly visible as punctate, vesicular structures throughout the cytoplasm (Figure 4A-G). We stained transfected cells with antibodies against

early endosome antigen-1 (EEA1, early endosomes), lysosomal-associated membrane protein 1 (LAMP1, lysosomes), RAB9 (late endosomes), M6PR (late endosomes), as well as with Golgi-, mitochondria- and endoplasmic reticulum-trackers. We found that Snx11 co-localized most strongly with markers of late endosomes (Figure 4A, G), and of the Golgi (Figure 4C) but little with EEA1 and other compartments (lysosome, mitochondria, endoplasmic reticulum) (Figure 4B, D-F). The presence of Snx11 in endosomes was evaluated by Western blot using subcellular fractions of cell lysates. After subcellular fractionation by gradient separation, some Snx11 was found in the fraction corresponding to early endosomes but it was mostly seen in late endosomal fractions (Figure 4H).

Knockdown of Snx11 in Xenopus laevis causes aberrant somitogenesis-To further characterize Snx11 functions, we investigated the effect of morpholino-induced knockdown of this gene during Xenopus laevis embryogenesis. We designed our morpholino to the translation start site and confirmed its ability to block translation of Xenopus Snx11 by Western blot (Figure 5H). Morphants had short tails with a deformation of the dorsal axis and disorganization of the somites. This disorganization was confirmed by histology and electron microscopy (Figure 5A-G). In Snx11MO-treated embryos somite boundaries were formed but disorganized, displaying incomplete development and a lack of regularity between somites. Also, knockdown embryos had large seemingly undifferentiated fibroblastic areas (5E'). The penetrance of this phenotype was low, as only 20-30% of SNX11MO-injected embryos were abnormal compared to 10% in injected controls and efficiently rescued with cDNA injections (data not shown).

SNX11 interacts with cytoskeleton proteins-In numerous SNXs, sorting events are accomplished through the formation of multimeric protein complexes. To better understand the function of SNX11, we screened for interacting partners using the yeast two-hybrid system.

Many of the positive isolates identified belong to the cytoskeleton (i.e, contractile apparatus, and extracellular matrix) as well as nuclear/perinuclear proteins (involved in DNA repair, transcription and translation), and are associated with many types of human diseases (Table 1). In accordance with these interactions, SNX11-GFP was found to co-localize with LASP1, CTSL, ITM2a and ATP1B1 in HEK293T cells (Figure 6A-D).

Snx11 promotes actin polymerization-The identification of several components of the cytoskeleton in our yeast two-hybrid screen, we tested the effect of Snx11 on actin polymerization over time. The baseline values for this assay were first determined using the nucleation-promoting factors, Arp2/3 and VCA, alone and in combination. As expected, we observed an increase in steady-state and equilibrium values when adding Arp2/3, VCA or Arp2/3-VCA (except for the slightly lower steady-state value of VCA alone). Interestingly, SNX11 alone or in combination with these enhancers increases both the steady-state and equilibrium values of this assay (Figure 7), pointing for an actin-nucleation promoting effect.

SNX11 is involved in trafficking of the delta-opioid receptor-Given the known role of other SNX-PX in receptor trafficking (PMID: 23416069), we set out to determine whether Snx11 is involved in receptor recycling. We used the delta-Opioid receptor (DOR) as a proxy to investigate the role of Snx11 in receptor recycling, since this receptor is known to traffic to late endosomes (18). Cells expressing the DOR were transfected with either non-silencing (negative control) or Snx11 shRNA and stimulated with DPDPE. Knockdown of SNX11 in shRNA-Snx11-treated cells was confirmed by Western blot. In unstimulated cells, the DOR remained at the plasma membrane. Following removal of the agonist DPDPE, we observed increased recycling of the DOR to the plasma membrane in cells treated with Snx11-shRNA (Figure 8C). Snx11 shRNA did not affect internalization of DOR nor the total amount of DOR, demonstrating that Snx11

did not affect the amount of receptor available for recycling after internalization (Figure 8A, B). In control conditions, 50% of internalized DOR was recycled back to the membrane but treatment with Snx11 shRNA cells increased this amount to 90%. As expected, inhibition of PtdIns(3)P kinase by treatment with BEZ235 (100nM) and wortmannin (100nM), produced a similar effect as Snx11 knockdown, supporting the necessity for binding of SNX11 to PtdIns(3)P during DOR recycling (Figure 8D). Since microtubules and actin filaments have been shown to be involved in protein sorting, we wanted to determine whether either of these cytoskeletal elements are involved in DOR recycling. We used nocodazole and cytochalasin, which interfere with microtubule and actin polymerization, respectively. Surprisingly, treatment with cytochalasin (100mM) did not produce any difference in DOR recycling but treatment with nocodazole (100mM) reduced the amount of DOR recycled from (Figure 8E). No co-localization was observed with the late endosome marker, RAB9 (Figure 8B, F) but upon stimulation with DPDPE, the DOR to co-localized with RAB9 (Figure 8F), marking a compartment also associated with Snx11 (Figure 4A, G).Taken together, these results demonstrate that Snx11 inhibits DOR recycling in an actin-independent fashion, that the DOR travels along microtubules during this process and that the site of action of Snx11 in DOR recycling is the late endosome.

Mutations of SNX11 are not associated with human Ehlers-Danlos syndrome-Since several interaction partners identified in our SNX11 yeast-two-hybrid screen point to a biologically plausible role of SNX11 in human Ehlers-Danlos syndrome (Table 1), we screened 14 patients for disease-causing mutations in SNX11. No disease-causing mutations were identified. Thus, SNX11 does not seem to play a major role in this disease spectrum.

DISCUSSION

In this study, our analysis of Snx11 in mouse, Xenopus and cells revealed a widely expressed gene that appears to be involved in at we provide evidence for the broad expression of Snx11 across many tissues originating from all three germ layers. This suggests Snx11 is a ubiquitous protein possibly involved in common cellular processes. Although expression of Snx11 was widespread, the level of Snx11 expression in the mouse was tissue-specific, suggesting that Snx11 follows organ-specific transcriptional regulation (Figure 1B). In addition to this, we propose two seemingly distinct functions of Snx11: regulation of actin-dependent processes that involve the interaction with or secretion of factors into the extra-cellular milieu; and an actin-independent role in receptor recycling that occurs from late endosomes.

First, we showed that proper segmentation of the Xenopus embryo requires Snx11. The formation of vertebrate segments, somitogenesis, is an evolutionarily conserved embryonic process that follows a “segmentation clock” (19). Regulating this clock are several pathways, including the Notch, FGF, Wnt and Retinoic acid (RA) signaling pathways (19). Factors from these pathways are secreted (or cell-bound) into the extra-cellular milieu, creating a gradient of morphogens that together regulate somitogenesis. Data from mouse knockouts suggest that somite border formation requires proper Notch signaling followed by activation of Mesp2 to suppress Notch signaling and delimit the somite boundary (20). The somite border defects seen in Snx11-knockdown embryos allude to an involvement of Snx11 in regulating Notch signaling, which requires extensive protein trafficking of ligands and receptors during signaling (21). However, this remains to be confirmed and does not exclude the possibility that Snx11 could also regulate FGF, Wnt and RA signaling.

Mechanistically, the secretion of factors and subsequent receptor activation both require extensive membrane remodeling that occurs during exo- and endocytosis. These processes are sensitive to actin (22,23) and interestingly, we found that Snx11 can promote actin polymerization as well as associate with components of the actin cytoskeleton. The majority of the proteins found in our Y2H screen were important for structural components of the cell like the cytoskeleton, and contractile, cell adhesion, and matrix proteins, while no other members of the sorting nexin family were identified. This was in accordance with our expression analysis and supports a function for SNX11 in the cartilaginous and smooth muscle tissues. SNX11 interacted with different actins (alpha and gamma) and Lasp1, an actin-binding protein (24). The implication of actin in receptor trafficking has been reported in studies of retromer function (6).

The other proteins identified in our screen were metabolic and translational protein such as ATP1B1. This latter gene is part of the β-subunit of Na+/K+ ATPase holoenzyme complex, which regulates the translation and transport of the catalytic α-subunit to the plasma membrane (25,26). The strong expression of SNX11 in the distal tubules of the kidney therefore makes it an interesting candidate to chaperone the Na+/K+ ATPase complex during its transport to the cell surface. The interactions of SNX11 with CTSL, ITM2a and ATP1B1 support a role for SNX11 in coupling the actin cytoskeleton to processes of protein trafficking at the plasma membrane.

The increase in actin polymerization in the presence of SNX11 alone could be the result of increased actin nucleation by recruitment of actin. In physiological conditions, the interaction between SNX11 and LASP1 could promote actin nucleation by recruiting actin and nucleation-

promoting factors. These results point toward a role for SNX11 in linking the actin cytoskeleton to membrane dynamics.

The similarity between protein sequences of SNX11 and SNX10 (83% sequence identity), as well as our findings, may point to similar functions. Snx10 is thought to play a role during osteoclast formation as it is strongly up-regulated during RANKL-induced osteoclast differentiation in vitro and expressed in osteoclasts in vivo (11). As such, a mutation in the PX domain of SNX10 (Arg51Gln) was recently found to induce malignant osteopetrosis of infancy (12). Given the recent findings that SNX10 and SNX11 act antagonistically in endosome vacuolation (17), it is possible that SNX11-binding proteins identified in our study could also be implicated in SNX10 function. Future studies of the uncharacterized protein domains of SNX10/11 and exhaustive protein interaction studies in different cellular contexts will be required for clarification. The presence of Snx11 in smooth muscle and cartilage is compatible with an involvement in the regulation of the extra-cellular matrix (ECM). Snx11 could thus play a role in exocytosis, similar to the role of SNX3 in the secretion of Wnt (2).

PX domains are known for binding to phospholipids, in particular PtdIns(3)P (27). This was not different for SNX11A and B which preferentially associated with PtdIns(3)P. The inability to bind to associate with lipids for each of the truncated versions of SNX11 is likely due to protein misfolding, as the adjacent protein sequence might also be required for proper folding of the PX domain. Similar results have been reported for other SNX's, including SNX9 (28). Although the C-terminus of Snx11 has yet to be recognized as functional domain, the region likely plays an important functional role. Such is the case for SNX10, which requires its C-terminal domains for function (29). PtdInsPs are critical determinants of membrane domain identity (30) and help recruit proteins events such as membrane trafficking, intracellular signaling, cytoskeleton

organization and apoptosis (31). PtdIns(3)P is found on the surface of early and late endosomes as well as on the membranes of the intralumenal vesicles of multivesicular bodies (MVBs) (7,32). The presence of SNX11 in late endosomes shown by confocal microscopy and subcellular fractionation supports of role for SNX11 in trafficking to and/or from late endosomes. Although late endosomes and the Golgi network are endosomal compartments used by the retromer, the lack of a BAR domain in SNX11 points towards retromer-independent functions. Many reports have shown that some retromer-independent sorting, involving membrane remodeling and receptor trafficking, still occurs when one of the retromer subcomplexes is missing (33,34). Late endosomes (or MVBs) can host a diverse set of proteins that do not always share the same fate and that therefore require tailored trafficking machinery. In contrast, the M6PR travels continuously between late endosomes and the trans-Golgi network (35).

Secondly, we show that Snx11 participates in trafficking of the DOR in an actin-independent manner. This was demonstrated in our recycling assay, where the DOR co-localized with SNX11 after stimulation with DPDPE and where knockdown of Snx11 increased DOR recycling. This along with the co-localizations of both RAB9-DOR (with DPDPE) and RAB9-SNX11, suggest that DOR recycling follows an SNX11-dependent route via late endosomes whereby SNX11 reduces DOR recycling. However, direct binding of SNX11 to DOR is not expected due to the fact that sorting nexins often bind indirectly with their cargo via accessory adaptor proteins. Proteins travelling to late endosomes are often en-route to lysosomes for degradation but it has also been shown that intralumenal vesicles can undergo “back-fusion” with the late endosome limiting membrane, suggesting some proteins can exit this compartment (36). The increase in DOR recycling observed in the absence of SNX11 is

perhaps due to a defective transport of DOR to late endosomes. Upon Snx11 knockdown, trafficking to late endosomes might fail and the receptor might instead be returned to the cell surface via a fast recycling mechanism. As expected, increased DOR recycling was observed by inhibition of PtdIns(3)P production, which supports a role for Snx11 in suppressing DOR recycling. Surprisingly, inhibition of de novo actin polymerization did not affect DOR recycling, while inhibition of microtubules did. Although the mechanism by which Snx11 inhibits DOR recycling is still unclear, these data therefore support a role for Snx11 in trafficking the DOR whereby membrane deformations are not dependent upon actin polymerization.

In conclusion, we propose that Snx11 has dual functions. First it associates with the actin cytoskeleton to regulate signaling pathways involved in secreting or responding to factors present in the extra-cellular milieu, such as the Wnt, FGF, RA and Notch pathways. Second, we describe an actin-independent role for Snx11 in receptor recycling, as demonstrated by the positive effect of Snx11 knockdown on recycling of the DOR. Advances in the biology of cellular trafficking are revealing a complex yet finely-tuned network of shuttles that regulates the fate of intracellular proteins. With a better understanding of cellular trafficking, we will better understand how signaling pathways are regulated.

Reference List

1. Lundmark, R., and Carlsson, S. R. (2003) The Journal of biological chemistry 278, 46772-46781

2. Harterink, M., Port, F., Lorenowicz, M. J., McGough, I. J., Silhankova, M., Betist, M. C., van Weering, J. R., van Heesbeen, R. G., Middelkoop, T. C., Basler, K., Cullen, P. J., and Korswagen, H. C. (2011) Nature cell biology 13, 914-923

3. Cullen, P. J., and Korswagen, H. C. (2012) Nature cell biology 14, 29-37

4. Seet, L. F., and Hong, W. (2006) Biochimica et biophysica acta 1761, 878-896

5. Cullen, P. J. (2008) Nature reviews. Molecular cell biology 9, 574-582

6. Seaman, M. N. (2012) Journal of cell science 125, 4693-4702

7. van Weering, J. R., Verkade, P., and Cullen, P. J. (2010) Seminars in cell & developmental biology 21, 371-380

8. Andelfinger, G., Hitte, C., Etter, L., Guyon, R., Bourque, G., Tesler, G., Pevzner, P., Kirkness, E., Galibert, F., and Benson, D. W. (2004) Genomics 83, 1053-1062

9. Chen, C., Garcia-Santos, D., Ishikawa, Y., Seguin, A., Li, L., Fegan, K. H., Hildick-Smith, G. J., Shah, D. I., Cooney, J. D., Chen, W., King, M. J., Yien, Y. Y., Schultz, I. J., Anderson, H., Dalton, A. J., Freedman, M. L., Kingsley, P. D., Palis, J., Hattangadi, S. M., Lodish, H. F., Ward, D. M., Kaplan, J., Maeda, T., Ponka, P., and Paw, B. H. (2013) Cell metabolism 17, 343-352

10. Lorenowicz, M. J., Macurkova, M., Harterink, M., Middelkoop, T. C., de Groot, R., Betist, M. C., and Korswagen, H. C. (2014) Cellular signalling 26, 19-31

11. Zhu, C. H., Morse, L. R., and Battaglino, R. A. (2012) Journal of cellular biochemistry 113, 1608-1615

12. Aker, M., Rouvinski, A., Hashavia, S., Ta-Shma, A., Shaag, A., Zenvirt, S., Israel, S., Weintraub, M., Taraboulos, A., Bar-Shavit, Z., and Elpeleg, O. (2012) Journal of medical genetics 49, 221-226

13. Nieuwkoop, P. D., and Faber, J. (1994) Normal Table of Xenopus laevis (Daudin), Garland Publishing Inc., New York

14. Lavallee, G., Andelfinger, G., Nadeau, M., Lefebvre, C., Nemer, G., Horb, M. E., and Nemer, M. (2006) Embo Journal 25, 5201-5213

15. Letunic, I., Doerks, T., and Bork, P. (2012) Nucleic acids research 40, D302-305

16. Schultz, J., Milpetz, F., Bork, P., and Ponting, C. P. (1998) Proc Natl Acad Sci U S A 95, 5857-5864

17. Xu, J., Xu, T., Wu, B., Ye, Y., You, X., Shu, X., Pei, D., and Liu, J. (2013) The Journal of biological chemistry 288, 16598-16605

18. Archer-Lahlou, E., Audet, N., Amraei, M. G., Huard, K., Paquin-Gobeil, M., and Pineyro, G. (2009) Journal of cellular and molecular medicine 13, 147-163

19. Dequeant, M. L., and Pourquie, O. (2008) Nature reviews. Genetics 9, 370-382

20. Saga, Y., and Takeda, H. (2001) Nature reviews. Genetics 2, 835-845

21. Ntziachristos, P., Lim, J. S., Sage, J., and Aifantis, I. (2014) Cancer Cell 25, 318-334

22. Nightingale, T. D., Cutler, D. F., and Cramer, L. P. (2012) Trends in cell biology 22, 329-337

23. Robertson, A. S., Smythe, E., and Ayscough, K. R. (2009) Cellular and molecular life sciences : CMLS 66, 2049-2065

24. Grunewald, T. G., and Butt, E. (2008) Molecular cancer 7, 31

25. Chow, D. C., and Forte, J. G. (1995) The Journal of experimental biology 198, 1-17

26. Geering, K. (2001) Journal of bioenergetics and biomembranes 33, 425-438

27. Teasdale, R. D., and Collins, B. M. (2012) The Biochemical journal 441, 39-59

28. Lundmark, R., and Carlsson, S. R. (2009) Journal of cell science 122, 5-11

29. Qin, B., He, M., Chen, X., and Pei, D. (2006) The Journal of biological chemistry 281, 36891-36896

30. Anitei, M., Wassmer, T., Stange, C., and Hoflack, B. (2010) Molecular membrane biology 27, 443-456

31. Saarikangas, J., Zhao, H., and Lappalainen, P. (2010) Physiological reviews 90, 259-289

32. Sasaki, T., Sasaki, J., Sakai, T., Takasuga, S., and Suzuki, A. (2007) Biological & pharmaceutical bulletin 30, 1599-1604

33. Nisar, S., Kelly, E., Cullen, P. J., and Mundell, S. J. (2010) Traffic 11, 508-519

34. Prosser, D. C., Tran, D., Schooley, A., Wendland, B., and Ngsee, J. K. (2010) Traffic. 11, 1347-1362

35. Arighi, C. N., Hartnell, L. M., Aguilar, R. C., Haft, C. R., and Bonifacino, J. S. (2004) The Journal of cell biology 165, 123-133

36. Falguieres, T., Luyet, P. P., and Gruenberg, J. (2009) Experimental cell research 315, 1567-1573

Table 1: List of interacting clones found by yeast two-hybrid, using mouse SNX11b as bait, and ordered by biological function. The major associated human phenotypes are also shown.

DESCRIPTION	GENE	GROUP / DESCRIPTION	BIOLOGICAL FUNCTION	HUMAN PHENOTYPE (OMIM#)
Cytoskeleton, Cell adhesion, Extra-cellular matrix	ACTC1	Cardiac Alpha actin	Cardiac actin	Dilated cardiomyopathy/left ventricular non-compaction (102540) Hypertrophic cardiomyopathy (115196) Atrial septal defect (612794)
	ACTG	Gamma actin	Cytoskeletal, Cell adhesion	Autosomal dominant deafness (604717) Baraitser-Winter syndrome 2(614583)
	MYBPC1	Myosin binding protein C, slow type	Cell contractility	Distal arthrogryposis (614335) Lethal congenital contracture syndrome 4 (614915)
	Col1a2	Procollagen, type I, alpha 2	Extra-cellular matrix	Ehlers-Danlos syndrome, cardiac valvular form (225320) Ehlers-Danlos syndrome, type VIIB (130060) Osteogenesis imperfecta II, III, IV (166210, 259420, 166220)
	Col5a2	Procollagen, type V	Extra-cellular matrix	Ehlers-Danlos type I (130000)
	Col11a1	Procollagen, type XI	Extra-cellular matrix	Fibrochondrogenesis (228520) Marshall syndrome (154780) Stickler syndrome type II (604841)
	Plod1	Procollagen-lysine, 2-oxoglutarate 5-dioxygenase 1	Collagen synthesis	Ehlers-Danlos syndrome type VI (225400)
	Itm2a	Integral membrane protein 2A	Myogenic, chondrogenic differentiation	
	Lasp1	LIM and SH3 protein 1	Cytoskeleton, focal adhesions	

Table 1: List of interacting clones found by yeast two-hybrid, using mouse SNX11b as bait, and ordered by biological function. The major associated human phenotypes are also shown. (continued)

DESCRIPTION	GENE	GROUP / DESCRIPTION	BIOLOGICAL FUNCTION	HUMAN PHENOTYPE (OMIM#)
Transcription, translation, DNA repair	Polr2c	Polymerase (RNA) II (DNA directed) polypeptide C	Transcription, subunit of RNA polymerase II complex	
	Supt4h	Suppressor of Ty 4 homolog	transcription initiation/elongation, chromatin remodeling	
	Rnf141	Ring finger protein 141	Transcription, Posttranslational modification, protein turnover, chaperones	
	Eif3s2	Eukaryotic translation initiation factor 3, subunit 2 (beta)	Translation initiation	
	Eif3s10	Eukaryotic translation initiation factor 3, subunit 10 (theta)	Translation initiation	
	Eef1a1	Eukaryotic translation elongation factor 1 alpha 1	Translation elongation	
	Eef2	Eukaryotic translation elongation factor 2	Translation elongation	Spinocerebellar ataxia 26 (609306)
	Arbp	Acidic ribosomal phosphoprotein P0	Translation elongation, ribosome assembly	
	RDM1	RAD52B, RAD52 homolog B	RNA recognition motif, DNA repair	

Table 1: List of interacting clones found by yeast two-hybrid, using mouse SNX11b as bait, and ordered by biological function. The major associated human phenotypes are also shown. (continued)

DESCRIPTION	GENE	GROUP / DESCRIPTION	BIOLOGICAL FUNCTION	HUMAN PHENOTYPE (OMIM#)
Trafficking	Gphn	Gephyrin	Synaptic receptor clustering, molybdene cofactor synthesis	Molybdenum cofactor deficiency C (615501)
Signaling	PIP5K1A	Phosphatidylinositol phosphate kinase	Signaling, Golgi, trafficking	
Lysosome	Ctsl	Cathepsin L	Proteolytic enzyme, lysosome	
	Npc2	Niemann Pick type C2	late endosomal/lysosomal system	Niemann Pick type C2 (607625)

Table 1: List of interacting clones found by yeast two-hybrid, using mouse SNX11b as bait, and ordered by biological function. The major associated human phenotypes are also shown. (continued)

DESCRIPTION	GENE	GROUP / DESCRIPTION	BIOLOGICAL FUNCTION	HUMAN PHENOTYPE (OMIM#)
Mitochondrial	Mrpl4 (S100A9)	Mitochondrial ribosomal protein L4	mitochondrial	
	Fech	Ferrochelatase	Porphyrin metabolism	Erythropoietic protoporphyria (17700)
	Ech1	Enoyl coenzyme A hydratase	Beta oxidation	
	Atp5d	ATP synthase, H+ transporting, mitochondrial F1 complex, delta subunit	Ion / proton transport	
	Ndufs8	NADH dehydrogenase (ubiquinone) Fe-S protein 8	Oxidoreductase	Leigh syndrome (256000)
	Cyc1	Cytochrome c1	Mitochondrial electron carrier	Mitochondrial complex III deficiency, nuclear type 6
Carbohydrate metabolism	Akr1a4	Aldo-keto reductase family 1, member A4 (aldehyde reductase)	Carbohydrate metabolism	
	FUCA2	Alpha-L-fucosidase		
	ALDOA	Aldolase A, fructose-bisphosphate	Pentose phosphate pathway	Aldolase A deficiency
	G6pd	Glucose-6-phosphate dehydrogenase	Pentose phosphate pathway	G6PD deficiency (134700, 300908)
	Eno1	Enolase 1, alpha non-neuron, 2-phospho-D-glycerate hydrolase	Glycolysis, gluconeogenesis	Enolase deficiency

Table 1: List of interacting clones found by yeast two-hybrid, using mouse SNX11b as bait, and ordered by biological function. The major associated human phenotypes are also shown. (continued)

DESCRIPTION	GENE	GROUP / DESCRIPTION	BIOLOGICAL FUNCTION	HUMAN PHENOTYPE (OMIM#)
Other	Atp1b1	ATPase, Na+/K+ transporting, beta 1 polypeptide	Membrane associated Na K pump	
	Ahsg	Fetuin-A ;alpha-2-HS-glycoprotein	MMP inhibitor	
	Wfdc1	WAP four-disulfide core domain 1	Protease inhibitor	
	Tbc1d22b	TBC1 domain family, member 22B	GTPase-activating protein	
	Dgcr6	DiGeorge syndrome critical region gene 6	Nuclear phosphoprotein	
	Lgals9	Lectin, galactose binding, soluble	Galactose binding, signal transduction, chemoattractant	
	LOC329575	FOG, Zn finger containing protein	hypothetical	
	2210412D01	Catalytic domain	hypothetical	
	Ntan1	N-terminal Asn amidase	Ubiquitination, protein turnover	
	H19	H19 fetal liver mRNA	gene with no protein product	Beckwith-Wiedemann (130650) Silver-Russell (180860) Wilms tumor 2 (194071)

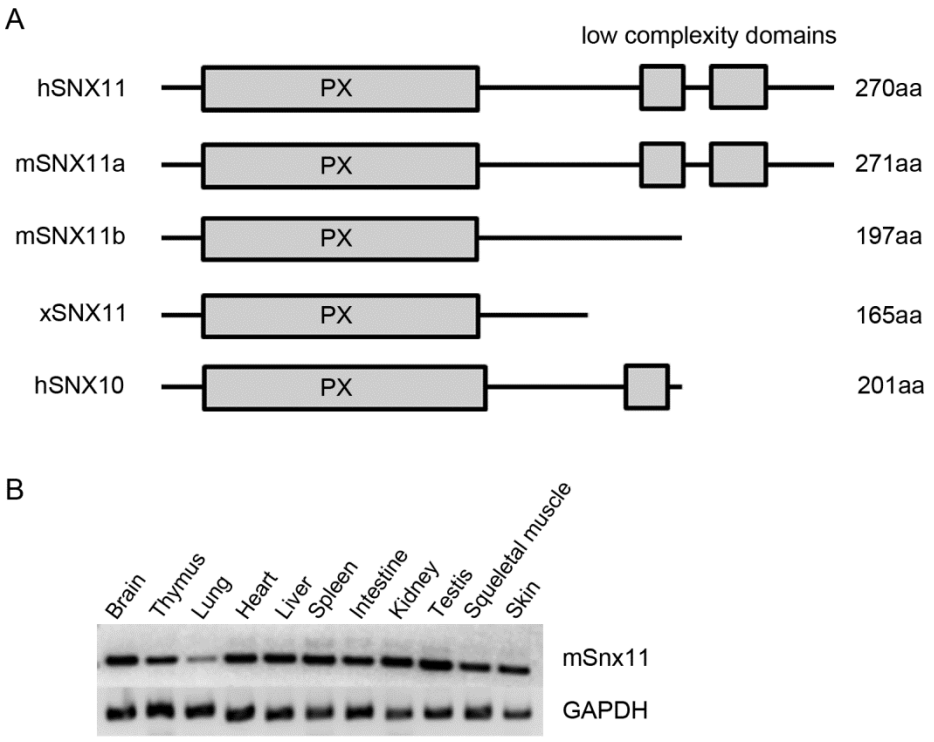

Figure 1. The domain structure of SNX11 and expression profile in various mouse tissues. A) Across all species and isoforms, the SNX11-PX domain is located at the N-terminal (as predicted by SMART). Two C-terminal low complexity domains (coiled-coils) are present in hSNX11 and mSNX11a but not in other isoforms or species. SNX10 (closest phylogenetic relative) contains an N-terminal PX domain and a single low complexity domain. Length in amino acid (aa) is indicated. B) RT-PCR of mSnx11, determined from tissue-derived cDNA. GAPDH was used as positive control.

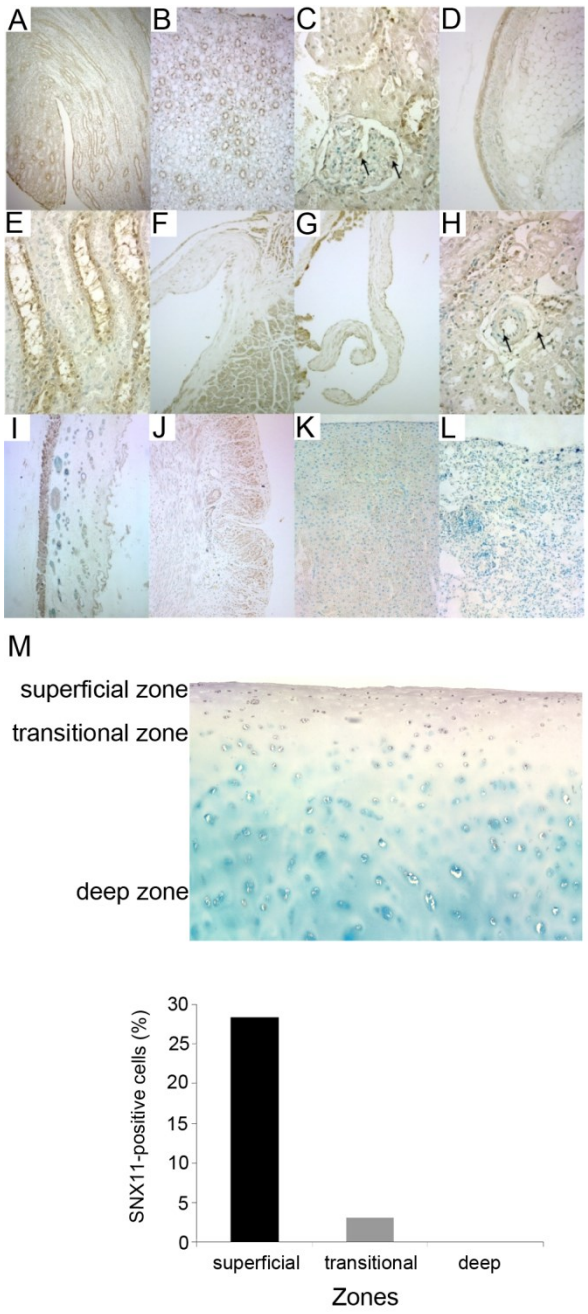

Figure 2. SNX11 is expressed ubiquitously. Seen here are rat and human histological sections stained with goat anti-SNX11 antibody (polyclonal) and counter-stained with methyl green. Tissue sections shown are as follows: A) human kidney tubules (10x) B) human kidney (10x) C) human kidney glomerular tissue (40x) D) human kidney (20x) E) human

kidney (40x) F) rat heart fibrous tissue (20x) G) rat heart valvular tissue (20x) H) rat vessel (40x) I) rat skin (10x) J) rat uterus (10x) K) rat liver (10x) L) rat lung (10x). M) As seen in this human knee cartilage section (upper panel) and bar graph (lower panel), SNX11 staining is strongest in the superficial zone.

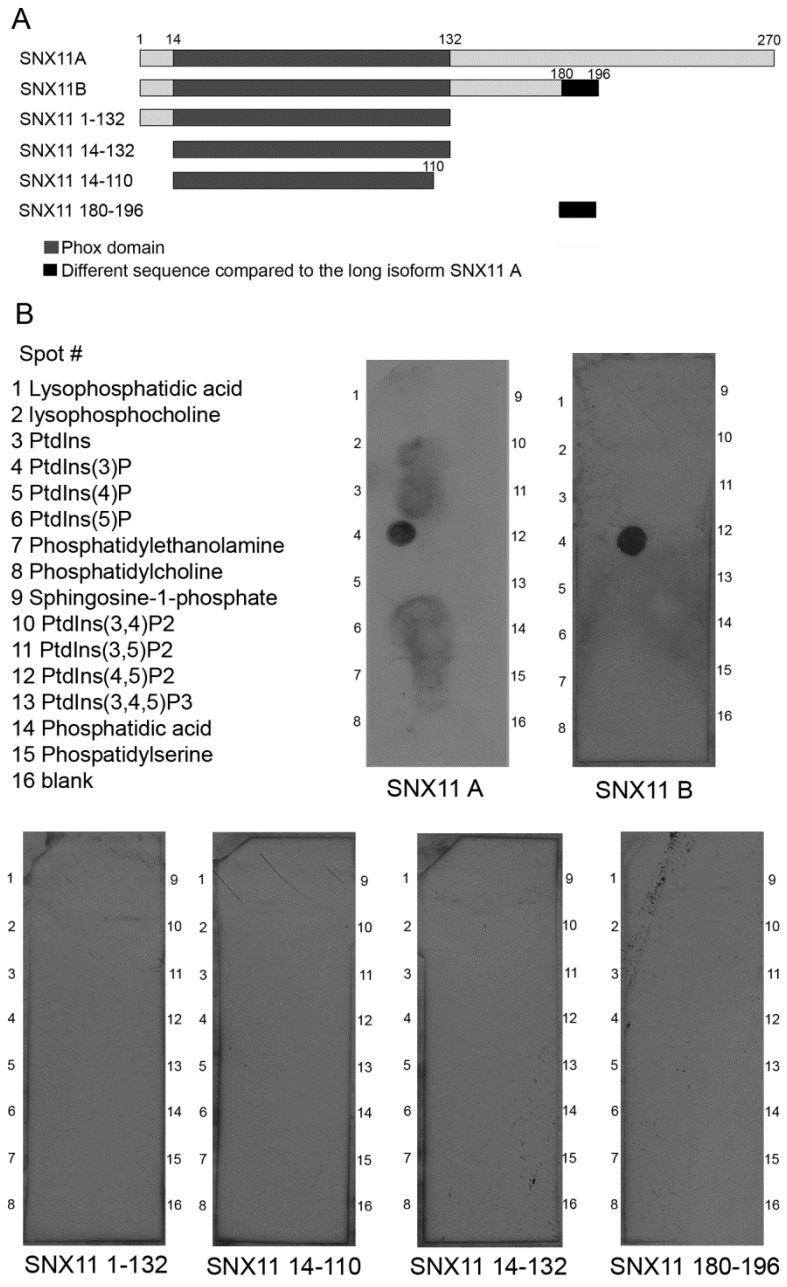

Figure 3. SNX11 bind to PtdIns(3)P. The production of various mouse isoforms and truncated versions of GST-tagged SNX11 (A) was induced (IPTG) in BL21-Gold bacteria (see Figure S1 for expression in BL21-Gold bacteria). Purified proteins were subjected to a phospholipid overlay assay (PIP-strips) and subsequent Western blotting. Binding to PtdIns(3)P can be seen in blots of SNX11A and SNX11B whereas all other constructs were unable to bind.

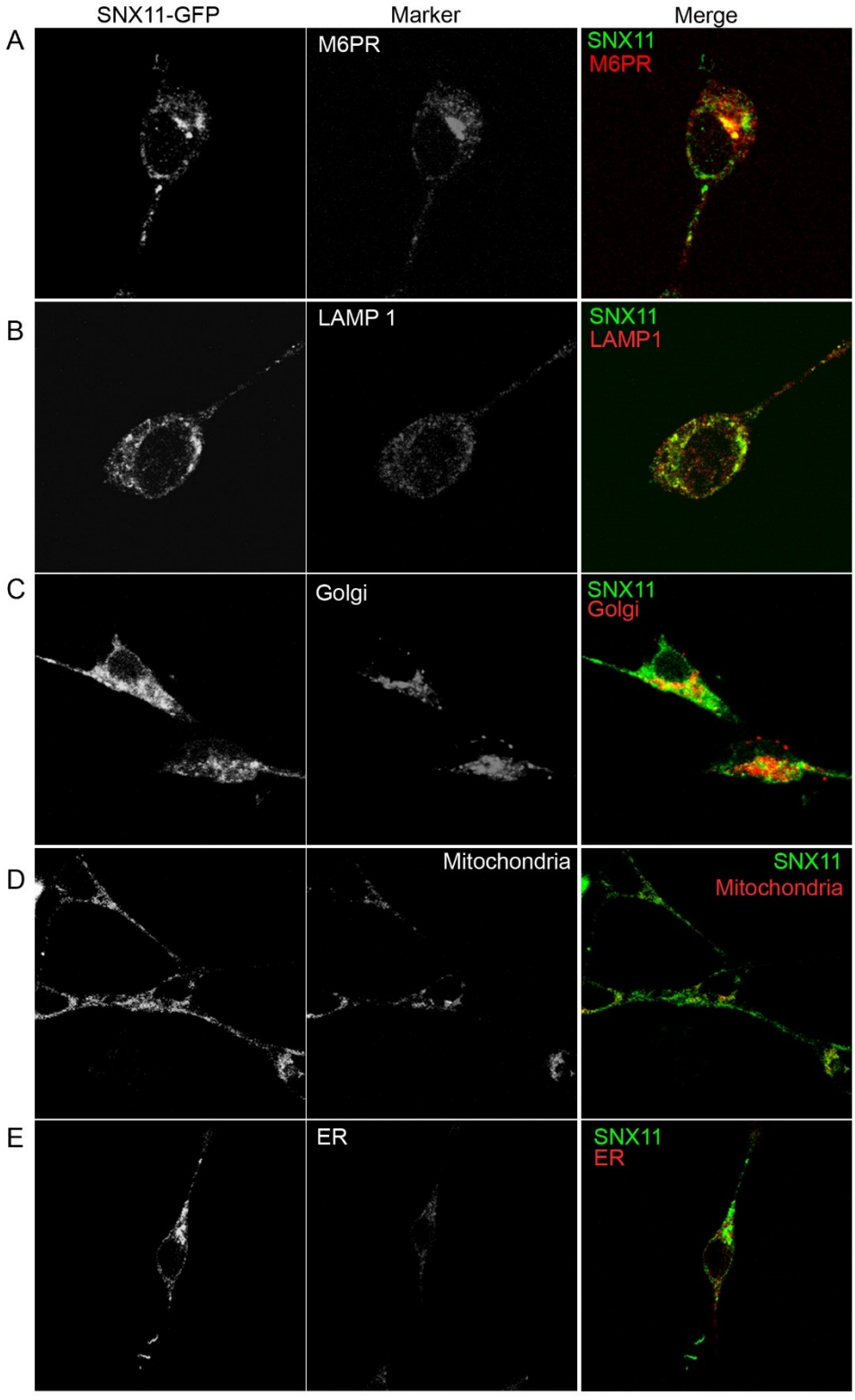
SNX11-GFP
Marker
Merge
A
M6PR
SNX11
M6PR
B
LAMP 1
SNX11
LAMP1
C
Golgi
SNX11
Golgi
D
Mitochondria
SNX11
Mitochondria
E
ER
SNX11
ER

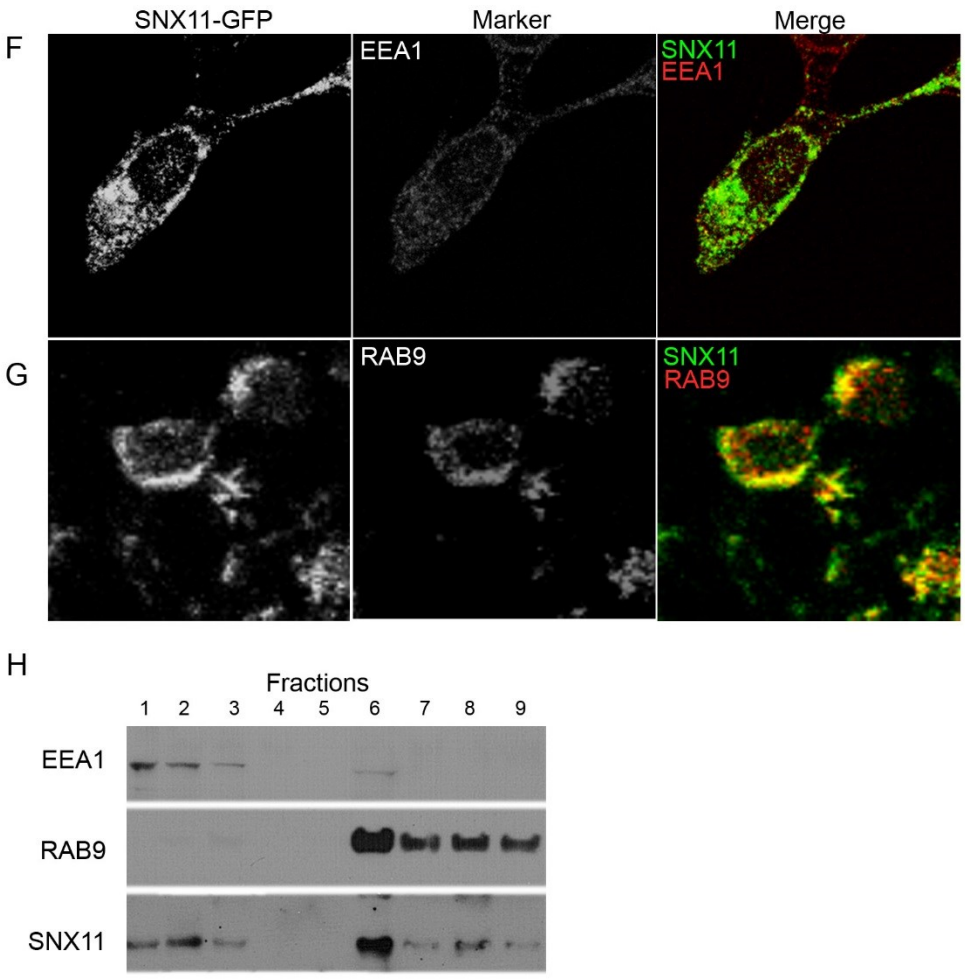

Figure 4. Distribution of SNX11-GFP in HEK293T cells. Localization of SNX11-GFP (green) and various endosomal markers (red) in HEK293T_SNX11-GFP cells; a yellow signal signifies co-localization. A) Cation-independent mannose-6-phosphate receptor (CI-M6PR) – late endosome. B) Lysosome-associated membrane protein-1 (LAMP1) – lysosomes. C) Golgi-tracker – Golgi network. D) Mito-tracker – mitochondria. E) ER-tracker – endoplasmic reticulum. F) Early endosome associated protein-1 (EEA1) – early endosomes. G) Rab9 – late endosomes. H) Distribution of EEA-1, RAB9 and SNX11 in a subcellular fractionation of HEK293T_SNX11-GFP cells.

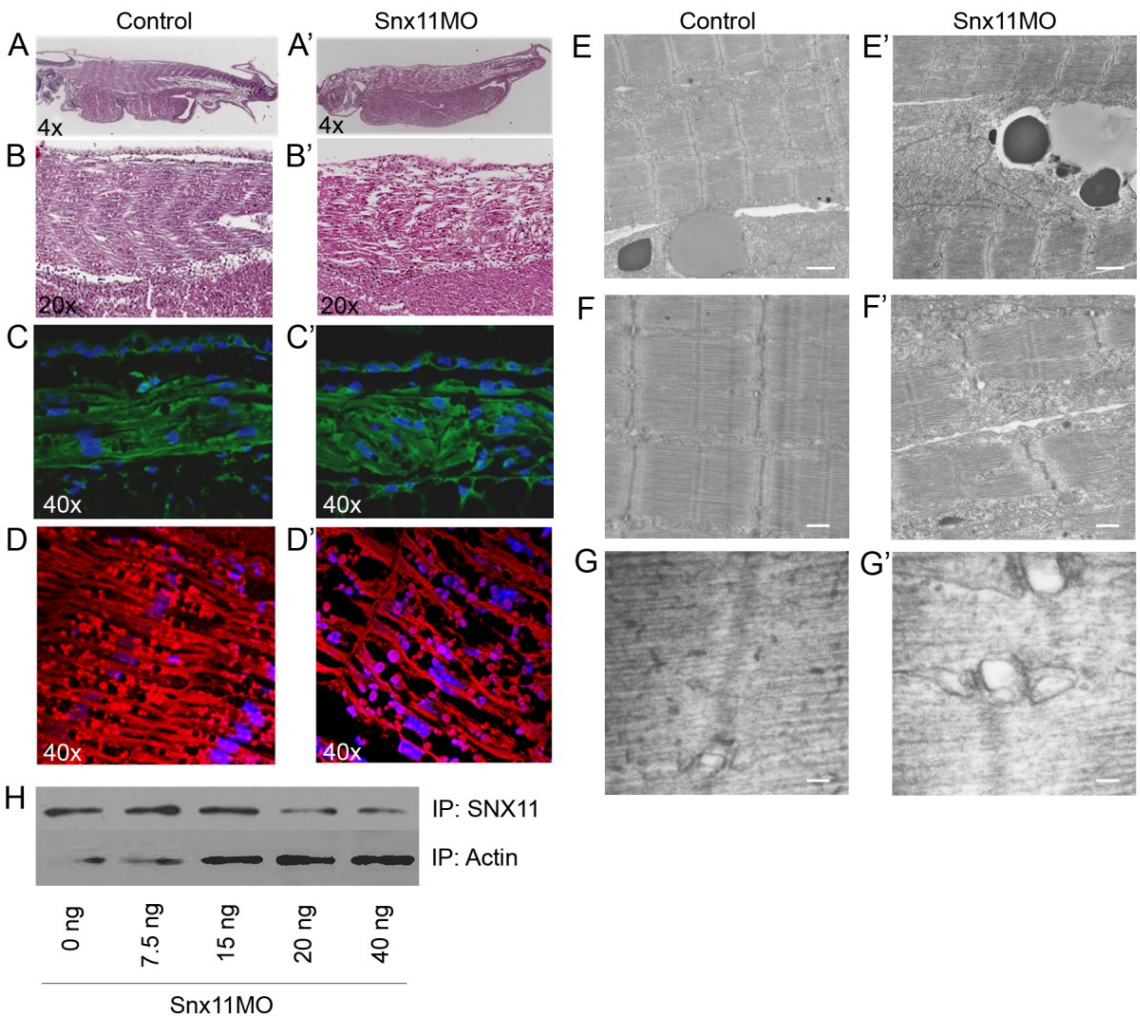

Figure 5. Morpholino-induced knockdown of Snx11 in *Xenopus laevis*. A-B) Staining with on fixed embryos injected with control or Snx11MO (magnification is indicated). Somites are well-formed in controls (A-B) but in knockdown embryos somite boundaries are abnormal and somite structure is disorganized (A'-B'). These defects are also seen with fibronectin (C-C') and phalloidin (D-D') staining. E-G) Electron microscopy scans of somites at stage 40 (scale = 1μm (E), 200nm (F), 50nm (G)). H) Western blot showing the increased SNX11 knockdown with an increasing dose of Snx11MO. Actin was used as loading control.

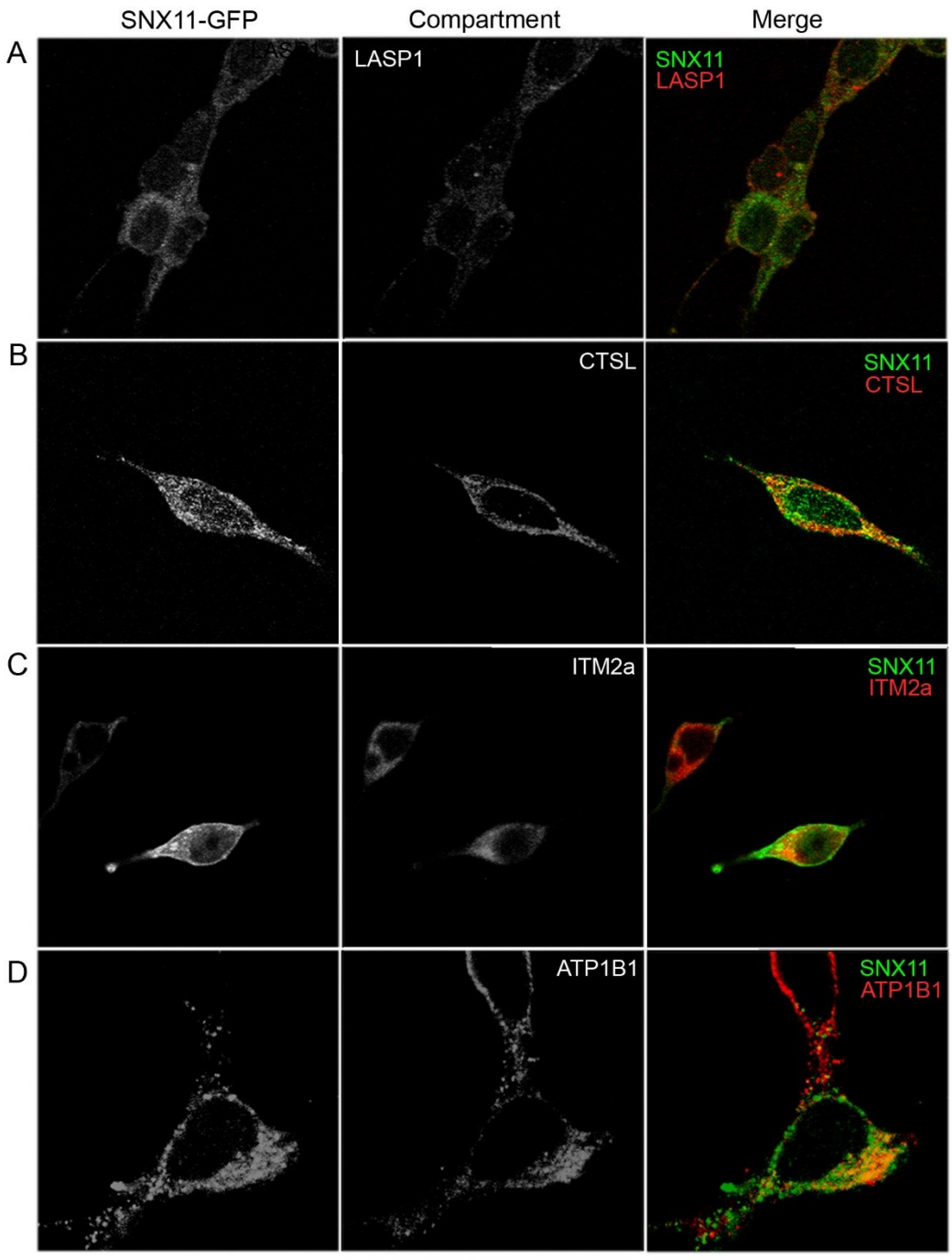

Figure 6: Co-localization of SNX11-GFP (green) and Y2H isolates (red) in HEK293T cells. SNX11-GFP co-localizes (yellow) with A) LASP1, B) CTSL, C) ITM2a and D) ATP1B1.

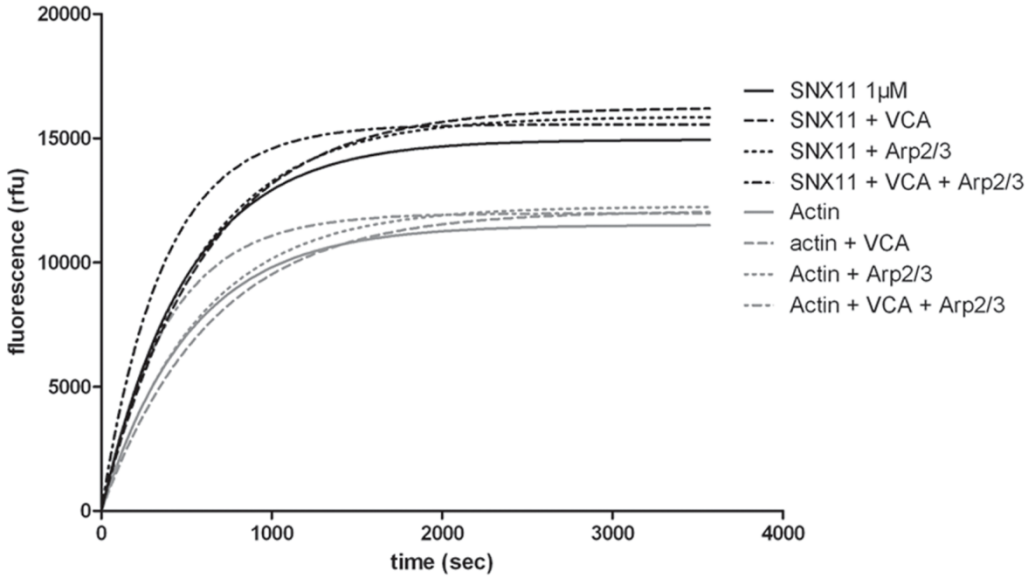

Figure 7: SNX11 promotes actin polymerization. The effect of various combinations of nucleation-promoting factors (Arp2/3 and VCA) on the relative rate of actin polymerization. The addition of SNX11 increases actin polymerization.

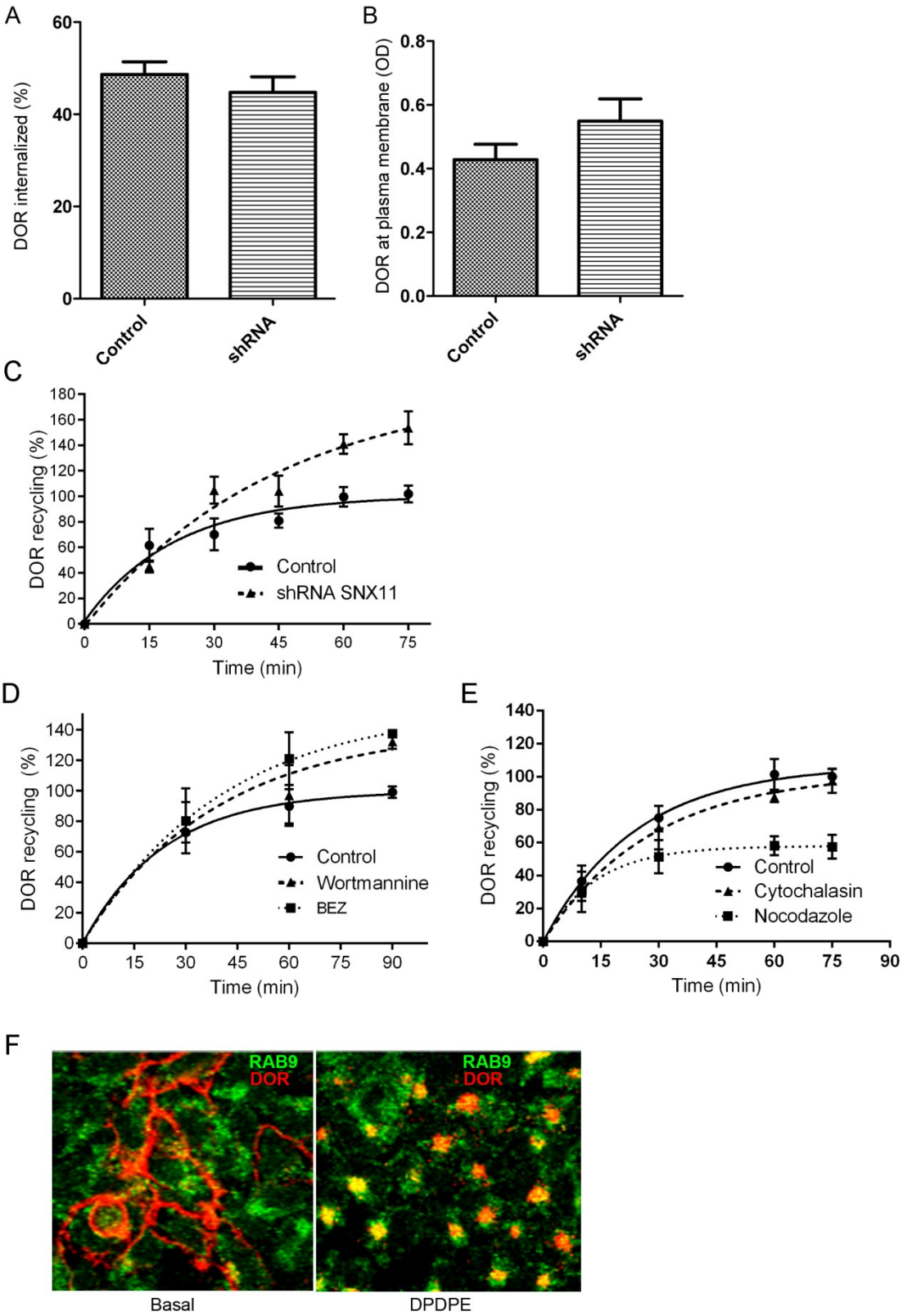
A
DOR internalized (%)
60
40
20
0
Control
shRNA
B
DOR at plasma membrane (OD)
0.8
0.6
0.4
0.2
0.0
Control
shRNA
C
DOR recycling (%)
180
160
140
120
100
80
60
40
20
0
0
15
30
45
60
75
Time (min)
Control
shRNA SNX11
D
DOR recycling (%)
140
120
100
80
60
40
20
0
0
15
30
45
60
75
90
Time (min)
Control
Wortmannine
BEZ
E
DOR recycling (%)
140
120
100
80
60
40
20
0
0
15
30
45
60
75
90
Time (min)
Control
Cytochalasin
Nocodazole
F
RAB9
DOR
RAB9
DOR
Basal
DPDPE

Figure 8: SNX11 negatively regulates DOR recycling to the membrane. A, C) Protein synthesis in HEK293 cells stably expressing Flag-DOR (Control) or Flag-DOR/shRNA Snx11 (shRNA) was blocked 1h before the start of internalization and recycling experiments. A) Internalization of Flag-DOR 30 minutes after induction with DPDPE (1μM; 30 min) in control and shRNA cells. B) Total amount of Flag-DOR at the plasma membrane after transfections with Flag-DOR or Flag-DOR/shRNA Snx11 without DPDPE. C) Internalization was induced as in A after which cells were placed in the incubator in an agonist-free medium (DMEM/HEPES/cycloheximide) for increasing periods of time. Percent of Flag-DOR recycled to the plasma membrane was determined by ELISA-based method. Results are expressed as percentage of maximal recovery of internalized receptor in control cells. The data represent mean ± S.E.M. from five independent experiments carried out in triplicate. Statistical comparison between curves (Control versus shRNA) was assessed using two-way ANOVA ($p<0.0001$). D) Recycling assays were carried out as in C except that recovery was done in an agonist-free medium containing either vehicle (control), wortmannin (10nM) or BEZ235 (10nM). E) Recycling assays were also carried out as in C except that recovery was done in an agonist-free medium containing either vehicle (control), cytochalasin (10μM) or nocodazole (μM). The data represents mean ± S.E.M. from three independent experiments carried out in triplicates. Statistical comparison between curves (Control vs Cytochalasin vs Nocodazole) was assessed by two-way ANOVA (p=). (E) HEK293T cells stably expressing Flag-DOR (red) were fixed before (basal) and after (DPDPE) treatment with DPDPE (1μM; 30min). Co-localization (yellow) with Rab9 (green) is seen in treated cells.

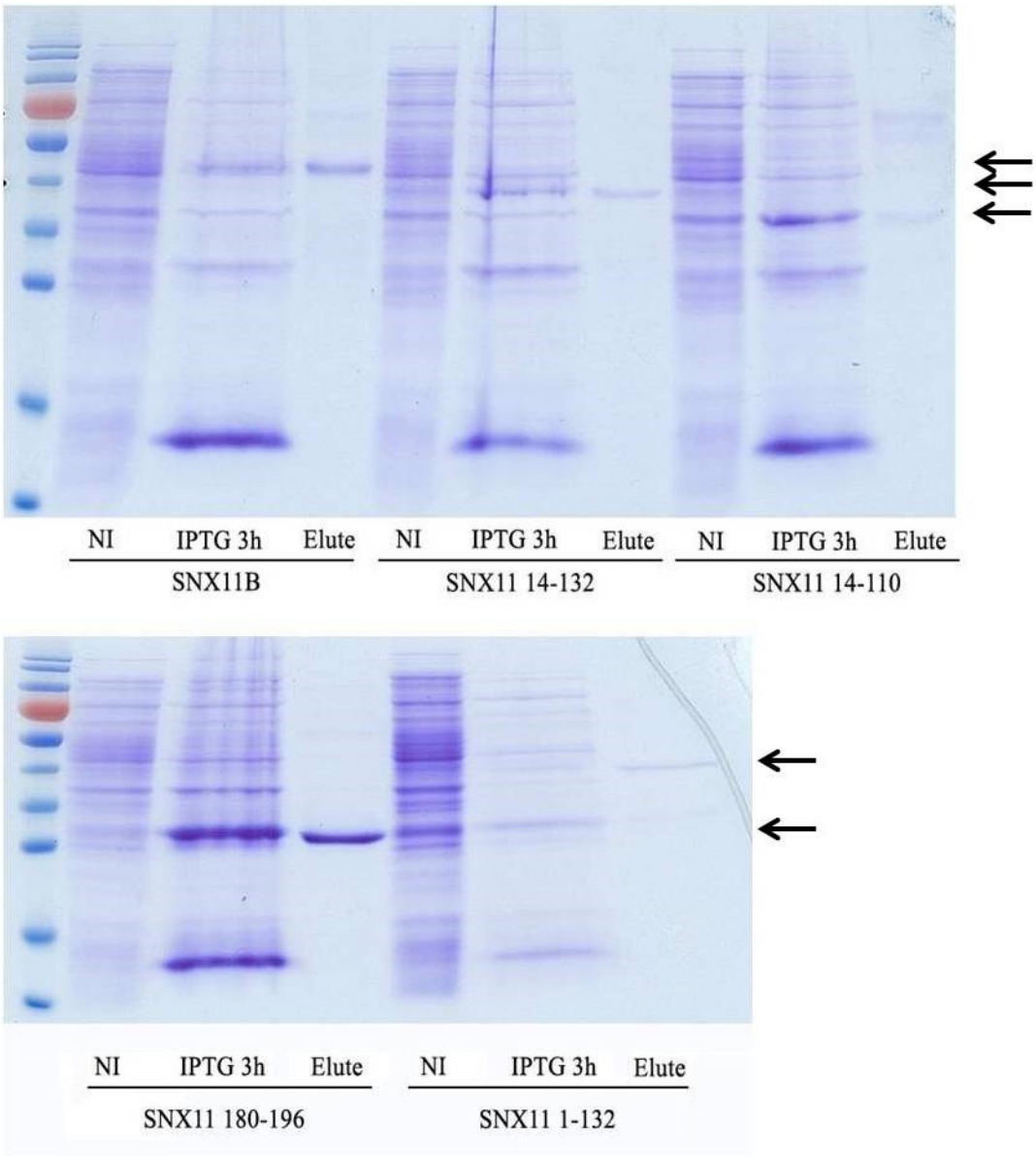

Figure S1. Expression of full length and truncated SNX11 in BL21-Gold bacteria. Shown here is a coomassie stain of total and purified protein (arrows) from BL21-Gold bacteria expressing various SNX11 constructs. The eluate was used for PIP-strip overlay assay.

Chapter 3: Journal article #2 (submitted to Traffic)

SNX30 negatively regulates Wnt/β-catenin signaling

Michel Cameron[1,2], Séverine Leclerc[1], Christian Beauséjour[1], Parker Antin[3], Nicole Dubois[4], Carmen Gagnon[1], Florian Wünnemann[1], Sylvain Chemtob[1], Gregor Andelfinger[1,2]

[1] Centre de Recherche, CHU Sainte Justine, Departments of Pediatrics and Biochemistry, Université de Montréal

[2] Départements de Pharmacologie et de Biochimie, Université de Montréal

[3] Cellular & Molecular Medicine, Molecular & Cellular Biology, University of Arizona

[4] McEwen Centre for Regenerative Medicine. University Health Network, University of Toronto

Synopsis and Graphical Table of Contents:

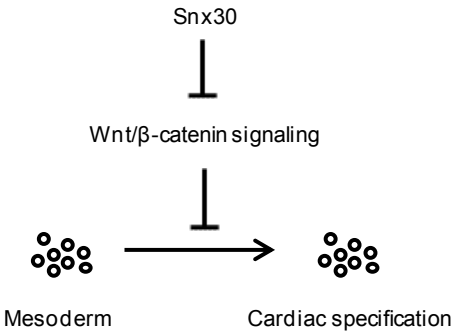

Snx30 negatively regulates Wnt/β-catenin signaling both in vivo and in vitro. Knockdown of Snx30 impaired cardiogenesis in Xenopus laevis increased Wnt/β-catenin signaling in both Xenopus and HEK293T cells. Inhibition of Wnt/β-catenin signaling is required for cardiac specification and was therefore insufficient upon loss of Snx30, as shown by a smaller cardiac population. In HEK293T cells, the Snx30-driven inhibition of Wnt/β-catenin was strongest upon expression of specific Frizzled receptors, such as Fz8. Snx30 may thus provide cells a means by which to fine-tune this pathway.

Abstract

During Wnt/β-catenin signalling, Fz/LRP/Wnt signaling complexes are sorted to multivesicular bodies where GSK3 is also sequestered to allow the accumulation of cytoplasmic β-catenin. However, the mechanisms regulating this trafficking are unknown. Sorting nexins are a large protein family that regulates endosomal trafficking of proteins such as receptors. Here, we provide the first functional characterization of sorting nexin-30 (Snx30). Snx30 was highly expressed during early Xenopus laevis and

Gallus gallus development and SNX30-GFP localized mainly to RAB9- and M6PR-positive endosomes (multivesicular bodies) in HEK293T cells. In Xenopus knockdown of Snx30 increased Wnt/β-catenin signaling, reduced Nkx2-5 expression and caused heart malformations. In accordance, knockdown of Snx30 in HEK293T co-expressing each of the ten Wnt receptors (Fz1-10) and LRP5, significantly increased Wnt/β-catenin signaling for all receptors except Fz1/Fz4/Fz9. The specificity of this effect was evaluated using cell-surface biotinylation, where knockdown of Snx30 reduced the localization of Fz8 at the cell membrane, while leaving Fz4 unaffected. Snx30 could be involved in trafficking components of this complex from this compartment. Supporting this argument, we found that SNX30 localized to intralumenal vesicles in a Wnt3a-dependent manner. We propose that Snx30 negatively regulates Wnt/β-catenin signaling and contributes to the inhibition of this pathway required during cardiogenesis.

Introduction

The Wnt signaling pathway is involved in a vast array of developmental and physiological processes, including cardiogenesis (1, 2), and diseases like cancer (3) and bone disease (4). Several studies point to a biphasic effect of activation of the Wnt cascade in cardiogenesis and while the formation of mesoderm requires Wnt/β-catenin signaling, this pathway must be inhibited for the subsequent commitment of these cells to the cardiac lineage (1). During this latter stage, many factors such as IGFBP-4, which competitively associates with the Wnt receptor Frizzled 8 (Fz8), contribute to this inhibition (5). Recent advances have revealed the importance of trafficking during Wnt signal transduction. Upon activation of Wnt/β-catenin

signaling, receptor-ligand complexes are internalized and sequestered into multivesicular bodies (6, 7). As such, transport vesicles shuttle Wnt receptors to and from the plasma membrane, sequentially fusing with dynamic intracellular compartments. However, the mechanisms responsible for sorting Wnt receptors within the endosomal network remain largely unknown.

Sorting nexins are a diverse family of membrane-associated proteins that orchestrate intracellular receptor trafficking (8). Through their PHOX-homology (PX) domain, sorting nexins can detect and bind to phosphatidylinositol phosphate (PtdIns)-enriched elements of membranes, where sorting events occur (9). Within the family of sorting nexins, a subgroup of 12 members contains an additional BAR domain that detects and induces membrane curvature (10, 11). Through the dimerization of their BAR domain, they can form higher order oligomeric complexes, leading to cargo sorting. Many studies have focused on the role of sorting nexins as part of the retromer protein complex, which mediates the retrograde transport of the mannose-6-phosphate receptor (M6PR) from the endosome to the trans-Golgi (12). However, retromer-independent processes responsible for endocytosis, recycling, secretion and degradation, have also been identified (13). Although SNX30 has not been shown to induce membrane tubulation in vitro, this SNX-BAR can homo- and heterodimerize with SNX4, suggesting roles in sensing membrane curvature (14). Aside from these findings, Snx30 remains largely uncharacterized. In this study, we demonstrate that SNX30 is required early during embryogenesis of Xenopus laevis and plays an important role in cardiogenesis. We also provide evidence that SNX30 inhibits Wnt/β-catenin, possibly by disrupting LRP6 signalosomes where the β-catenin inhibitor GSK3 is also sequestered during signaling.

Results and Discussion

Snx30 is expressed in early embryogenesis with strong expression in cardiac tissue

X. laevis (BC097784) and Gallus gallus (BB-GG17906) SNX30 are 79% and 87% identical in amino acid sequence, respectively, to human Snx30 (AK127013), and share the same protein structure, with an N-terminal PX domain and a C-terminal BAR domain (Figure S1) as predicted by the Simple Modular Architecture Research Tool (SMART) (15, 16). To determine the spatio-temporal expression profile of Snx30, we performed in situ hybridization with DIG-labeled antisense RNA probe on chick and Xenopus embryos. In Xenopus Snx30 transcripts were detected in the animal pole of the embryo at NF10.5, and later was found in latero-anterior mesoderm tissue near the cardiac crescent (NF21), as well as in head and heart tissue (NF35) (Figure 1A). In the chick, Snx30 was detected at all stages examined (Figure 1C). At HH stage 3, Snx30 transcripts were localized to the primitive streak and mesoderm. At late gastrula stages (stages 6-7), expression was observed in the primitive streak, notochord and head process. Snx30 expression was observed in the heart beginning at the onset of heart tube formation. At stage 23, Snx30 was broadly expressed with highest levels in the heart.

We analyzed Snx30 expression by RT-PCR on stage-matched Xenopus embryos and human heart tissue. In Xenopus, Snx30 was expressed throughout development, from stage NF1 to NF42 (Figure 1B) and peaked prior to gastrulation at stages NF7-11. These stages coincide with mesoderm specification, which occurs in the equatorial region of the mid- to late blastula (NF7-9) from which a subset of mesoderm-derived cells commit to the cardiac lineage during gastrulation (1). In human heart tissue, expression of Snx30 was at least two-fold stronger in all fetal cardiac tissue (gestational day 20) except for fetal right atrium, where expression of

Snx30 was still stronger than in adult tissue (Figure 1D). These results suggest an evolutionarily conserved role for Snx30 in heart development.

SNX30 localizes to multivesicular bodies

We assessed by immunohistochemistry the intracellular distribution of SNX30 in HEK293T cells transfected with a SNX30-GFP construct. SNX30-GFP was mobile within these cells (Movie M1) and was mainly visible as punctuate, vesicular structures throughout the cytoplasm (Figure 2). Although many SNX-BARs are found in early endosomes (17), we found little co-localization of SNX30-GFP with EEA1 (early endosomes) (Figure 2A), and no co-localization with RAB11 (recycling endosomes) (Figure 2B), or LAMP1 (lysosomes) (Figure 2D). SNX30-GFP co-localized with RAB9 and M6PR, both markers of multivesicular bodies (MVBs) (Figure 2C,E). These results suggest that Snx30 is mainly involved in trafficking events that occur in MVBs. The association of SNX-BARs to specific endosomal compartments is dependent upon the association of the PX domain with phosphatidylinositol-phosphates (PtdInsP) (9). To assess the lipid-binding properties of SNX30, we performed a lipid-overlay with GST-purified human SNX30 (GST-SNX30). GST-SNX30 associated with PtdIns(3)P, PtdIns(4)P and PtdIns(5)P (Figure S2). PtdIns(3)P is found in early endosomes and intralumenal vesicles of MVBs (18), in accordance with our previous data.

To identify possible binding partners of Snx30, we performed tandem affinity purification on human SNX30. HEK293T cells were transfected either with pCTAP-hSNX30 or pCTAP (negative control). Purified proteins were separated by SDS-PAGE and a single band unique to pCTAP-hSNX30 analyzed by LC-MS/MS. After peptide analysis with the MASCOT

database, SNX4 and SNX30 were identified as the interacting partner to SNX30. To confirm the ability of SNX30 to homo- and hetero-dimerize, we immunoprecipitated GFP-tagged SNX30 and SNX4 from cells co-transfected with V5-SNX30 and –SNX4. Both SNX4 and SNX30 formed homo- and heterodimers, confirming a previous report (Figure S3 A) (14). We also found SNX4 to bind the retromer component VPS35 but not VPS26, whereas no association was found with SNX30 (Figure S3 B). Despite these findings, we did not see any co-localization between SNX4 and SNX30 in HEK293T cells (Figure S4).

The existence of SNX30-SNX30 and SNX30-SNX4 dimers demonstrates the complexities of protein sorting alluded to by others (19) and would provide a diversity of interactions required for fine-tuning signaling pathways. Each Snx30 dimer likely has distinct membrane-binding properties that could be responsible for different sorting functions, in multiple signaling pathways, similar to the multiple roles of Snx1 (20, 21). However, the identification of cargo associated with each dimer may prove challenging due to the fact that these interactions likely occur indirectly through associations with a cargo-recognition sub-complex and due to difficulties in isolating the instance when interactions occur.

Snx30 regulates gastrulation and is important for cardiogenesis

To gain insight on Snx30 function during embryogenesis, we produced a knockdown phenotype using anti-sense morpholino (MO) oligonucleotides. A 25-mer morpholino was designed to complement the 5'-UTR sequence immediately upstream to the start codon (Snx30MO). The efficacy of our morpholino in preventing translation of Xenopus Snx30 was confirmed by co-injecting GFP-tagged Xenopus Snx30 mRNA (100ng) and Snx30MO (20ng), since we were

unable to obtain an appropriate antibody (Figure S5A). Embryos responded in a dose-dependent manner to Snx30MO: while 10ng produced no effect, 20ng decreased survival to about 30%, and 40ng was lethal (Figure S6). Co-injection of 100pg of human Snx30 mRNA in Snx30MO-treated (20ng) embryos increased survivability by about 20% but we were unable to completely rescue the Snx30MO phenotype (Figure S6). For all following morpholino analysis, 20ng of Snx30MO was used. The first defects appeared during gastrulation (Figure 3B, 3G), as blastopore closure defects, leading in some cases to the spilling out of cells (Movie M2). This stage was also marked by a sharp decrease in survival (Figure S6). From this point on, knockdown embryos were developmentally delayed (Figure 3A-3J, movie M1), shorter in length with anterior defects, including generalized malformations of the head and gut as well as ventral oedema (Figure 3E, 3J).

We next examined heart morphology in transverse cross-sections of Snx30MO-injected embryos at stage 42 (Figure 3K-3N). Snx30-knockdown embryos had many heart defects including a hypoplastic ventricle, poorly developed trabeculations, pericardial oedema, and an absent interatrial septum. In accordance, staining for Nkx2-5 transcripts, an early cardiac marker, was markedly reduced (Figure 4O, 4P).

Snx30 downregulates Wnt/β-catenin signaling by altering cell-surface expression of specific Wnt receptors

Since the Snx30 phenotype appeared at the onset of gastrulation with a delay in blastopore closure and that expression was in proximity to cardiac tissue, we looked at variations in gene expression of genes involved in Wnt/β-catenin signaling, known to be important during

gastrulation and cardiogenesis (1). In SNX30MO-treated embryos, genes upstream of β-catenin signaling were unaffected (Wnt3A, Wnt8 and β-catenin), however downstream target genes were upregulated (Xnr3, Siamois) (Figure 4A). Xnr3 remained activated up to stage NF19, whereas expression in controls was markedly reduced at stage NF15. Expression of Xbra, an early mesodermal marker and downstream target of Xnr3 (22), was also stronger in Snx30MO-treated embryos.

To validate the effect of Snx30 knockdown on Wnt/β-catenin signaling observed in Xenopus, we used stable HEK293T cells expressing the TOPflash β-catenin-dependent luciferase reporter (firefly luciferase and Renilla luciferase (HEK293T+TF) (23). These cells were infected with either Snx30 or control shRNAs via lentivirus (Figure S5B) and later co-transfected with each mouse Frizzled receptor (mFz1-10) and LRP5, and stimulated with WNT3A-conditionned medium. In control conditions (non-silencing shRNA), cells transfected with each of the ten Wnt Fz receptors activated β-catenin signaling in response to WNT3A stimulation (Figure 4B). In shRNA Snx30 cells, stimulation with WNT3A-conditioned medium significantly increased Wnt/β-catenin signaling for a subset of Fz receptors (Figure 4B). The effect of Snx30-knockdown was strongest in cells were transfected with Fz8 (25 fold increase), while no difference was observed in cells transfected with Fz1, Fz4 and Fz9. An important step in Wnt/β-catenin signaling is the inhibition of GSK3, which normally prevents the accumulation of cytoplasmic β-catenin (24). The Snx30 knockdown-dependent increase in Wnt/β-catenin signaling was also observed in HEK293T cells without the need for overexpression of Frizzled receptors (Figure S9). This supports the finding that Snx30 effects Wnt/β-catenin signaling with endogenous expression of sigaling components. Treatment of HEK293T+TF cells with non-specific (LiCl) (25), or specific (CHIR 99021) GSK3 inhibitors induced a stronger fold

activation of Wnt/β-catenin signaling upon Snx30 knockdown compared to controls (Figure 4D). This confirmed our previous observations that knockdown of Snx30 in Xenopus embryos increases expression of Wnt/β-catenin target genes (Xnr3 and Siamois).

An essential component of Wnt signaling is the localization of Wnt receptors at the cell surface to receive Wnt-mediated extracellular signaling and the subsequent sequestration of a LRP signalosome to multivesicular bodies (6). To determine whether Snx30 is involved in Frizzled receptor localization to the cell surface, we performed a biotinylation assay on HEK293T+TF cells transfected with either Fz4 or Fz8. In accordance with our previous results, knockdown of Snx30 did not change the localization of Fz4 (Figure 4C). On the other hand, we did observe reduced cell-surface expression of Fz8 (Figure 4C). In both cases, total protein levels of Fz4 and Fz8 appeared unchanged by knockdown of Snx30 (Figure 4C), suggesting that Snx30 is not responsible for degradation of the Fz receptors. Also, we did not find any direct physical interaction between either Fz4 or Fz8 and Snx30, using GFP-trap pull-down (Figure S7).

These results suggest that knockdown of Snx30 in Xenopus embryos caused a delay in the inhibition of Wnt/β-catenin usually observed during gastrulation and required for cardiogenesis (1). The appearance of gastrulation defects in Snx30MO-treated embryos coincides with the upregulation of Wnt/β-catenin target genes, Xnr3 and Siamois, and immediately follows the peak in XSnx30 expression observed by RT-PCR. In addition, the upregulation of Xbra and the reduced Nkx2-5 staining denotes overactive Wnt/β-catenin signaling, as the activation of this pathway is required for mesoderm specification followed by inhibition for cardiac specification (1, 2). Although we detected strong expression of Snx30 in later stages of heart development such as chamber formation, we did not evaluate expression of downstream target genes due to technical difficulties in isolating heart tissue from Xenopus embryos. Nevertheless, the role

of Snx30 in regulating Wnt/β-catenin signaling in later stages of cardiogenesis may hold as Wnt/β-catenin signaling could still undergo phases of activation/inhibition.

The increased signaling for certain Fz receptors in Snx30-knockdown cells might be due to the specificity of Snx30 towards these receptors and may be a fine-tuning mechanism of Wnt signaling. In the case of Fz1, Fz4 and Fz9, for which knockdown of Snx30 had no significant effect, Snx30 might not be implicated in sorting these receptors. Alternatively, stimulation of these receptors with Wnt3A could induce the use of Snx30-independent routes, while stimulation with another ligand might recruit Snx30. The increase in Wnt/β-catenin signaling observed upon Snx30 knockdown in cells treated with both GSK3 inhibitors (LiCl and CHIR 99021) indicates that Snx30 regulates Wnt signaling independently of GSK3 and that knockdown of Snx30 acts synergistically with these inhibitors to increase signaling.

Here, we found that Snx30 can influence the localization of Fz8, as shown by reduced cell-surface expression of this receptor in Snx30-knockdown cells. This was specific to Fz8 as no effect was observed with Fz4, which was neither affected by Snx30 knockdown in our TOPflash assay. It is likely that upon Wnt3a stimulation, Fz8 is sequestered to in Xenopus embryos MVBs as part of a LRP6/GSK3 signalosomes (6). The fate of Fz and LRP after their passage in MVBs is still unknown. A common fate of proteins found in these compartments is degradation. However, after Wnt stimulation, levels of GSK3 do not drop suggesting an alternative fate (6). Another possibility is that intralumenal vesicles may be recycled back into the cytosol by “back-fusion” to the late endosome limiting membrane (26). If this is the case for LRP6 signalosomes, Snx30 would be a likely candidate for mediating this type of sorting. In agreement, Wnt3a stimulation induced a relocalization of SNX30-GFP to intralumenal vesicles of giant endosomes (induced by expression of RAB5QL-dsRed) (Figure S8). We speculate that Snx30 may sort

specific Fz receptors out of MVBs, thereby disrupting the LRP6 signalosome and releasing GSK3 back into the cytoplasm. This would explain a simultaneous decrease of Fz8 at the cell surface and increase in Wnt/β-catenin signaling, upon Snx30 knockdown. The synergistic effect of Snx30 knockdown in Wnt/β-catenin signaling for cells treated with GSK3 inhibitors could be due to the presence of certain Fz receptors in MVBs, which unable to exit due to inefficient sorting, although this requires confirmation.

Taken together, our results show that Snx30 plays a negative role in Wnt/β-catenin signaling during gastrulation possibly by regulating the localization of specific Fz receptors within the cell. The localization of Snx30 in multivesicular bodies suggests a function in sorting Fz receptors from this compartment. We thus propose that Snx30 contributes to the biphasic nature of Wnt/β-catenin signaling that occurs during early cardiogenesis (1). As cell-based therapies continue to make progress, understanding every step of cardiac differentiation is essential to apply these techniques in clinical settings.

Materials and Methods

Cloning of Gateway Entry and Expression clones

All expression clones were generated with the Gateway cloning system (Invitrogen). Entry clones were produced using a two-step Gateway cloning procedure (27): 1) open reading frames (ORF) were amplified from cDNA clones (human Snx4: BC018762; human Snx30: BC165765; X. laevis Snx30: IMAGE 6868636 – Open Biosystems) for 11 cycles using gene-specific primers, and 2) 5μL of step-1 PCR products were used as template for amplification (24 cycles) of target sequence with step-2 primers (Table S1). Reverse primers were designed

to produce an ORF with or without a stop codon, thus allowing the production of N- or C-terminal fusion proteins. Clones were sequenced (Sanger) at the McGill University and Génome Québec Innovation Center. PCR products were purified by gel extraction (QIAguick gel extraction kit, QIAGEN) and used in recombination reactions according to manufacturer protocol.

Expression plasmids were made by recombinations between entry clones and the following destination clones: pDS-X-GFP (C-terminal GFP, ATCC: 1032336345), pDS-GFP-X (N-terminal GFP, ATCC: 1032336345), pcDNA3.1_nV5-DEST (N-terminal V5 tag, Invitrogen), pDEST565 (N-terminal GST tag, Addgene), pDEST_CS-CeGFP (C-terminal eGFP tag). pDEST_CS-CeGFP was made by amplifying eGFP from pEGFP-N1 and inserted into pCS-DEST (a generous gift from Nathan Lawson) with XhoI and XbaI restriction enzymes.

Whole-mount in situ hybridization

All animals were handled in accordance with the guidelines of the Sainte-Justine Hospital bioethics committee. X. laevis embryos were generated by in vitro fertilization, their handling, culture, and staging followed standard procedures (28). Whole-mount in situ hybridization was performed as described (29) using digoxygenin-UTP-labeled probes (Roche). For antisense DIG-labeled RNA probes, pEXP-CS_Xsnx30 was linearized with BglII (T3), and pCS-Xnkx2-5 was linearized with HindIII (T7) (Fermentas). Probes were detected with the DIG detection kit (Roche) according to the manufacturer's manual. Fertile chicken (Gallus gallus) eggs were obtained from Hy-Line International (Spencer, IA) and incubated 37°C in a humid environment until the desired Hamburger-Hamilton stage (1951, 1992). Embryos were fixed in 4%

paraformaldehyde in PBS overnight at 4ºC. In situ hybridizations were performed as described (30) with minor modifications (protocol available at http://geisha.arizona.edu). The antisense DIG-labeled RNA probe for SNX30 was transcribed from a cDNA template corresponding to nt 20-830 of the chicken SNX30 mRNA sequence (XM_424910).

RT-PCR (Xenopus) and RT-qPCR (human)

Total Xenopus RNA was extracted with TRIzol reagent (Invitrogen) from three stage-matched embryos at indicated stages. Primer sequences for the following genes can be found in Table S1: β-catenin, Brachyury (Xbra), Nkx2-5, Nodal-related 3 (Xnr3), Ornithine decarboxylase (ODC), Siamois (Sia), Sorting nexin-30 (Xsnx30), Wnt3A, Wnt8.

Total human RNA was prepared and treated with RNase-free DNase (Ambion). 500 ng to 1 µg of RNA was reverse transcribed into cDNA using random hexamers and Oligo (dT) with Superscript III Reverse Transcriptase (Invitrogen). QPCR was performed on a MasterCycler EP RealPlex (Eppendorf) using QuantiFast SYBR Green PCR Kit (Qiagen). Expression levels were normalized to the housekeeping gene TATA box binding protein (TBP). In addition to TBP for normalization across samples, genomic DNA was used as a DNA standard. The y axis of RT-qPCR graphs represents copy numbers of the gene of interest divided by copy numbers of TBP, and therefore is an arbitrary but absolute unit, that can be compared between experiments. Error bars represent standard error of the mean (s.e.m.).

Immunohistochemistry

HEK293T cells were seeded on Poly-L-lysine-coated coverslips in 12-well plates and fixed in methanol for 10 minutes at 4˚C, blocked for 1 hour at room temperature in blocking buffer (TBS/5% fat-free milk/5% goat serum) and incubated overnight with primary antibodies at 4˚C. Cells were washed 3 x 5 minutes in TBS and incubated 1 hour at room temperature with secondary antibody (1:1000) in blocking buffer (Alexa 594 anti-rabbit, anti-mouse, Invitrogen). Cells were washed 3x 5 minutes and placed on microslides with ProLong Gold antifade reagent (Invitrogen). Pictures were taken on a ImageDisc confocal microscope.

Antibodies

Anti-SNX30 (HPA019346), anti-EEA-1 (HPA03158) and anti-GST (G 1160) antibodies were from Sigma. Anti-Vps26 (ab23892), anti-Vps35 (ab57632), anti-, anti-LAMP1 (ab24178), and anti-M6PR (ab2733) antibodies were from Abcam. Anti-V5 (MA1-81617) antibodies were from ThermoScientific. Anti-Rab9 (sc-53145) and anti-Rab11 (sc-166523) antibodies were from Santa Cruz. Anti-1D4 antibody was a generous gift from Jeremy Nathans.

Antisense morpholinos, RNA transcription and microinjection

Antisense morpholino oligonucleotides were designed and manufactured by Gene Tools LLC. The antisense 25-mer morpholino for Xsnx30 was designed against the 5'UTR immediately preceding the start codon (5'-GTTTTTGTACCTCCCAGCACTCACA-3'). As a control, a 25-mer morpholino with no target and no significant biological activity was used (5'-

CCTCTTACCTCAGTTACAATTTATA-3'). Morpholinos were injected in stage 1 embryos after fertilization. Only the embryos that went on to stage 2 were used and accounted for during all experiments. Comparisons between Snx30MO- and CtlMO-treated embryos were done in same-fertilization batches to avoid non-specific effects. Capped RNAs were transcribed in vitro using the mMessage mMachine kit (Ambion) from the pEXP-CS_Xsnx30-3UTR clone. We injected 100pg of Snx30 RNA into stage 1 embryos.

Biotinylation

Biotinylation was performed as previously described (31). Briefly, cells were washed with ice-cold PBS/CM (1x PBS, 0.9mM CaCl2, 0.33mM MgCl2) and incubated with PBS/CM + 0.5mg/mL Sulfo-NSH-SS-biotin (Fisher, PI21331). After quenching with PBS/CM + 50mM NH4Cl, cells were lysed in 500µL ice-cold lysis buffer (50mM Tris-Cl, pH 8.0, 1.25% Triton X-100, 0.25% SDS, 150mM NaCl, 5mM EDTA and 10µg/mL PMSF). Biotinylated proteins were immobilized on streptavidin beads (GE Healthcare) and separated on SDS-PAGE. Vectors for mouse Frizzled receptors, pRK5_Fz1-10, pRK5_Fz4-1D4 and pRK5_Fz8-1D4, were obtained as a generous gift from Jeremy Nathans (32).

GFP-Trap

HEK293 cells were co-transfected with pEXP_V5-SNX30 or pEXP_V5-SNX4 and SNX30-GFP or pEXP_SNX4-GFP, SNX30-GFP and Fz4-1D4 or Fz8-1D4 and harvested 48h later for GFP co-immunopurification. GFP-tagged proteins purified from cellular extracts by GFP-trap_M

(Chromotek, Martinsried, Germany) following the manufacturer's manual. Purified samples were separated on SDS-PAGE and co-immunopurification of GFP- and V5-tagged constructs, Fz4/8-1D4, Vps26 and Vps35 were determined by Western blot.

Lentivirus production

The lentiviruses encoding shRNAs against human and mouse Snx30, and control vector were purchased from OpenBiosystems (pGIPZ-shRNA_hSnx30-338031 and pGIPZ-shRNA_mSnx30-86452, pGIPZ). Viruses were produced as described previously (33) and titers adjusted when necessary to achieve ~90% infectivity.

TOPflash reporter assay

HEK293T cells stably expressing the β-catenin-dependent luciferase reporter (firefly luciferase) and Renilla luciferase (23) (under the control of the constitutive EF1α promoter as a normalization probe) were infected with Snx30 lentivirus. Conditioned media were produced as previously described (23). Briefly, mouse L cells expressing Wnt3A (CRL-2647) were cultured to 100% confluence, after which the medium was harvested and replaced every 2 days for a total of 6 days. Medium from different days was assayed by using the TOPflash reporter assay and fractions with greatest activation were pooled and subsequently used for stimulation experiments. Conditioned medium from parental mouse L cells not producing Wnt3A (CRL-2648) was produced in parallel and used as control. Cells were transfected with Fz receptors (pRK5-Fz1 to -10, a generous gift from Jeremy Nathans) and LRP5 (pRK5-LRP5), and

stimulated with conditioned media 48h after. Stimulated cells were assayed 24h after stimulation according to the dual luciferase protocol (Promega) using an Envision plate reader (Perkin-Elmer). The GSK3β inhibitors LiCl and CHIR 99021 (Selleckchem, S1263) were used to activate the TOPflash reporter. Cells were treated with LiCl or CHIR 99021 for 24h prior to performing the dual luciferase assay (Promega).

Protein-lipid overlay assay

The expression clone pEXP565-hSnx30 was transformed into E. coli BL21 and expression of the GST-tagged construct was induced with 1mM IPTG. Purification was performed with the MagneGST system (Promega). Purified proteins were incubated (1µg/mL) with PIP Strips (Echelon-inc) according to manufacturer protocol. Binding to phospholipids was detected by Western blot using anti-GST antibody.

Tandem Affinity Purification

SNX30 was cloned into a mammalian expression vector (pCTAP-A) that has a C-terminal TAP-tag composed of a streptavidin-binding protein and a calmodulin-binding protein (InterPlay Mammalian TAP System, Stratagene). HEK293T cells were transfected with pCTAP_SNX30 and with the empty vector as a negative control (pCTAP-A). Tagged proteins were purified according to manufacturer protocol, separated on SDS-PAGE and silver-stained. A single band only present in our Snx30-TAP sample was cut, digested (trypsin) and analyzed by mass

spectrometry LC-MS/MS (Institute for Research in Immunology and Cancer). Proteins were identified with the MASCOT database.

Statistical analysis

Data are expressed as mean ± standard deviation. Differences were considered significant if $p<0.05$ threshold.

Acknowledgements

We would like to thank Robert Hamilton and Linn Strandberg for assistance in obtaining fetal tissue samples. We would also like to thank Stéphane Angers, Gilles Hickson, Gregory Emery and Carl Laflamme for their help, and Jeremy Nathans for providing us with the Fz and Lrp plasmids. The authors confirm that they have not conflicts of interest to declare.

References

1. Gessert S, Kuhl M. The multiple phases and faces of wnt signaling during cardiac differentiation and development. Circulation research 2010;107(2):186-199.

2. Nakajima Y, Sakabe M, Matsui H, Sakata H, Yanagawa N, Yamagishi T. Heart development before beating. Anatomical science international 2009;84(3):67-76.

3. Barker N, Clevers H. Catenins, Wnt signaling and cancer. BioEssays : news and reviews in molecular, cellular and developmental biology 2000;22(11):961-965.

4. Monroe DG, McGee-Lawrence ME, Oursler MJ, Westendorf JJ. Update on Wnt signaling in bone cell biology and bone disease. Gene 2012;492(1):1-18.

5. Zhu W, Shiojima I, Ito Y, Li Z, Ikeda H, Yoshida M, Naito AT, Nishi J, Ueno H, Umezawa A, Minamino T, Nagai T, Kikuchi A, Asashima M, Komuro I. IGFBP-4 is an inhibitor of canonical Wnt signalling required for cardiogenesis. Nature 2008;454(7202):345-349.

6. Taelman VF, Dobrowolski R, Plouhinec JL, Fuentealba LC, Vorwald PP, Gumper I, Sabatini DD, De Robertis EM. Wnt signaling requires sequestration of glycogen synthase kinase 3 inside multivesicular endosomes. Cell 2010;143(7):1136-1148.

7. Dobrowolski R, Vick P, Ploper D, Gumper I, Snitkin H, Sabatini DD, De Robertis EM. Presenilin deficiency or lysosomal inhibition enhances Wnt signaling through relocalization of GSK3 to the late-endosomal compartment. Cell reports 2012;2(5):1316-1328.

8. Cullen PJ. Endosomal sorting and signalling: an emerging role for sorting nexins. Nature reviews Molecular cell biology 2008;9(7):574-582.

9. Seet LF, Hong W. The Phox (PX) domain proteins and membrane traffic. Biochimica et biophysica acta 2006;1761(8):878-896.

10. van Weering JR, Verkade P, Cullen PJ. SNX-BAR proteins in phosphoinositide-mediated, tubular-based endosomal sorting. Seminars in cell & developmental biology 2010;21(4):371-380.

11. Frost A, Unger VM, De Camilli P. The BAR domain superfamily: membrane-molding macromolecules. Cell 2009;137(2):191-196.

12. Sakane H, Yamamoto H, Kikuchi A. LRP6 is internalized by Dkk1 to suppress its phosphorylation in the lipid raft and is recycled for reuse. Journal of cell science 2010;123(Pt 3):360-368.

13. Teasdale RD, Collins BM. Insights into the PX (phox-homology) domain and SNX (sorting nexin) protein families: structures, functions and roles in disease. Biochem J 2012;441(1):39-59.

14. van Weering JR, Sessions RB, Traer CJ, Kloer DP, Bhatia VK, Stamou D, Carlsson SR, Hurley JH, Cullen PJ. Molecular basis for SNX-BAR-mediated assembly of distinct endosomal sorting tubules. The EMBO journal 2012;31(23):4466-4480.

15. Letunic I, Doerks T, Bork P. SMART 7: recent updates to the protein domain annotation resource. Nucleic acids research 2012;40(Database issue):D302-305.

16. Schultz J, Milpetz F, Bork P, Ponting CP. SMART, a simple modular architecture research tool: identification of signaling domains. Proc Natl Acad Sci U S A 1998;95(11):5857-5864.

17. Teasdale RD, Loci D, Houghton F, Karlsson L, Gleeson PA. A large family of endosome-localized proteins related to sorting nexin 1. Biochem J 2001;358(Pt 1):7-16.

18. De Matteis MA, Godi A. PI-loting membrane traffic. Nat Cell Biol 2004;6(6):487-492.

19. Cullen PJ, Korswagen HC. Sorting nexins provide diversity for retromer-dependent trafficking events. Nat Cell Biol 2012;14(1):29-37.

20. Kurten RC, Cadena DL, Gill GN. Enhanced degradation of EGF receptors by a sorting nexin, SNX1. Science 1996;272(5264):1008-1010.

21. Wang Y, Zhou Y, Szabo K, Haft CR, Trejo J. Down-regulation of protease-activated receptor-1 is regulated by sorting nexin 1. Molecular biology of the cell 2002;13(6):1965-1976.

22. Haramoto Y, Takahashi S, Asashima M. Monomeric mature protein of Nodal-related 3 activates Xbra expression. Development genes and evolution 2007;217(1):29-37.

23. Lui TT, Lacroix C, Ahmed SM, Goldenberg SJ, Leach CA, Daulat AM, Angers S. The ubiquitin-specific protease USP34 regulates axin stability and Wnt/beta-catenin signaling. Molecular and cellular biology 2011;31(10):2053-2065.

24. Niehrs C. The complex world of WNT receptor signalling. Nature reviews Molecular cell biology 2012;13(12):767-779.

25. Klein PS, Melton DA. A molecular mechanism for the effect of lithium on development. Proc Natl Acad Sci U S A 1996;93(16):8455-8459.

26. Falguieres T, Luyet PP, Gruenberg J. Molecular assemblies and membrane domains in multivesicular endosome dynamics. Experimental cell research 2009;315(9):1567-1573.

27. Hartley JL, Temple GF, Brasch MA. DNA cloning using in vitro site-specific recombination. Genome research 2000;10(11):1788-1795.

28. Sive HL, Grainger, R.M., Harland, R.M. Early development of Xenopus laevis. A laboratory manual. New York: Cold Spring Harbor Laboratory Press; 2000.

29. Harland RM. In situ hybridization: an improved whole-mount method for Xenopus embryos. Methods in cell biology 1991;36:685-695.

30. Nieto MA, Patel K, Wilkinson DG. In situ hybridization analysis of chick embryos in whole mount and tissue sections. Methods in cell biology 1996;51:219-235.

31. Morimoto S, Nishimura N, Terai T, Manabe S, Yamamoto Y, Shinahara W, Miyake H, Tashiro S, Shimada M, Sasaki T. Rab13 mediates the continuous endocytic recycling of occludin to the cell surface. The Journal of biological chemistry 2005;280(3):2220-2228.

32. Yu H, Ye X, Guo N, Nathans J. Frizzled 2 and frizzled 7 function redundantly in convergent extension and closure of the ventricular septum and palate: evidence for a network of interacting genes. Development (Cambridge, England) 2012;139(23):4383-4394.

33. Beausejour CM, Krtolica A, Galimi F, Narita M, Lowe SW, Yaswen P, Campisi J. Reversal of human cellular senescence: roles of the p53 and p16 pathways. The EMBO journal 2003;22(16):4212-4222.

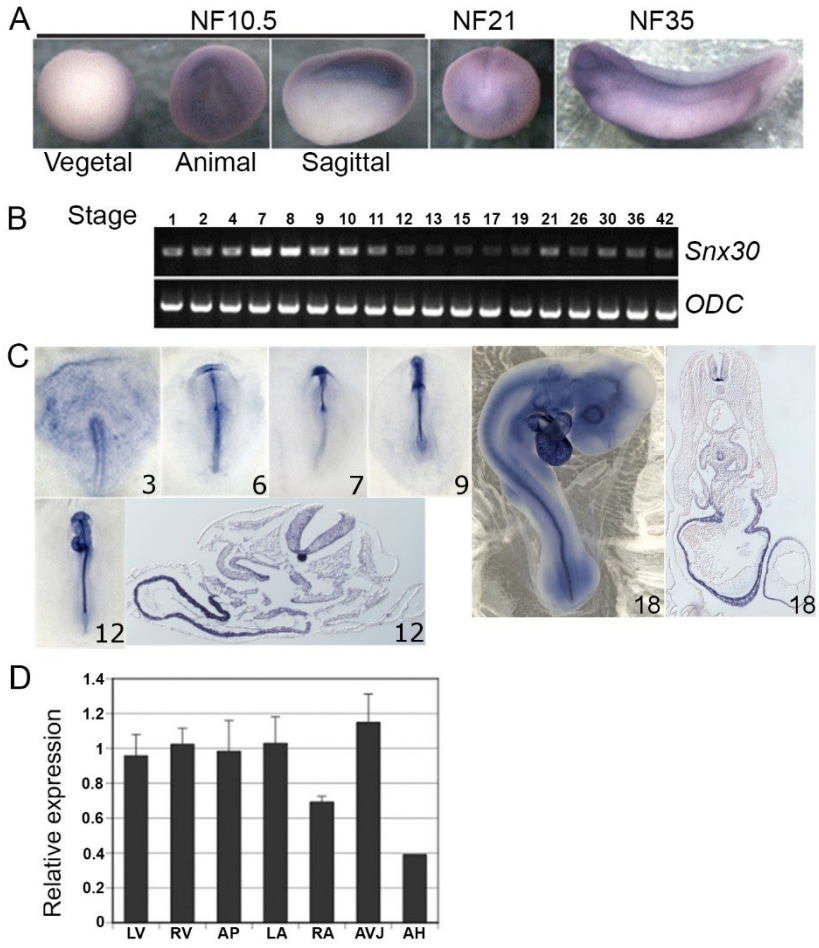

Figure 1. Expression profile of Snx30 in Xenopus laevis and Gallus gallus. A) In situ hybridization in X. laevis shows expression in the animal pole at NF10.5, in latero-anterior mesoderm tissue at NF21 and in head and heart (arrow) at NF35. B) RT-PCR of Xenopus laevis Snx30 shows expression throughout development with increased expression at stages NF7-11 (ODC was used as control) C) In situ hybridization in Gallus gallus embryos at indicated stages shows Snx30 expression in the primitive streak, early mesoderm, heart tube, neural tube and notochord. At stage 12 and 18, expression was strongest in the heart and notochord. D) RT-qPCR analysis for Snx30 in human fetal heart tissue and adult heart. LV, left ventricle; RV, right ventricle; AP, Apex; LA, left atria; RA, right atria, AVJ, atrioventricular junction; AH, adult heart. Error bars represent s.e.m., n = 6.

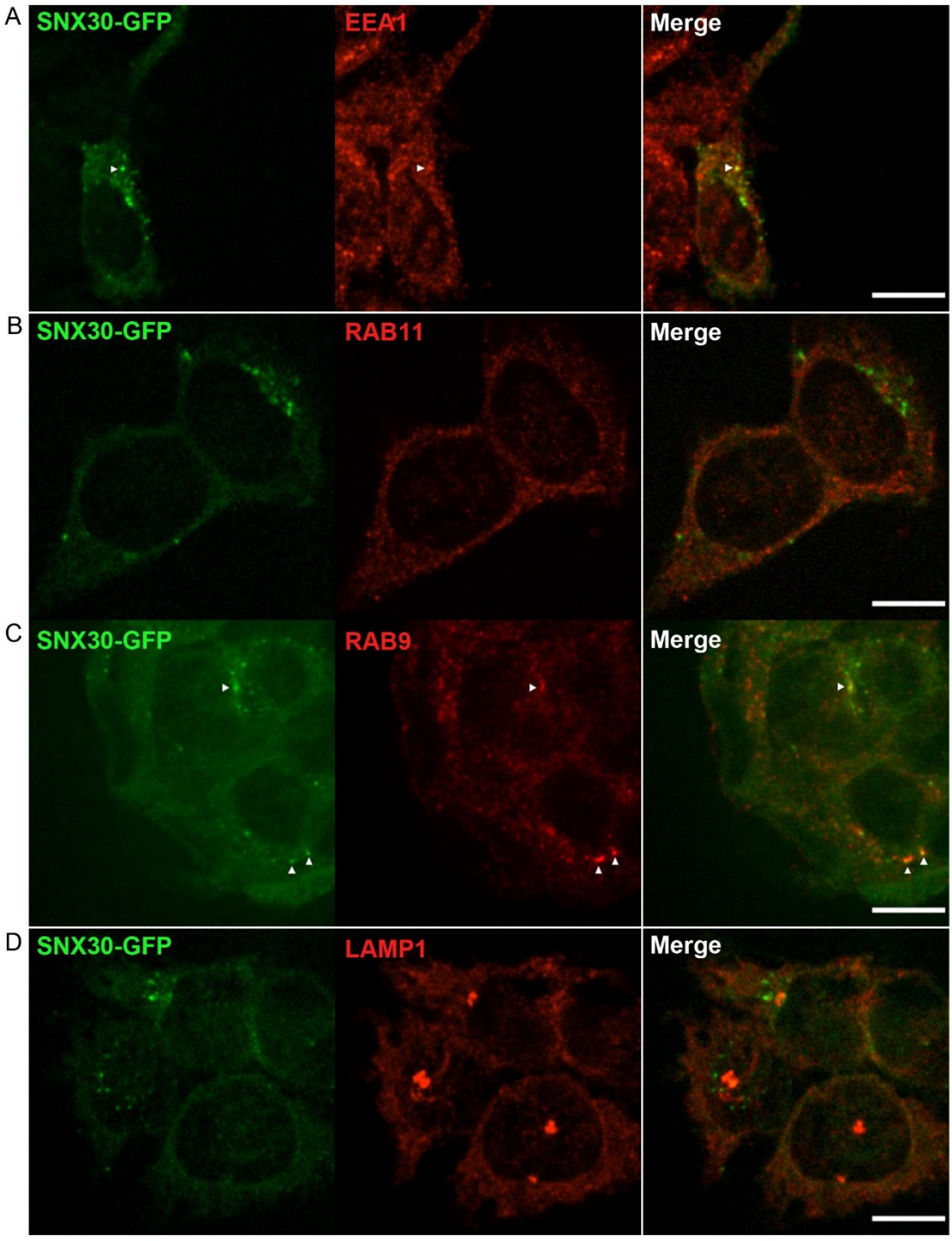
A
SNX30-GFP
EEA1
Merge
B
SNX30-GFP
RAB11
Merge
C
SNX30-GFP
RAB9
Merge
D
SNX30-GFP
LAMP1
Merge

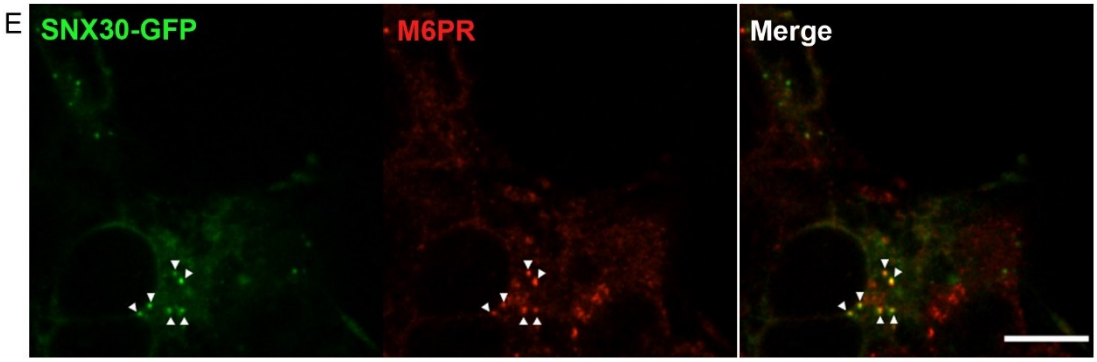

Figure 2. Intracellular localization of SNX30-GFP in HEK293T cells. HEK293T cells transfected with pEXP- SNX30-GFP were stained using markers of specific intracellular compartments (red). These markers were A) EEA1 (early endosome), B) RAB11 (recycling endosomes), C) RAB9 (multivesicular bodies), D) LAMP1 (lysosomes), and M6PR (multivesicular bodies). The panels on the right are merged channels and a yellow signal indicates co-localization (arrows). Scale bar = 10μm.

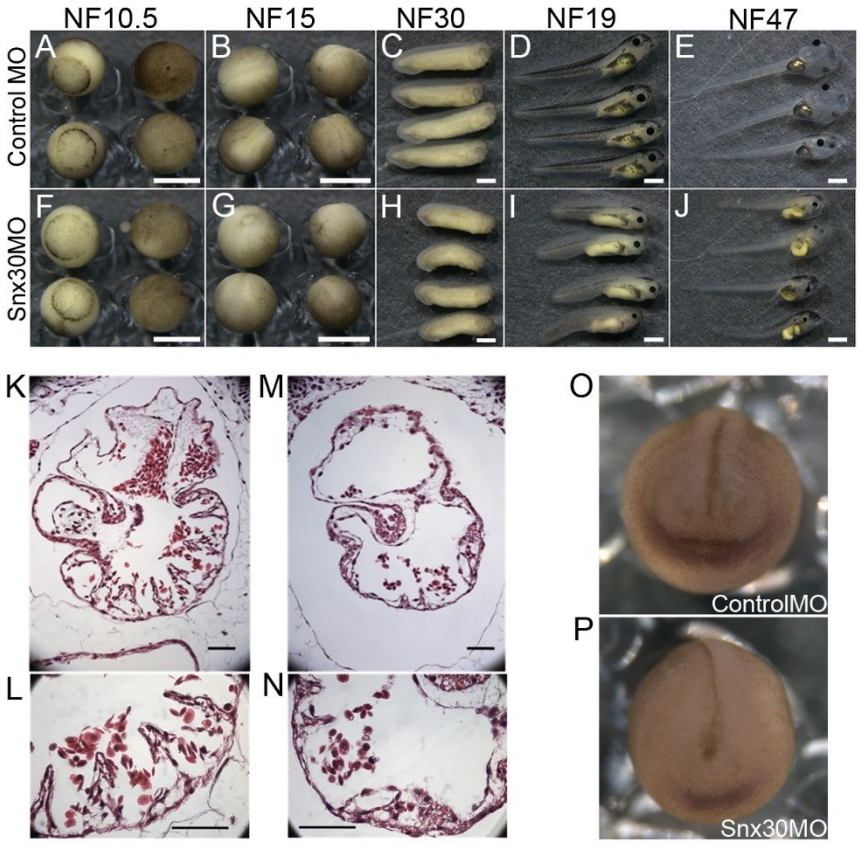

Figure 3. Phenotype of Snx30 knockdown in X. laevis. A-J) Single-cell embryos injected with Snx30 morpholino were developmentally delayed, starting after gastrulation. Embryos were shorter in length with anterior defects (scale = 1mm). K-N) Heart morphology in control embryos (K, L) vs Snx30 knockdown embryos (M, N) (scale = 25μm). Knockdown of Snx30 caused pericardial oedema, hypoplastic ventricle, absent interatrial septum, poorly formed trabeculations (M). Trabeculations were normal in controls (L) but almost inexistent in Snx30 knockdown embryos (N). O,P) Nkx2-5 staining by in situ hybridization was reduced in SNX30MO-treated embryos at stage NF21 compared to controls.

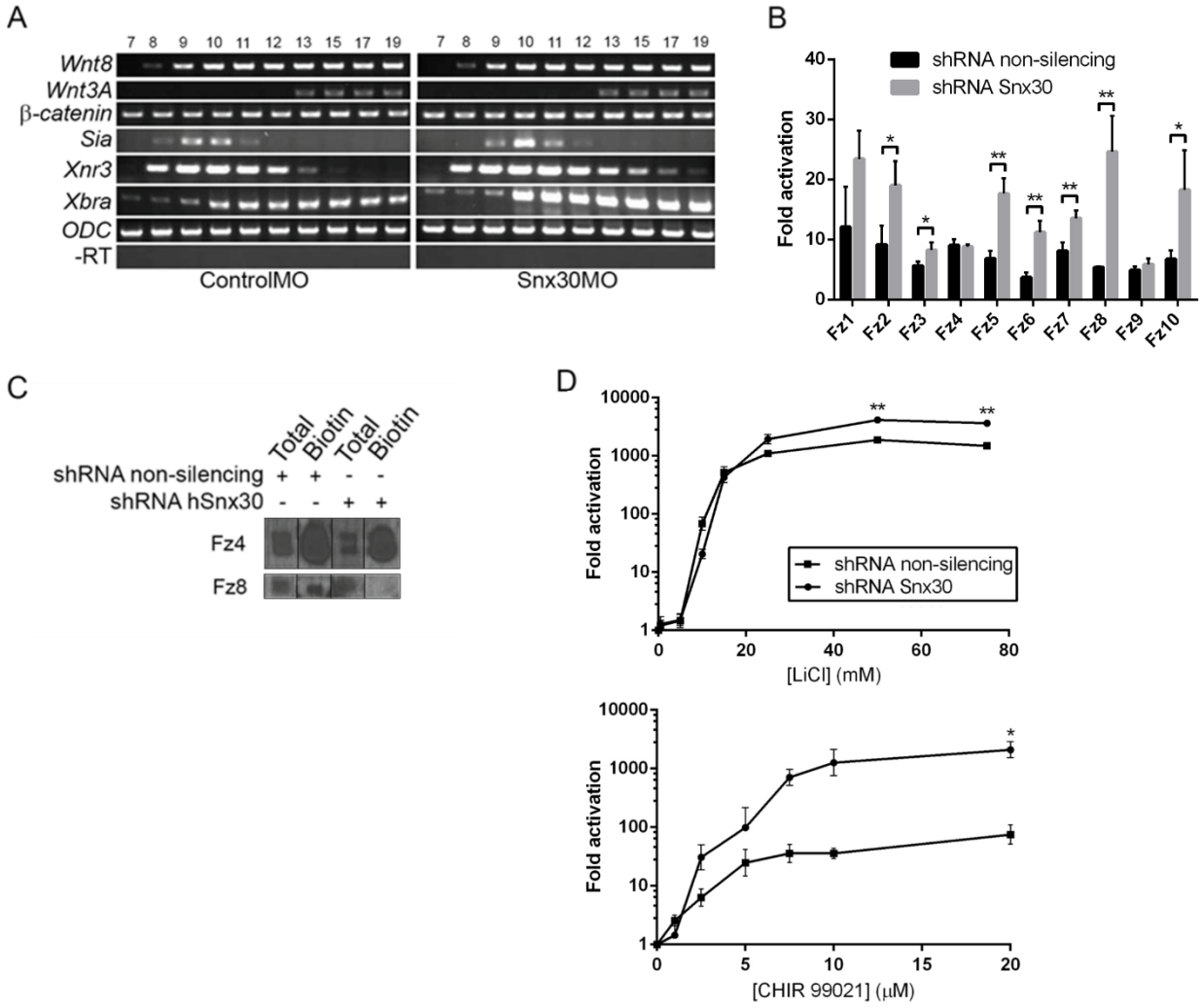

Figure 4. Effect of Snx30 knockdown on Wnt/β-catenin signaling. A) RT-PCR analysis of genes involved in Wnt/β-catenin signaling. The β-catenin targets *Siamois* and *Xnr3* were upregulated as well as the mesoderm marker *Xbra*. Expression of Wnt8, Wnt3A and β-catenin were unaffected. B) HEK293T cells stably expressing the β-catenin-dependent luciferase reporter (TOPflash) and either non-silencing or hSnx30 shRNA were co-transfected with each of the ten Frizzleds (Fz1-10) and LRP5. Fold activation of Wnt/β-catenin signaling after stimulation with Wnt3A is shown (n = 9). C) Cell-surface expression of Fzd4 and Fzd8 was assessed by biotinylation and subsequent isolation with streptavidin beads. Compared to controls, knockdown of Snx30 reduced cell-surface expression of Fz8 (6% band density compared to control) while that of Fz4 (123% band density compared to control) remained unchanged. D)

Treatment of HEK293T+TF cells with increasing doses of the non-specific (LiCl) and specific (CHIR 99021) GSK3 inhibitors caused a stronger fold activation of Wnt/β-catenin signaling in Snx30-knockdown cells than in controls (n = 3). *p<0.05, **p<0.01, error bars represent standard deviation.

Cameron_Supplemental Movie M1

Live cell imaging of SNX30-GFP. SNX30-GFP is mobile inside the cell. Each frame represents a 5 minute time-lapse. Scale bar = 6μm.

Cameron_Supplemental Movie M2

Time-lapse of gastrulation and neurulation up to stage Nieuwkoop-Faber 35 in Snx30 knockdown versus normal controls (Xenopus laevis).

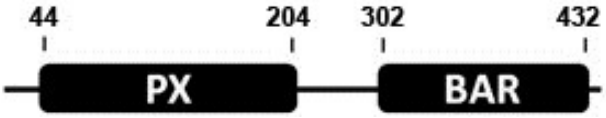

Figure S1. SNX30 protein structure. Amino acid positions are indicated at the start and end of each predicted protein domain.

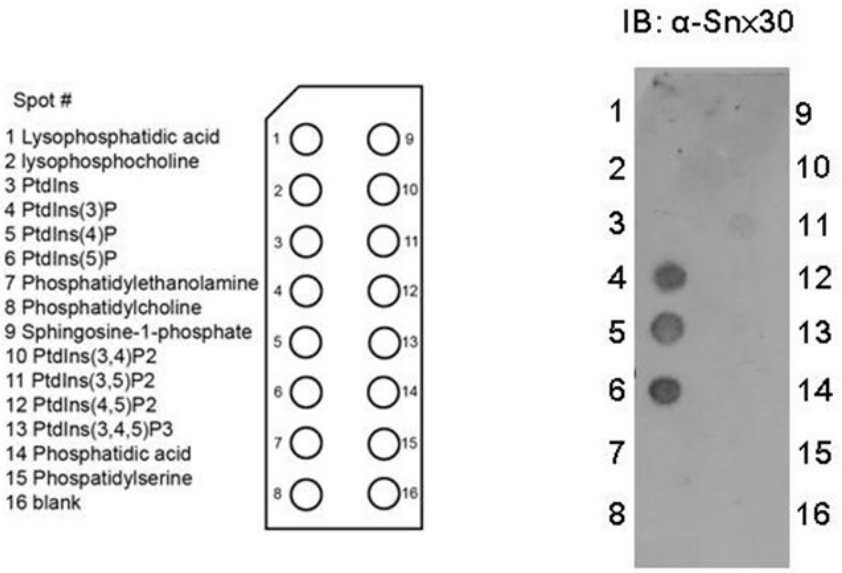

Figure S2. Lipid overlay assay. Purified GST-SNX30 from bacterial culture was incubated with a PIP-strip (Echelon). SNX30 bound to PtdIns(3)P, PtdIns(4)P and PtdIns(5)P.

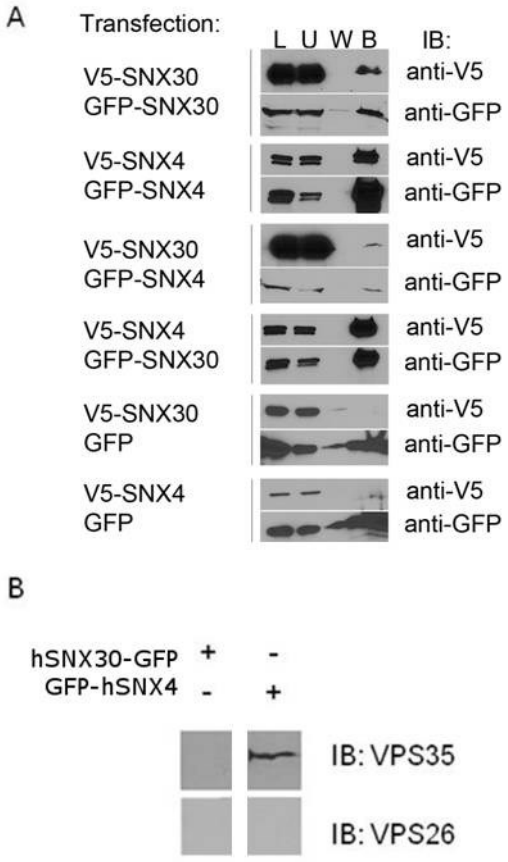

Figure S3. Co-immunoprecipitation of SNX30 and SNX4. A) GFP-trap was used to immunoprecipitate GFP-SNX30 or GFP-SNX4 from cell lysates transfected with V5-tagged or GFP-tagged constructs (L: load; U: unbound; W: wash; B: bound). In all conditions, SNX30 and SNX4 homo- and hetero-dimerize. GFP was used as a negative control. B) Interactions between SNX4/30 with endogenous retromer components VPS35 and VPS26 were evaluated. Only SNX4 bound to VPS35.

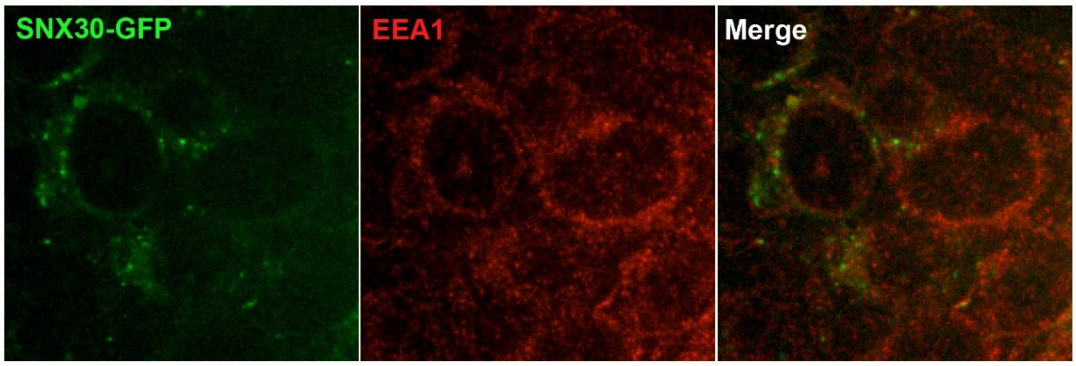

Figure S4. Distribution of SNX30-GFP and SNX4 in HEK293T cells. HEK293T cells were transfected with SNX30-GFP and stained with anti-SNX4 antibody. No co-localization was seen between SNX30-GFP and SNX4.

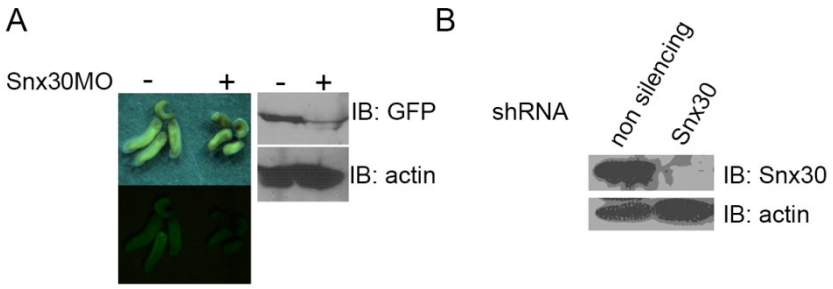

Figure S5. Proof of Snx30 knockdown. A) Proof of knockdown in X. laevis injected with GFP-SNX30 capped mRNA (100ng). Left panel shows reduced GFP expression in Snx30MO-treated embryos. Right panel shows reduced expression as shown by Western blot. B) HEK293T cells were infected via lentivirus with shRNAs (non-silencing and Snx30). shRNA-Snx30 was effective at reducing endogenous protein expression.

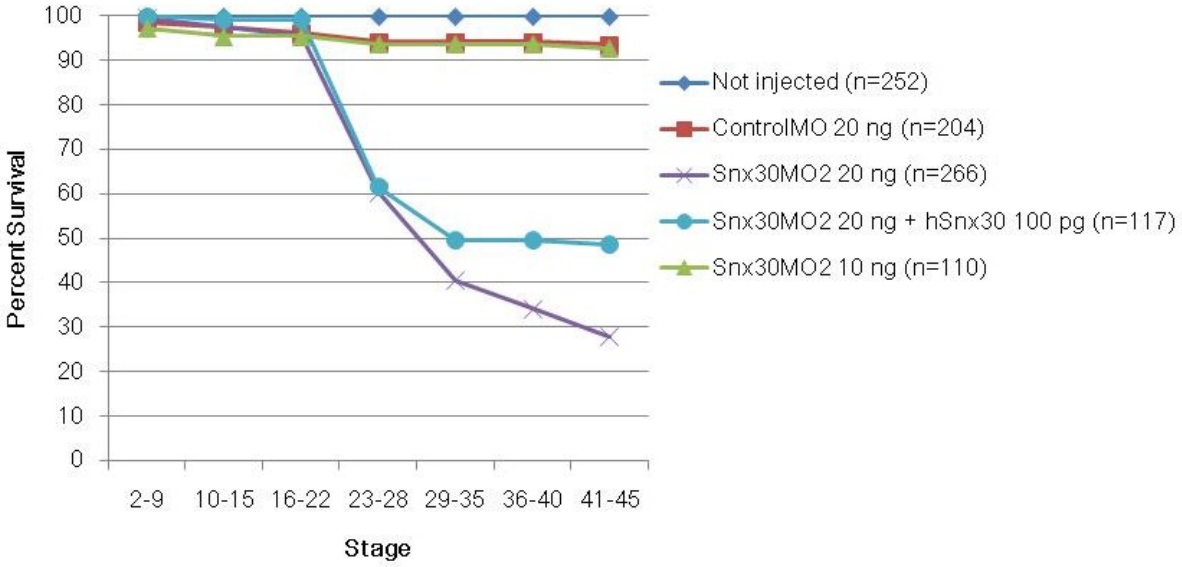

Figure S6. Survival curve of one-cell X. laevis embryos injected with indicated morpholinos.

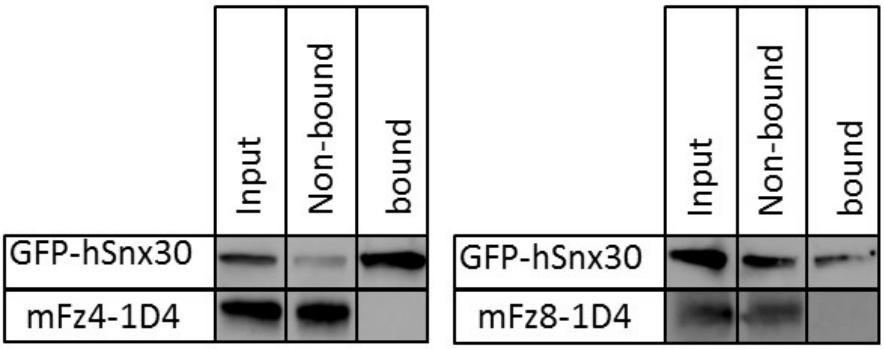

Figure S7. GFP-trap of SNX30 and Fz4/Fz8. This pull-down experiment shows the lack of physical interaction between SNX30 and the Wnt receptors Fz4 and Fz8.

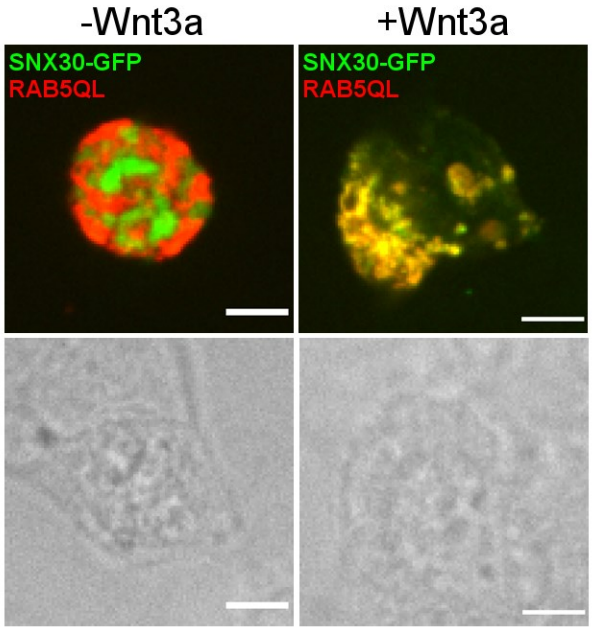

Figure S8. Confocal analysis of SNX30 localization upon Wnt stimulation. Top panel: green, SNX30-GFP; red, RAB5QL-dsRed. Bottom panel: DIC photograph providing cell contours. SNX30-GFP localizes to intralumenal vesicles after stimulation with Wnt3a. Cells transfected with RAB5QL-dsRed and SNX30-GFP were treated with control and Wnt3a conditioned medium for 4 hours. Cells were then fixed and observed with a confocal microscope. After stimulation with Wnt3a, SNX30-GFP localized to the intralumenal vesicles of giant endosomes created by expression of RAB5QL (6).

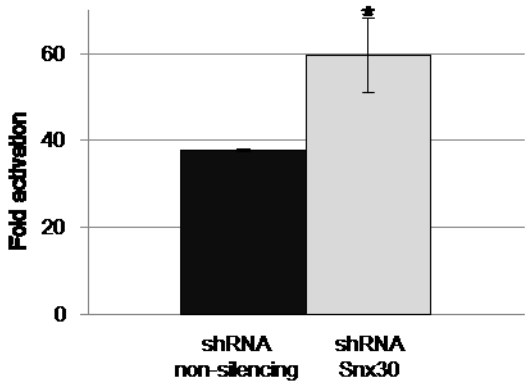

Figure S9. Knockdown of Snx30 (shRNA Snx30) increases Wnt/β-catenin signaling. TOPflash HEK293T treated with either shRNA non-silencing or shRNA Snx30 were treated with Wnt3A-conditioned medium and assayed for activation of the Wnt/β-catenin signaling using a dual luciferase assay. (* $p < 0.05$)

Table 1. Primer sequences (S: sense, AS: antisense; Y corresponds to T or C).

Gene	Primers
β-catenin	S: 5'-CACACTGGCCTTTGATAAAG-3'
	AS: 5'-TTCAACAATCTCCTCCATGC-3'
Human *Snx4*	S: 5'-GGCTCCACCATGGCGGGCGGGCCCCCC-3'
	AS: 5'-TGGGTGGATYCACTTGGCCTCTTGTTTCTCC-3'
Human *Snx30*	S: 5'-GGCTCCACCATGGCGGGCGGGCCCCCC-3'
	AS: 5'-TGGGTGGATYCACTTGGCCTCTTGTTTCTCC-3'
Siamois	S: 5'-AAGATAACTGGCATTCCTGAGC-3'
	AS: 5'-GGTAGGGCTGTGTATTTGAAGG-3'
Wnt3A	S: 5'-CTGGGGAAGGCTGGAAGTG-3'
	AS: 5'-TTGGGGGAGCTCTCATAGTAAATC-3'
Wnt8	S: 5'-AGATGACGGCATTCCAGA-3'
	AS: 5'-TCTCCCGATATCTCAGGA-3'
Xbra	S: 5'-GCCTGTCTGTCAATGCTCCA-3'
	AS: 5'-TGTGCTCCATGCTCATACAA-3'
Xnr3	S: 5'-ACCGTCCAAAGCTTCATCGCTA-3'
	AS: 5'-TCCTTGCCGTCATTGGTATGGT-3'
Xenopus snx30 (for cloning)	S: 5'-GGCTCCACCATGTCAGGCTCCAGTTCTCC-3'
	AS: 5'-TGGGTGGATYCACTTTGGTTCCTGTTTGTCTTGTAGC-3'
Xenopus snx30 (for RT-PCR)	S: 5'-TGCGGAATTTGCCACCGTAACA-3'
	AS: 5'-AGCAGTTTCCAACACAGGCTGA-3'
eGFP	S: 5'-AATTCTCGAGATGGTGAGCAAGGGCGAGGAG-3'
	AS: 5'-TTATGATCTAGAGTCGCGGCC-3'
Step-2 Gateway Cloning	S: 5'-GGGGACAAGTTTGTACAAAAAAGCAGGCTCCACCATG-3'
	AS: 5'-GGGGACCACTTTGTACAAGAAAGCTGGGTGGATYCA-3'

Chapter 4: Conclusion

The work presented here is the first to explicitly address the roles of two sorting nexins, Snx11 and Snx30, during embryogenesis. These proteins are part of a network of molecules that regulate endosomal protein trafficking. The data presented in this work contributes to our understanding of how protein trafficking can affect signaling pathways. However, since these studies are the first to address the function of Snx11 and Snx30, there are still many questions to be answered before a clear picture about their function can be made. Nevertheless, these results shed light upon two proteins that may eventually become as therapeutic targets.

Characterization of two new sorting nexins

When studying a new gene, a few classical “fishing” experiments must be performed. Expression profile analysis and knockdown (or knockout) experiments are the most important. Protein-protein interaction assays can also be very informative but even when using independent assays, they run the risk of identifying too many candidates, of which many can be false-positives.

Having analyzed the expression profile, knockdown effects, and potential protein-protein interactions, Snx30 seems to behave as a dimerizing protein (with another SNX-BAR) that is expressed early on during embryogenesis with the potential to not only affect heart development but also the development of other organs and systems. Due to the scope of this study and based on previous unpublished data, the focus of analysis of developmental defects

caused by knockdown of Snx30 was limited to the heart. However, upon evaluation of the effect of knockdown of Snx30, it is clear that Snx30 is not only implicated in cardiogenesis but also in many other developmental processes. Aside from cardiac defects, other visible malformations were observed in Snx30 knockdown embryos: they are shorter in length, and they have malformations of the eyes and digestive system. CNS defects may also be present but this was not evaluated. The fact that Snx30 seems to be implicated in multiple developmental pathways hints towards a characteristic of many sorting nexins: their promiscuous nature. This is not surprising if you take into account the presence of the BAR domain. This dimerization domain offers many potential SNX-BAR combinations. Indeed, at least *in vitro*, Snx30 can homodimerize as well as form a dimer with Snx4. How this affects various signaling pathways and developmental processes has yet to be discovered but does increase the complexity of this group of proteins. Do the combinations of Snx30-Snx30 and Snx30-Snx4 have different functions or are they redundant? Cells would benefit from both options. In one case, the diversity of interactions offered by various SNX-BARs would provide the cell with an efficient way to regulate multiple pathways. On the other hand, redundancy is a good way to prevent catastrophic outcomes in case a single protein is mutated or misfolded. Of course, not all BAR domains dimerize together. For example, in retromer, Snx1 will dimerize with Snx5 or Snx6 but not with Snx2 [114]. Likewise, Snx5 will dimerize with Snx1 or Snx2 but not with Snx6 [114]. However in yeast only two proteins forming the Snx dimer exist (Vps5p and Vps17p). The specialized roles of multicellular organisms like vertebrates require higher specialization, which may have resulted in the expansion of the Snx family. Future studies will be needed to answer these questions.

SNX30 and Wnt/β-catenin signaling

Recently, Taelman *et al.* (2010) found that Wnt/β-catenin signaling is dependent upon intracellular trafficking of LRP6 signalosomes to MVBs [103]. The fact that altering Snx30 expression in HEK293T cells significantly alters the output of Wnt/β-catenin signaling supports the idea that intracellular trafficking is an essential part of this signaling pathway. To substantiate the strength of this experience, an evaluation of the expression of each receptor would be needed. However, the finding that this effect is only detectable for a certain set of Wnt receptors is indicative of increased specificity. Indeed, Snx30 has differing effects on Wnt/β-catenin signaling depending on the receptor present. While RABs and the ESCRT are well-known to be essential for vesicle movement and MVB formation, their requirement during Wnt signaling is fundamental. In other words, any change in expression of these crucial genes affects every trafficking events to MVBs, at all stages of development, in every cells. On the other hand, Snx30 is expressed in a specific set of cells and plays a role on the trafficking of a specific set of Wnt receptors. Therefore, altering its expression does not cause generalized Wnt signaling variations nor is it lethal during development. For example, knockdown of Snx30 did not affect Wnt/β-catenin signaling via the Fz4 receptor, neither did it affect its localization. This characteristic is interesting pharmacologically because of its specific mode of action. Endogenous variability in Snx30 expression across time and space may be a way of fine-tuning Wnt/β-catenin signaling.

How does Snx30 accomplish its negative effect on Wnt/β-catenin signaling? One possibility is that it mediates the recycling of LRP6 signalosomes back to membranes facing the cytoplasm, thereby releasing GSK3 from intralumenal vesicles (Figure 19). Data on trafficking

to and from the internal membranes of MVBs is scarce. In mammalian cells that have impaired LBPA functions, CI-M6PR accumulates in the internal membranes of late endosomes [83]. Therefore, proteins may at least to some extent cycle between the outer and inner membranes of MVBs. Although essential to MVB formation, the ESCRT machinery can be considered as a generic mediator of this process that does not show any cargo specificity. Therefore, additional factors likely come into play when a protein complex like the LRP6 signalosome gets sorted to MVBs. The extent of this work did not address whether or not Snx30 plays this role but this possibility would be interesting to examine.

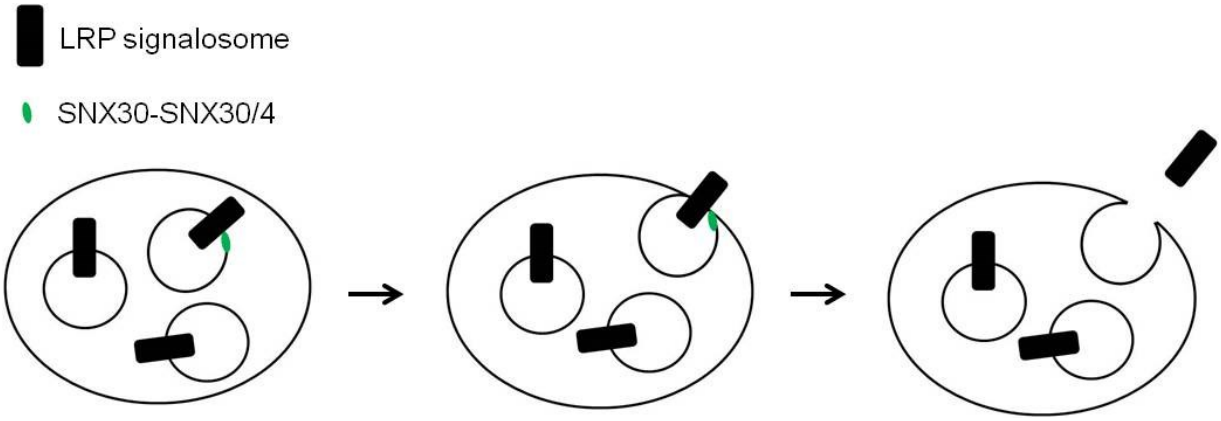

Figure 19. First model for a mechanism of Wnt/β-catenin signaling inhibition by SNX30. In order to reduce the levels of cytoplasmic β-catenin, LRP signalosomes could be released from MVBs through sorting by SNX30 (homo- or heterodimer of SNX-BAR, SNX30 or SNX4).

Another possibility is that Snx30 sorts receptors found in MVBs to the lysosome (Figure 20). This would ultimately limit the amount of receptors available for activation at the cell membrane and reduce Wnt signaling via those receptors. Both models suggest a trafficking decision taken at MVBs, based mainly on immunohistochemistry data. Co-localization studies of Snx30 and the various candidate cargos may help in clarifying the mechanism of Snx30 function.

There is often a gap of unanswered questions between biomolecular and physiological research. As such integrating biomolecular data into a holistic model requires both *in vivo* and *in vitro* experiments. Here, we found that *Snx30*'s expression profile corresponds to periods of rapidly changing Wnt/β-catenin signaling activity, namely the period at which the *Xnr3* and *Siamois* target genes are downregulated in *X. laevis*. This and other results suggest that *Snx30* is a developmentally regulated gene that allows cardiac specification of mesoderm cells. It does so carrying out intracellular trafficking events that lead to the inhibition of Wnt/β-catenin signaling (phosphorylation of β-catenin by GSK3). The Fz8 receptor is expressed in the Spemann organizer and early dorsal mesoderm [363]. As this was one of the receptors that responded the most to knockdown of Snx30, it would make sense physiologically and biomolecularly that Snx30 downregulates Wnt/β-catenin signaling by mediating trafficking of Fz8 receptor complexes. By doing so, activation of Wnt/β-catenin signaling via Fz8 would be inhibited without necessarily causing its degradation, which may be energetically expensive for the cell. Instead, Snx30 could release Fz8-containing LRP signalosomes from MVBs, returning Fz8 to the plasma membrane and at the same time allowing GSK3 to phosphorylate β-catenin. Again further study will be needed to address this question.

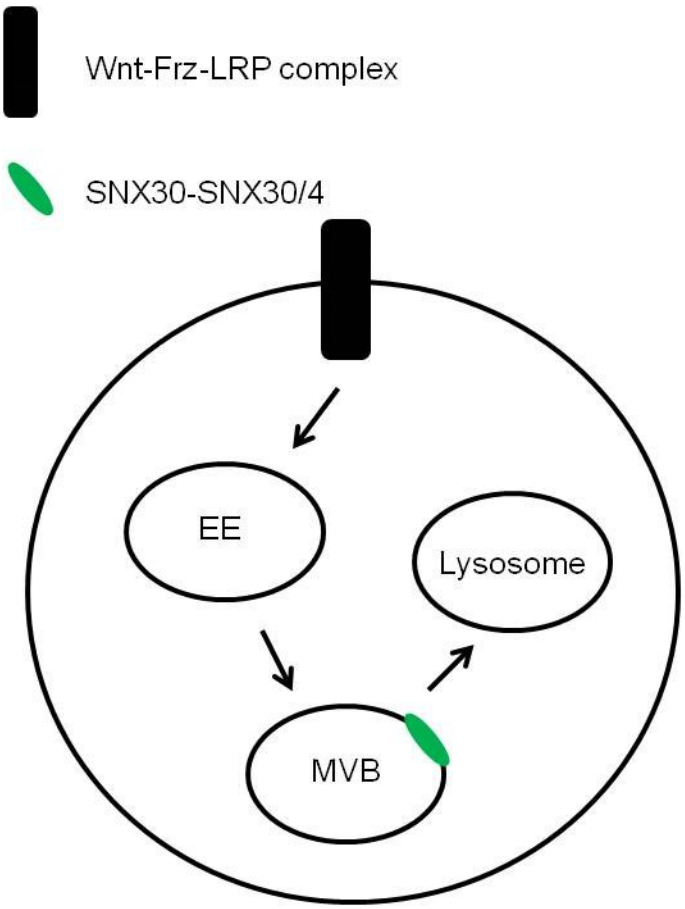

Figure 20. Second model for a mechanism of Wnt/β-catenin signaling inhibition by SNX30. SNX30 could inhibit Wnt/β-catenin signaling by sorting receptors towards the degradative pathway.

Although our current data clearly suggests a role for Snx30 in regulating Wnt/β-catenin signaling, many new and remaining questions will have to be addressed before we can include Snx30 as a *bona fide* regulator of Wnt signaling. What is the nature of Snx30's cargo and does it bind directly to it? Does Snx30 mediate the sequestration of the LRP6 complex to late endosomes as previously described or does it rather help release LRP signalosome from the

MVB [103]. Are *in vivo* TopFlash reporters similar to results from cell culture? Is Snx30 associated with proteins involved with trafficking LRP6 to multivesicular bodies? Are any other signaling pathways regulated by Snx30?

The fundamental importance of Wnt signaling during vertebrate embryogenesis and its link with many diseases makes any new finding on the regulation of Wnt signaling very exciting. However, it must be taken into account that other signaling pathways may be controlled by Snx30 through the formation of various BAR dimers (SNX30-Snx30 and SNX30-SNX4). As the precise role of Snx30 becomes better understood, therapeutic applications may begin to appear.

The dual functions of SNX11

As previously mentioned, Snx11 appears to have at least two functions. The first function seems to involve actin-dependent processes that involve either the production or indirect modification of extracellular proteins. Although this remains to be proven, many lines of evidence suggest such a function. First, expression of Snx11 in cartilage and its requirement for somitogenesis suggest an underlying function in either sending or receiving signals from the extracellular matrix. Second, actin remodelling is not uncommon during processes that engage the extra-cellular matrix and Snx11 clearly seems to have a positive effect on actin polymerization. It would be interesting to evaluate the link between Snx11 and actin, and to evaluate if it localizes preferentially to the cell membrane.

The second function that was discovered is the Snx11-dependent inhibition of DOR recycling, in which recycling was actin-independent and seems to occur from late endosomes, which is relatively far from interactions with the extra-cellular matrix. However, further work into this process would be required to determine whether this inhibition is dependent upon actin polymerization and what is the trafficking outcome of the receptor after the involvement of SNX11. A possible outcomes include trafficking towards the degradative pathway and this could involve actin polymerization. In addition, due to the availability of the DOR recycling assay, this experiment was used to evaluate the role of SNX11 in receptor recycling. However, it would be interesting and more relevant to evaluate the effect of Snx11 on the trafficking of other receptors, especially those involved in the main signaling pathways of somitogenesis (e.g. Notch receptor). Unfortunately, a mechanistic model for such functions is still lacking due to insufficient data. In addition, it would be interesting to determine whether overexpression of SNX11 inhibits DOR recycling and whether it can counter the effect of shRNA-mediated knockdown. This would substantially increase the strength of the conclusions found in this paper.

Both studies have evaluated the role of these proteins *in vivo* and *in vitro*. Taken together, the work presented here will provide valuable background information for future studies of Snx11 and Snx30.

References

1. Fortini, M.E., *Notch signaling: the core pathway and its posttranslational regulation.* Dev Cell, 2009. **16**(5): p. 633-47.
2. Conner, S.D. and S.L. Schmid, *Regulated portals of entry into the cell.* Nature, 2003. **422**(6927): p. 37-44.
3. Mercer, J., M. Schelhaas, and A. Helenius, *Virus entry by endocytosis.* Annu Rev Biochem, 2010. **79**: p. 803-33.
4. Lanzetti, L. and P.P. Di Fiore, *Endocytosis and cancer: an 'insider' network with dangerous liaisons.* Traffic, 2008. **9**(12): p. 2011-21.
5. Di Guglielmo, G.M., et al., *Distinct endocytic pathways regulate TGF-beta receptor signalling and turnover.* Nat Cell Biol, 2003. **5**(5): p. 410-21.
6. Mills, I.G., *The interplay between clathrin-coated vesicles and cell signalling.* Semin Cell Dev Biol, 2007. **18**(4): p. 459-70.
7. McMahon, H.T. and E. Boucrot, *Molecular mechanism and physiological functions of clathrin-mediated endocytosis.* Nat Rev Mol Cell Biol, 2011. **12**(8): p. 517-33.
8. Stimpson, H.E., et al., *Early-arriving Syp1p and Ede1p function in endocytic site placement and formation in budding yeast.* Mol Biol Cell, 2009. **20**(22): p. 4640-51.
9. Henne, W.M., et al., *FCHo proteins are nucleators of clathrin-mediated endocytosis.* Science, 2010. **328**(5983): p. 1281-4.
10. Reider, A., et al., *Syp1 is a conserved endocytic adaptor that contains domains involved in cargo selection and membrane tubulation.* EMBO J, 2009. **28**(20): p. 3103-16.
11. Divecha, N., *Lipid kinases: charging PtdIns(4,5)P2 synthesis.* Curr Biol, 2010. **20**(4): p. R154-7.
12. Lundmark, R. and S.R. Carlsson, *Sorting nexin 9 participates in clathrin-mediated endocytosis through interactions with the core components.* J Biol Chem, 2003. **278**(47): p. 46772-81.
13. Pearse, B.M., *Clathrin: a unique protein associated with intracellular transfer of membrane by coated vesicles.* Proc Natl Acad Sci U S A, 1976. **73**(4): p. 1255-9.
14. Fujimoto, L.M., et al., *Actin assembly plays a variable, but not obligatory role in receptor-mediated endocytosis in mammalian cells.* Traffic, 2000. **1**(2): p. 161-71.
15. Iwasa, J.H., *Animating the model figure.* Trends Cell Biol, 2010. **20**(12): p. 699-704.
16. Collins, B.M., et al., *Molecular architecture and functional model of the endocytic AP2 complex.* Cell, 2002. **109**(4): p. 523-35.
17. Kelly, B.T., et al., *A structural explanation for the binding of endocytic dileucine motifs by the AP2 complex.* Nature, 2008. **456**(7224): p. 976-79.
18. Yu, A., et al., *Association of Dishevelled with the clathrin AP-2 adaptor is required for Frizzled endocytosis and planar cell polarity signaling.* Dev Cell, 2007. **12**(1): p. 129-41.
19. Chidambaram, S., J. Zimmermann, and G.F. von Mollard, *ENTH domain proteins are cargo adaptors for multiple SNARE proteins at the TGN endosome.* J Cell Sci, 2008. **121**(Pt 3): p. 329-38.
20. Dittman, J.S. and J.M. Kaplan, *Factors regulating the abundance and localization of synaptobrevin in the plasma membrane.* Proc Natl Acad Sci U S A, 2006. **103**(30): p. 11399-404.

21. Tebar, F., et al., *Eps15 is a component of clathrin-coated pits and vesicles and is located at the rim of coated pits.* J Biol Chem, 1996. **271**(46): p. 28727-30.
22. Saffarian, S., E. Cocucci, and T. Kirchhausen, *Distinct dynamics of endocytic clathrin-coated pits and coated plaques.* PLoS Biol, 2009. **7**(9): p. e1000191.
23. Kosaka, T. and K. Ikeda, *Reversible blockage of membrane retrieval and endocytosis in the garland cell of the temperature-sensitive mutant of Drosophila melanogaster, shibirets1.* J Cell Biol, 1983. **97**(2): p. 499-507.
24. Wigge, P., et al., *Amphiphysin heterodimers: potential role in clathrin-mediated endocytosis.* Mol Biol Cell, 1997. **8**(10): p. 2003-15.
25. Ferguson, S.M., et al., *Coordinated actions of actin and BAR proteins upstream of dynamin at endocytic clathrin-coated pits.* Dev Cell, 2009. **17**(6): p. 811-22.
26. Sundborger, A., et al., *An endophilin-dynamin complex promotes budding of clathrin-coated vesicles during synaptic vesicle recycling.* J Cell Sci, 2011. **124**(Pt 1): p. 133-43.
27. Schlossman, D.M., et al., *An enzyme that removes clathrin coats: purification of an uncoating ATPase.* J Cell Biol, 1984. **99**(2): p. 723-33.
28. Ungewickell, E., et al., *Role of auxilin in uncoating clathrin-coated vesicles.* Nature, 1995. **378**(6557): p. 632-5.
29. Brodsky, F.M., *Diversity of clathrin function: new tricks for an old protein.* Annu Rev Cell Dev Biol, 2012. **28**: p. 309-36.
30. Howes, M.T., et al., *Clathrin-independent carriers form a high capacity endocytic sorting system at the leading edge of migrating cells.* J Cell Biol, 2010. **190**(4): p. 675-91.
31. Sandvig, K., et al., *Acidification of the cytosol inhibits endocytosis from coated pits.* J Cell Biol, 1987. **105**(2): p. 679-89.
32. van Deurs, B., et al., *The ways of endocytosis.* Int Rev Cytol, 1989. **117**: p. 131-77.
33. Parton, R.G. and M.A. del Pozo, *Caveolae as plasma membrane sensors, protectors and organizers.* Nat Rev Mol Cell Biol, 2013. **14**(2): p. 98-112.
34. Thorn, H., et al., *Cell surface orifices of caveolae and localization of caveolin to the necks of caveolae in adipocytes.* Mol Biol Cell, 2003. **14**(10): p. 3967-76.
35. Zhuang, Z., et al., *Is caveolin involved in normal proximal tubule function? Presence in model PT systems but absence in situ.* Am J Physiol Renal Physiol, 2011. **300**(1): p. F199-206.
36. Howes, M.T., S. Mayor, and R.G. Parton, *Molecules, mechanisms, and cellular roles of clathrin-independent endocytosis.* Curr Opin Cell Biol, 2010. **22**(4): p. 519-27.
37. Breen, M.R., et al., *Cholesterol depletion in adipocytes causes caveolae collapse concomitant with proteosomal degradation of cavin-2 in a switch-like fashion.* PLoS One, 2012. **7**(4): p. e34516.
38. Fairn, G.D., et al., *High-resolution mapping reveals topologically distinct cellular pools of phosphatidylserine.* J Cell Biol, 2011. **194**(2): p. 257-75.
39. Mayor, S. and R.E. Pagano, *Pathways of clathrin-independent endocytosis.* Nat Rev Mol Cell Biol, 2007. **8**(8): p. 603-12.
40. Pelkmans, L., et al., *Caveolin-stabilized membrane domains as multifunctional transport and sorting devices in endocytic membrane traffic.* Cell, 2004. **118**(6): p. 767-80.
41. Kozera, L., E. White, and S. Calaghan, *Caveolae act as membrane reserves which limit mechanosensitive I(Cl,swell) channel activation during swelling in the rat ventricular myocyte.* PLoS One, 2009. **4**(12): p. e8312.

42. Sinha, B., et al., *Cells respond to mechanical stress by rapid disassembly of caveolae.* Cell, 2011. **144**(3): p. 402-13.
43. Garcia-Cardena, G., et al., *Dissecting the interaction between nitric oxide synthase (NOS) and caveolin. Functional significance of the nos caveolin binding domain in vivo.* J Biol Chem, 1997. **272**(41): p. 25437-40.
44. Sowa, G., M. Pypaert, and W.C. Sessa, *Distinction between signaling mechanisms in lipid rafts vs. caveolae.* Proc Natl Acad Sci U S A, 2001. **98**(24): p. 14072-7.
45. Lamaze, C., et al., *Interleukin 2 receptors and detergent-resistant membrane domains define a clathrin-independent endocytic pathway.* Mol Cell, 2001. **7**(3): p. 661-71.
46. Naslavsky, N., R. Weigert, and J.G. Donaldson, *Convergence of non-clathrin- and clathrin-derived endosomes involves Arf6 inactivation and changes in phosphoinositides.* Mol Biol Cell, 2003. **14**(2): p. 417-31.
47. Sabharanjak, S., et al., *GPI-anchored proteins are delivered to recycling endosomes via a distinct cdc42-regulated, clathrin-independent pinocytic pathway.* Dev Cell, 2002. **2**(4): p. 411-23.
48. Robertson, A.S., E. Smythe, and K.R. Ayscough, *Functions of actin in endocytosis.* Cell Mol Life Sci, 2009. **66**(13): p. 2049-65.
49. Rohn, J.L. and B. Baum, *Actin and cellular architecture at a glance.* J Cell Sci, 2010. **123**(Pt 2): p. 155-8.
50. van Weering, J.R., P. Verkade, and P.J. Cullen, *SNX-BAR proteins in phosphoinositide-mediated, tubular-based endosomal sorting.* Semin Cell Dev Biol, 2010. **21**(4): p. 371-80.
51. Yarar, D., C.M. Waterman-Storer, and S.L. Schmid, *SNX9 couples actin assembly to phosphoinositide signals and is required for membrane remodeling during endocytosis.* Dev Cell, 2007. **13**(1): p. 43-56.
52. Sandvig, K. and B. van Deurs, *Delivery into cells: lessons learned from plant and bacterial toxins.* Gene Ther, 2005. **12**(11): p. 865-72.
53. Kumari, S., S. Mg, and S. Mayor, *Endocytosis unplugged: multiple ways to enter the cell.* Cell Res, 2010. **20**(3): p. 256-75.
54. Pust, S., H. Barth, and K. Sandvig, *Clostridium botulinum C2 toxin is internalized by clathrin- and Rho-dependent mechanisms.* Cell Microbiol, 2010. **12**(12): p. 1809-20.
55. Gibert, M., et al., *Endocytosis and toxicity of clostridial binary toxins depend on a clathrin-independent pathway regulated by Rho-GDI.* Cell Microbiol, 2011. **13**(1): p. 154-70.
56. Ait-Slimane, T., et al., *Basolateral internalization of GPI-anchored proteins occurs via a clathrin-independent flotillin-dependent pathway in polarized hepatic cells.* Mol Biol Cell, 2009. **20**(17): p. 3792-800.
57. Payne, C.K., et al., *Internalization and trafficking of cell surface proteoglycans and proteoglycan-binding ligands.* Traffic, 2007. **8**(4): p. 389-401.
58. Glebov, O.O., N.A. Bright, and B.J. Nichols, *Flotillin-1 defines a clathrin-independent endocytic pathway in mammalian cells.* Nat Cell Biol, 2006. **8**(1): p. 46-54.
59. Yamamoto, H., H. Komekado, and A. Kikuchi, *Caveolin is necessary for Wnt-3a-dependent internalization of LRP6 and accumulation of beta-catenin.* Dev Cell, 2006. **11**(2): p. 213-23.
60. Yamamoto, H., et al., *Wnt3a and Dkk1 regulate distinct internalization pathways of LRP6 to tune the activation of beta-catenin signaling.* Dev Cell, 2008. **15**(1): p. 37-48.
61. Huotari, J. and A. Helenius, *Endosome maturation.* EMBO J, 2011. **30**(17): p. 3481-500.

62. Mayor, S., J.F. Presley, and F.R. Maxfield, *Sorting of membrane components from endosomes and subsequent recycling to the cell surface occurs by a bulk flow process.* J Cell Biol, 1993. **121**(6): p. 1257-69.
63. Sigismund, S., et al., *Clathrin-mediated internalization is essential for sustained EGFR signaling but dispensable for degradation.* Dev Cell, 2008. **15**(2): p. 209-19.
64. Gruenberg, J., *The endocytic pathway: a mosaic of domains.* Nat Rev Mol Cell Biol, 2001. **2**(10): p. 721-30.
65. Mellman, I., *Endocytosis and molecular sorting.* Annu Rev Cell Dev Biol, 1996. **12**: p. 575-625.
66. Christoforidis, S., et al., *Phosphatidylinositol-3-OH kinases are Rab5 effectors.* Nat Cell Biol, 1999. **1**(4): p. 249-52.
67. Jovic, M., et al., *The early endosome: a busy sorting station for proteins at the crossroads.* Histol Histopathol, 2010. **25**(1): p. 99-112.
68. van Dam, E.M., et al., *Endocytosed transferrin receptors recycle via distinct dynamin and phosphatidylinositol 3-kinase-dependent pathways.* J Biol Chem, 2002. **277**(50): p. 48876-83.
69. Lawe, D.C., et al., *Sequential roles for phosphatidylinositol 3-phosphate and Rab5 in tethering and fusion of early endosomes via their interaction with EEA1.* J Biol Chem, 2002. **277**(10): p. 8611-7.
70. Lawe, D.C., et al., *The FYVE domain of early endosome antigen 1 is required for both phosphatidylinositol 3-phosphate and Rab5 binding. Critical role of this dual interaction for endosomal localization.* J Biol Chem, 2000. **275**(5): p. 3699-705.
71. Nielsen, E., et al., *Rabenosyn-5, a novel Rab5 effector, is complexed with hVPS45 and recruited to endosomes through a FYVE finger domain.* J Cell Biol, 2000. **151**(3): p. 601-12.
72. Ellson, C.D., et al., *The PX domain: a new phosphoinositide-binding module.* J Cell Sci, 2002. **115**(Pt 6): p. 1099-105.
73. Mills, I.G., A.T. Jones, and M.J. Clague, *Involvement of the endosomal autoantigen EEA1 in homotypic fusion of early endosomes.* Curr Biol, 1998. **8**(15): p. 881-4.
74. Mills, I.G., A.T. Jones, and M.J. Clague, *Regulation of endosome fusion.* Mol Membr Biol, 1999. **16**(1): p. 73-9.
75. Naslavsky, N., et al., *Rabenosyn-5 and EHD1 interact and sequentially regulate protein recycling to the plasma membrane.* Mol Biol Cell, 2004. **15**(5): p. 2410-22.
76. Cozier, G.E., et al., *The phox homology (PX) domain-dependent, 3-phosphoinositide-mediated association of sorting nexin-1 with an early sorting endosomal compartment is required for its ability to regulate epidermal growth factor receptor degradation.* J Biol Chem, 2002. **277**(50): p. 48730-6.
77. Teasdale, R.D. and B.M. Collins, *Insights into the PX (phox-homology) domain and SNX (sorting nexin) protein families: structures, functions and roles in disease.* Biochem J, 2012. **441**(1): p. 39-59.
78. Hanson, P.I. and A. Cashikar, *Multivesicular body morphogenesis.* Annu Rev Cell Dev Biol, 2012. **28**: p. 337-62.
79. Falguieres, T., P.P. Luyet, and J. Gruenberg, *Molecular assemblies and membrane domains in multivesicular endosome dynamics.* Exp Cell Res, 2009. **315**(9): p. 1567-73.
80. Ostrowski, M., et al., *Rab27a and Rab27b control different steps of the exosome secretion pathway.* Nat Cell Biol, 2010. **12**(1): p. 19-30; sup pp 1-13.

81. Uytterhoeven, V., et al., *Loss of skywalker reveals synaptic endosomes as sorting stations for synaptic vesicle proteins.* Cell, 2011. **145**(1): p. 117-32.
82. Pols, M.S. and J. Klumperman, *Trafficking and function of the tetraspanin CD63.* Exp Cell Res, 2009. **315**(9): p. 1584-92.
83. Kobayashi, T., et al., *A lipid associated with the antiphospholipid syndrome regulates endosome structure and function.* Nature, 1998. **392**(6672): p. 193-7.
84. Ghosh, P., N.M. Dahms, and S. Kornfeld, *Mannose 6-phosphate receptors: new twists in the tale.* Nat Rev Mol Cell Biol, 2003. **4**(3): p. 202-12.
85. Settembre, C., et al., *Signals from the lysosome: a control centre for cellular clearance and energy metabolism.* Nat Rev Mol Cell Biol, 2013. **14**(5): p. 283-96.
86. Bankaitis, V.A., R. Garcia-Mata, and C.J. Mousley, *Golgi membrane dynamics and lipid metabolism.* Curr Biol, 2012. **22**(10): p. R414-24.
87. Farquhar, M.G. and G.E. Palade, *The Golgi apparatus (complex)-(1954-1981)-from artifact to center stage.* J Cell Biol, 1981. **91**(3 Pt 2): p. 77s-103s.
88. Sharma, M., et al., *Misfolding diverts CFTR from recycling to degradation: quality control at early endosomes.* J Cell Biol, 2004. **164**(6): p. 923-33.
89. Wang, S., G. Thibault, and D.T. Ng, *Routing misfolded proteins through the multivesicular body (MVB) pathway protects against proteotoxicity.* J Biol Chem, 2011. **286**(33): p. 29376-87.
90. Schoenheimer, R., et al., *THE APPLICATION OF THE NITROGEN ISOTOPE N15 FOR THE STUDY OF PROTEIN METABOLISM.* Science, 1938. **88**(2295): p. 599-600.
91. Ciehanover, A., Y. Hod, and A. Hershko, *A heat-stable polypeptide component of an ATP-dependent proteolytic system from reticulocytes.* Biochem Biophys Res Commun, 1978. **81**(4): p. 1100-5.
92. Etlinger, J.D. and A.L. Goldberg, *A soluble ATP-dependent proteolytic system responsible for the degradation of abnormal proteins in reticulocytes.* Proc Natl Acad Sci U S A, 1977. **74**(1): p. 54-8.
93. Matyskiela, M.E. and A. Martin, *Design principles of a universal protein degradation machine.* J Mol Biol, 2013. **425**(2): p. 199-213.
94. Sauer, R.T. and T.A. Baker, *AAA+ proteases: ATP-fueled machines of protein destruction.* Annu Rev Biochem, 2011. **80**: p. 587-612.
95. Gruenberg, J. and H. Stenmark, *The biogenesis of multivesicular endosomes.* Nat Rev Mol Cell Biol, 2004. **5**(4): p. 317-23.
96. Piper, R.C. and P.J. Lehner, *Endosomal transport via ubiquitination.* Trends Cell Biol, 2011. **21**(11): p. 647-55.
97. Clague, M.J. and S. Urbe, *Ubiquitin: same molecule, different degradation pathways.* Cell, 2010. **143**(5): p. 682-5.
98. Clague, M.J. and S. Urbe, *Endocytosis: the DUB version.* Trends Cell Biol, 2006. **16**(11): p. 551-9.
99. Jouvenet, N., *Dynamics of ESCRT proteins.* Cell Mol Life Sci, 2012. **69**(24): p. 4121-33.
100. Raiborg, C., et al., *Hrs sorts ubiquitinated proteins into clathrin-coated microdomains of early endosomes.* Nat Cell Biol, 2002. **4**(5): p. 394-8.
101. Hanyaloglu, A.C., E. McCullagh, and M. von Zastrow, *Essential role of Hrs in a recycling mechanism mediating functional resensitization of cell signaling.* EMBO J, 2005. **24**(13): p. 2265-83.

102. Hasdemir, B., N.W. Bunnett, and G.S. Cottrell, *Hepatocyte growth factor-regulated tyrosine kinase substrate (HRS) mediates post-endocytic trafficking of protease-activated receptor 2 and calcitonin receptor-like receptor.* J Biol Chem, 2007. **282**(40): p. 29646-57.
103. Taelman, V.F., et al., *Wnt signaling requires sequestration of glycogen synthase kinase 3 inside multivesicular endosomes.* Cell, 2010. **143**(7): p. 1136-48.
104. Maxfield, F.R. and T.E. McGraw, *Endocytic recycling.* Nat Rev Mol Cell Biol, 2004. **5**(2): p. 121-32.
105. Hopkins, C.R. and I.S. Trowbridge, *Internalization and processing of transferrin and the transferrin receptor in human carcinoma A431 cells.* J Cell Biol, 1983. **97**(2): p. 508-21.
106. Sheff, D.R., et al., *The receptor recycling pathway contains two distinct populations of early endosomes with different sorting functions.* J Cell Biol, 1999. **145**(1): p. 123-39.
107. Sonnichsen, B., et al., *Distinct membrane domains on endosomes in the recycling pathway visualized by multicolor imaging of Rab4, Rab5, and Rab11.* J Cell Biol, 2000. **149**(4): p. 901-14.
108. Deneka, M. and P. van der Sluijs, *'Rab'ing up endosomal membrane transport.* Nat Cell Biol, 2002. **4**(2): p. E33-5.
109. Kurten, R.C., D.L. Cadena, and G.N. Gill, *Enhanced degradation of EGF receptors by a sorting nexin, SNX1.* Science, 1996. **272**(5264): p. 1008-10.
110. Nesterov, A., R.C. Kurten, and G.N. Gill, *Association of epidermal growth factor receptors with coated pit adaptins via a tyrosine phosphorylation-regulated mechanism.* J Biol Chem, 1995. **270**(11): p. 6320-7.
111. Chin, L.S., et al., *Hrs interacts with sorting nexin 1 and regulates degradation of epidermal growth factor receptor.* J Biol Chem, 2001. **276**(10): p. 7069-78.
112. Pons, V., et al., *Enterophilin-1 interacts with focal adhesion kinase and decreases beta1 integrins in intestinal Caco-2 cells.* J Biol Chem, 2004. **279**(10): p. 9270-7.
113. Haft, C.R., et al., *Identification of a family of sorting nexin molecules and characterization of their association with receptors.* Mol Cell Biol, 1998. **18**(12): p. 7278-87.
114. Cullen, P.J., *Endosomal sorting and signalling: an emerging role for sorting nexins.* Nat Rev Mol Cell Biol, 2008. **9**(7): p. 574-82.
115. Ponting, C.P., *Novel domains in NADPH oxidase subunits, sorting nexins, and PtdIns 3-kinases: binding partners of SH3 domains?* Protein Sci, 1996. **5**(11): p. 2353-7.
116. Ago, T., et al., *Phosphorylation of p47phox directs phox homology domain from SH3 domain toward phosphoinositides, leading to phagocyte NADPH oxidase activation.* Proc Natl Acad Sci U S A, 2003. **100**(8): p. 4474-9.
117. Ago, T., et al., *Mechanism for phosphorylation-induced activation of the phagocyte NADPH oxidase protein p47(phox). Triple replacement of serines 303, 304, and 328 with aspartates disrupts the SH3 domain-mediated intramolecular interaction in p47(phox), thereby activating the oxidase.* J Biol Chem, 1999. **274**(47): p. 33644-53.
118. Banfi, B., et al., *Two novel proteins activate superoxide generation by the NADPH oxidase NOX1.* J Biol Chem, 2003. **278**(6): p. 3510-3.
119. Geiszt, M., et al., *Proteins homologous to p47phox and p67phox support superoxide production by NAD(P)H oxidase 1 in colon epithelial cells.* J Biol Chem, 2003. **278**(22): p. 20006-12.

120. Takeya, R., et al., *Novel human homologues of p47phox and p67phox participate in activation of superoxide-producing NADPH oxidases.* J Biol Chem, 2003. **278**(27): p. 25234-46.
121. Seet, L.F. and W. Hong, *The Phox (PX) domain proteins and membrane traffic.* Biochim Biophys Acta, 2006. **1761**(8): p. 878-96.
122. Horazdovsky, B.F., et al., *A sorting nexin-1 homologue, Vps5p, forms a complex with Vps17p and is required for recycling the vacuolar protein-sorting receptor.* Mol Biol Cell, 1997. **8**(8): p. 1529-41.
123. Nothwehr, S.F. and A.E. Hindes, *The yeast VPS5/GRD2 gene encodes a sorting nexin-1-like protein required for localizing membrane proteins to the late Golgi.* J Cell Sci, 1997. **110 (Pt 9)**: p. 1063-72.
124. Voos, W. and T.H. Stevens, *Retrieval of resident late-Golgi membrane proteins from the prevacuolar compartment of Saccharomyces cerevisiae is dependent on the function of Grd19p.* J Cell Biol, 1998. **140**(3): p. 577-90.
125. Ekena, K. and T.H. Stevens, *The Saccharomyces cerevisiae MVP1 gene interacts with VPS1 and is required for vacuolar protein sorting.* Mol Cell Biol, 1995. **15**(3): p. 1671-8.
126. Hettema, E.H., et al., *Retromer and the sorting nexins Snx4/41/42 mediate distinct retrieval pathways from yeast endosomes.* EMBO J, 2003. **22**(3): p. 548-57.
127. Kanai, F., et al., *The PX domains of p47phox and p40phox bind to lipid products of PI(3)K.* Nat Cell Biol, 2001. **3**(7): p. 675-8.
128. Cheever, M.L., et al., *Phox domain interaction with PtdIns(3)P targets the Vam7 t-SNARE to vacuole membranes.* Nat Cell Biol, 2001. **3**(7): p. 613-8.
129. Ellson, C.D., et al., *PtdIns(3)P regulates the neutrophil oxidase complex by binding to the PX domain of p40(phox).* Nat Cell Biol, 2001. **3**(7): p. 679-82.
130. Song, X., et al., *Phox homology domains specifically bind phosphatidylinositol phosphates.* Biochemistry, 2001. **40**(30): p. 8940-4.
131. Xu, Y., et al., *SNX3 regulates endosomal function through its PX-domain-mediated interaction with PtdIns(3)P.* Nat Cell Biol, 2001. **3**(7): p. 658-66.
132. Yu, J.W. and M.A. Lemmon, *All phox homology (PX) domains from Saccharomyces cerevisiae specifically recognize phosphatidylinositol 3-phosphate.* J Biol Chem, 2001. **276**(47): p. 44179-84.
133. Zhang, J., W.S. Talbot, and A.F. Schier, *Positional cloning identifies zebrafish one-eyed pinhead as a permissive EGF-related ligand required during gastrulation.* Cell, 1998. **92**(2): p. 241-51.
134. Zhong, Q., et al., *Endosomal localization and function of sorting nexin 1.* Proc Natl Acad Sci U S A, 2002. **99**(10): p. 6767-72.
135. Balla, T., Z. Szentpetery, and Y.J. Kim, *Phosphoinositide signaling: new tools and insights.* Physiology (Bethesda), 2009. **24**: p. 231-44.
136. De Matteis, M.A. and A. Godi, *PI-loting membrane traffic.* Nat Cell Biol, 2004. **6**(6): p. 487-92.
137. Krauss, M. and V. Haucke, *Phosphoinositide-metabolizing enzymes at the interface between membrane traffic and cell signalling.* EMBO Rep, 2007. **8**(3): p. 241-6.
138. Heraud, J.M., et al., *Lipid products of phosphoinositide 3-kinase and phosphatidylinositol 4',5'-bisphosphate are both required for ADP-dependent platelet spreading.* J Biol Chem, 1998. **273**(28): p. 17817-23.

139. Stauffer, T.P., S. Ahn, and T. Meyer, *Receptor-induced transient reduction in plasma membrane PtdIns(4,5)P2 concentration monitored in living cells.* Curr Biol, 1998. **8**(6): p. 343-6.
140. Payrastre, B., et al., *Phosphoinositides: key players in cell signalling, in time and space.* Cell Signal, 2001. **13**(6): p. 377-87.
141. Haucke, V., *Phosphoinositide regulation of clathrin-mediated endocytosis.* Biochem Soc Trans, 2005. **33**(Pt 6): p. 1285-9.
142. Falasca, M. and T. Maffucci, *Rethinking phosphatidylinositol 3-monophosphate.* Biochim Biophys Acta, 2009. **1793**(12): p. 1795-803.
143. Schu, P.V., et al., *Phosphatidylinositol 3-kinase encoded by yeast VPS34 gene essential for protein sorting.* Science, 1993. **260**(5104): p. 88-91.
144. Vieira, O.V., et al., *Distinct roles of class I and class III phosphatidylinositol 3-kinases in phagosome formation and maturation.* J Cell Biol, 2001. **155**(1): p. 19-25.
145. Panaretou, C. and S.A. Tooze, *Regulation and recruitment of phosphatidylinositol 4-kinase on immature secretory granules is independent of ADP-ribosylation factor 1.* Biochem J, 2002. **363**(Pt 2): p. 289-95.
146. De Matteis, M., A. Godi, and D. Corda, *Phosphoinositides and the golgi complex.* Curr Opin Cell Biol, 2002. **14**(4): p. 434-47.
147. Rozelle, A.L., et al., *Phosphatidylinositol 4,5-bisphosphate induces actin-based movement of raft-enriched vesicles through WASP-Arp2/3.* Curr Biol, 2000. **10**(6): p. 311-20.
148. Klopfenstein, D.R., et al., *Role of phosphatidylinositol(4,5)bisphosphate organization in membrane transport by the Unc104 kinesin motor.* Cell, 2002. **109**(3): p. 347-58.
149. Carlton, J.G. and P.J. Cullen, *Coincidence detection in phosphoinositide signaling.* Trends Cell Biol, 2005. **15**(10): p. 540-7.
150. Bhatia, V.K., et al., *Amphipathic motifs in BAR domains are essential for membrane curvature sensing.* EMBO J, 2009. **28**(21): p. 3303-14.
151. Frost, A., V.M. Unger, and P. De Camilli, *The BAR domain superfamily: membrane-molding macromolecules.* Cell, 2009. **137**(2): p. 191-6.
152. Peter, B.J., et al., *BAR domains as sensors of membrane curvature: the amphiphysin BAR structure.* Science, 2004. **303**(5657): p. 495-9.
153. Shimada, A., et al., *Curved EFC/F-BAR-domain dimers are joined end to end into a filament for membrane invagination in endocytosis.* Cell, 2007. **129**(4): p. 761-72.
154. Frost, A., P. De Camilli, and V.M. Unger, *F-BAR proteins join the BAR family fold.* Structure, 2007. **15**(7): p. 751-3.
155. Frost, A., et al., *Structural basis of membrane invagination by F-BAR domains.* Cell, 2008. **132**(5): p. 807-17.
156. Cullen, P.J., *Phosphoinositides and the regulation of tubular-based endosomal sorting.* Biochem Soc Trans, 2011. **39**(4): p. 839-50.
157. Stenmark, H., *Rab GTPases as coordinators of vesicle traffic.* Nat Rev Mol Cell Biol, 2009. **10**(8): p. 513-25.
158. Bonifacino, J.S. and J.H. Hurley, *Retromer.* Curr Opin Cell Biol, 2008. **20**(4): p. 427-36.
159. Stenmark, H. and V.M. Olkkonen, *The Rab GTPase family.* Genome Biol, 2001. **2**(5): p. REVIEWS3007.
160. Stenmark, H., *The Rabs: a family at the root of metazoan evolution.* BMC Biol, 2012. **10**: p. 68.

161. Villar, V.A., et al., *Novel role of sorting nexin 5 in renal D(1) dopamine receptor trafficking and function: implications for hypertension.* FASEB J, 2013. **27**(5): p. 1808-19.
162. Xu, J., et al., *Structure of Sorting Nexin 11 (SNX11) Reveals a Novel Extended PX Domain (PXe Domain) Critical for the Inhibition of Sorting Nexin 10 (SNX10) Induced Vacuolation.* J Biol Chem, 2013.
163. Qin, B., et al., *Sorting nexin 10 induces giant vacuoles in mammalian cells.* J Biol Chem, 2006. **281**(48): p. 36891-6.
164. Zhu, C.H., L.R. Morse, and R.A. Battaglino, *SNX10 is required for osteoclast formation and resorption activity.* J Cell Biochem, 2012. **113**(5): p. 1608-15.
165. Aker, M., et al., *An SNX10 mutation causes malignant osteopetrosis of infancy.* J Med Genet, 2012. **49**(4): p. 221-6.
166. Chen, Y., et al., *A SNX10/V-ATPase pathway regulates ciliogenesis in vitro and in vivo.* Cell Res, 2012. **22**(2): p. 333-45.
167. Pippig, S., S. Andexinger, and M.J. Lohse, *Sequestration and recycling of beta 2-adrenergic receptors permit receptor resensitization.* Mol Pharmacol, 1995. **47**(4): p. 666-76.
168. Temkin, P., et al., *SNX27 mediates retromer tubule entry and endosome-to-plasma membrane trafficking of signalling receptors.* Nat Cell Biol, 2011. **13**(6): p. 715-21.
169. Cao, T.T., et al., *A kinase-regulated PDZ-domain interaction controls endocytic sorting of the beta2-adrenergic receptor.* Nature, 1999. **401**(6750): p. 286-90.
170. Riederer, M.A., et al., *Lysosome biogenesis requires Rab9 function and receptor recycling from endosomes to the trans-Golgi network.* J Cell Biol, 1994. **125**(3): p. 573-82.
171. Lombardi, D., et al., *Rab9 functions in transport between late endosomes and the trans Golgi network.* EMBO J, 1993. **12**(2): p. 677-82.
172. Semerdjieva, S., et al., *Coordinated regulation of AP2 uncoating from clathrin-coated vesicles by rab5 and hRME-6.* J Cell Biol, 2008. **183**(3): p. 499-511.
173. Wu, X.S., et al., *Identification of an organelle receptor for myosin-Va.* Nat Cell Biol, 2002. **4**(4): p. 271-8.
174. Hales, C.M., J.P. Vaerman, and J.R. Goldenring, *Rab11 family interacting protein 2 associates with Myosin Vb and regulates plasma membrane recycling.* J Biol Chem, 2002. **277**(52): p. 50415-21.
175. Salminen, A. and P.J. Novick, *A ras-like protein is required for a post-Golgi event in yeast secretion.* Cell, 1987. **49**(4): p. 527-38.
176. Luders, J. and T. Stearns, *Microtubule-organizing centres: a re-evaluation.* Nat Rev Mol Cell Biol, 2007. **8**(2): p. 161-7.
177. Anitei, M. and B. Hoflack, *Bridging membrane and cytoskeleton dynamics in the secretory and endocytic pathways.* Nat Cell Biol, 2012. **14**(1): p. 11-9.
178. Schliwa, M. and G. Woehlke, *Molecular motors.* Nature, 2003. **422**(6933): p. 759-65.
179. Chung, B.M., J.D. Rotty, and P.A. Coulombe, *Networking galore: intermediate filaments and cell migration.* Curr Opin Cell Biol, 2013. **25**(5): p. 600-12.
180. Galletta, B.J., O.L. Mooren, and J.A. Cooper, *Actin dynamics and endocytosis in yeast and mammals.* Curr Opin Biotechnol, 2010. **21**(5): p. 604-10.
181. Campellone, K.G. and M.D. Welch, *A nucleator arms race: cellular control of actin assembly.* Nat Rev Mol Cell Biol, 2010. **11**(4): p. 237-51.

182. Faini, M., et al., *Vesicle coats: structure, function, and general principles of assembly.* Trends Cell Biol, 2013. **23**(6): p. 279-88.
183. Springer, S., A. Spang, and R. Schekman, *A primer on vesicle budding.* Cell, 1999. **97**(2): p. 145-8.
184. Hara-Kuge, S., et al., *En bloc incorporation of coatomer subunits during the assembly of COP-coated vesicles.* J Cell Biol, 1994. **124**(6): p. 883-92.
185. Aridor, M. and L.M. Traub, *Cargo selection in vesicular transport: the making and breaking of a coat.* Traffic, 2002. **3**(8): p. 537-46.
186. Seaman, M.N., *Identification of a novel conserved sorting motif required for retromer-mediated endosome-to-TGN retrieval.* J Cell Sci, 2007. **120**(Pt 14): p. 2378-89.
187. Chen, D., et al., *Retromer is required for apoptotic cell clearance by phagocytic receptor recycling.* Science, 2010. **327**(5970): p. 1261-4.
188. Strochlic, T.I., et al., *Grd19/Snx3p functions as a cargo-specific adapter for retromer-dependent endocytic recycling.* J Cell Biol, 2007. **177**(1): p. 115-25.
189. Wang, Y., et al., *Down-regulation of protease-activated receptor-1 is regulated by sorting nexin 1.* Mol Biol Cell, 2002. **13**(6): p. 1965-76.
190. Drin, G., et al., *A general amphipathic alpha-helical motif for sensing membrane curvature.* Nat Struct Mol Biol, 2007. **14**(2): p. 138-46.
191. Gallop, J.L., et al., *Mechanism of endophilin N-BAR domain-mediated membrane curvature.* EMBO J, 2006. **25**(12): p. 2898-910.
192. McGough, I.J. and P.J. Cullen, *Recent advances in retromer biology.* Traffic, 2011. **12**(8): p. 963-71.
193. Beck, R., et al., *Coatomer and dimeric ADP ribosylation factor 1 promote distinct steps in membrane scission.* J Cell Biol, 2011. **194**(5): p. 765-77.
194. Lee, M.C., et al., *Sar1p N-terminal helix initiates membrane curvature and completes the fission of a COPII vesicle.* Cell, 2005. **122**(4): p. 605-17.
195. Borner, G.H., et al., *Comparative proteomics of clathrin-coated vesicles.* J Cell Biol, 2006. **175**(4): p. 571-8.
196. Skanland, S.S., et al., *SNX4 in complex with clathrin and dynein: implications for endosome movement.* PLoS One, 2009. **4**(6): p. e5935.
197. Bocking, T., et al., *Single-molecule analysis of a molecular disassemblase reveals the mechanism of Hsc70-driven clathrin uncoating.* Nat Struct Mol Biol, 2011. **18**(3): p. 295-301.
198. Popoff, V., et al., *Analysis of articulation between clathrin and retromer in retrograde sorting on early endosomes.* Traffic, 2009. **10**(12): p. 1868-80.
199. Shi, A., et al., *Regulation of endosomal clathrin and retromer-mediated endosome to Golgi retrograde transport by the J-domain protein RME-8.* EMBO J, 2009. **28**(21): p. 3290-302.
200. Cai, H., K. Reinisch, and S. Ferro-Novick, *Coats, tethers, Rabs, and SNAREs work together to mediate the intracellular destination of a transport vesicle.* Dev Cell, 2007. **12**(5): p. 671-82.
201. Hammer, J.A., 3rd and X.S. Wu, *Rabs grab motors: defining the connections between Rab GTPases and motor proteins.* Curr Opin Cell Biol, 2002. **14**(1): p. 69-75.
202. Matanis, T., et al., *Bicaudal-D regulates COPI-independent Golgi-ER transport by recruiting the dynein-dynactin motor complex.* Nat Cell Biol, 2002. **4**(12): p. 986-92.
203. Short, B., et al., *The Rab6 GTPase regulates recruitment of the dynactin complex to Golgi membranes.* Curr Biol, 2002. **12**(20): p. 1792-5.

204. Sztul, E. and V. Lupashin, *Role of tethering factors in secretory membrane traffic.* Am J Physiol Cell Physiol, 2006. **290**(1): p. C11-26.
205. Whyte, J.R. and S. Munro, *Vesicle tethering complexes in membrane traffic.* J Cell Sci, 2002. **115**(Pt 13): p. 2627-37.
206. Hanson, P.I., et al., *Structure and conformational changes in NSF and its membrane receptor complexes visualized by quick-freeze/deep-etch electron microscopy.* Cell, 1997. **90**(3): p. 523-35.
207. Lin, R.C. and R.H. Scheller, *Structural organization of the synaptic exocytosis core complex.* Neuron, 1997. **19**(5): p. 1087-94.
208. Kaksonen, M., Y. Sun, and D.G. Drubin, *A pathway for association of receptors, adaptors, and actin during endocytic internalization.* Cell, 2003. **115**(4): p. 475-87.
209. Boettner, D.R., et al., *The F-BAR protein Syp1 negatively regulates WASp-Arp2/3 complex activity during endocytic patch formation.* Curr Biol, 2009. **19**(23): p. 1979-87.
210. Soulard, A., et al., *Saccharomyces cerevisiae Bzz1p is implicated with type I myosins in actin patch polarization and is able to recruit actin-polymerizing machinery in vitro.* Mol Cell Biol, 2002. **22**(22): p. 7889-906.
211. Le Clainche, C., et al., *A Hip1R-cortactin complex negatively regulates actin assembly associated with endocytosis.* EMBO J, 2007. **26**(5): p. 1199-210.
212. Merrifield, C.J., et al., *Imaging actin and dynamin recruitment during invagination of single clathrin-coated pits.* Nat Cell Biol, 2002. **4**(9): p. 691-8.
213. Lundmark, R. and S.R. Carlsson, *SNX9 - a prelude to vesicle release.* J Cell Sci, 2009. **122**(Pt 1): p. 5-11.
214. Alto, N.M., et al., *The type III effector EspF coordinates membrane trafficking by the spatiotemporal activation of two eukaryotic signaling pathways.* J Cell Biol, 2007. **178**(7): p. 1265-78.
215. Haberg, K., R. Lundmark, and S.R. Carlsson, *SNX18 is an SNX9 paralog that acts as a membrane tubulator in AP-1-positive endosomal trafficking.* J Cell Sci, 2008. **121**(Pt 9): p. 1495-505.
216. Soulet, F., et al., *SNX9 regulates dynamin assembly and is required for efficient clathrin-mediated endocytosis.* Mol Biol Cell, 2005. **16**(4): p. 2058-67.
217. Worby, C.A., et al., *Drosophila Ack targets its substrate, the sorting nexin DSH3PX1, to a protein complex involved in axonal guidance.* J Biol Chem, 2002. **277**(11): p. 9422-8.
218. Worby, C.A., et al., *The sorting nexin, DSH3PX1, connects the axonal guidance receptor, Dscam, to the actin cytoskeleton.* J Biol Chem, 2001. **276**(45): p. 41782-9.
219. Yarar, D., et al., *SNX9 activities are regulated by multiple phosphoinositides through both PX and BAR domains.* Traffic, 2008. **9**(1): p. 133-46.
220. Pylypenko, O., et al., *The PX-BAR membrane-remodeling unit of sorting nexin 9.* EMBO J, 2007. **26**(22): p. 4788-800.
221. Shin, N., et al., *SNX9 regulates tubular invagination of the plasma membrane through interaction with actin cytoskeleton and dynamin 2.* J Cell Sci, 2008. **121**(Pt 8): p. 1252-63.
222. Wu, S.Y., M. Ferkowicz, and D.R. McClay, *Ingression of primary mesenchyme cells of the sea urchin embryo: a precisely timed epithelial mesenchymal transition.* Birth Defects Res C Embryo Today, 2007. **81**(4): p. 241-52.

223. Thiery, J.P., et al., *Epithelial-mesenchymal transitions in development and disease.* Cell, 2009. **139**(5): p. 871-90.
224. Nelson, W.J., *Remodeling epithelial cell organization: transitions between front-rear and apical-basal polarity.* Cold Spring Harb Perspect Biol, 2009. **1**(1): p. a000513.
225. Winklbauer, R. and M. Nagel, *Directional mesoderm cell migration in the Xenopus gastrula.* Dev Biol, 1991. **148**(2): p. 573-89.
226. Sepich, D.S., et al., *Initiation of convergence and extension movements of lateral mesoderm during zebrafish gastrulation.* Dev Dyn, 2005. **234**(2): p. 279-92.
227. Kimelman, D. and K.J. Griffin, *Vertebrate mesendoderm induction and patterning.* Curr Opin Genet Dev, 2000. **10**(4): p. 350-6.
228. Acloque, H., et al., *Reciprocal repression between Sox3 and snail transcription factors defines embryonic territories at gastrulation.* Dev Cell, 2011. **21**(3): p. 546-58.
229. Buckingham, M., S. Meilhac, and S. Zaffran, *Building the mammalian heart from two sources of myocardial cells.* Nat Rev Genet, 2005. **6**(11): p. 826-35.
230. Srivastava, D., *Making or breaking the heart: from lineage determination to morphogenesis.* Cell, 2006. **126**(6): p. 1037-48.
231. Lohr, J.L. and H.J. Yost, *Vertebrate model systems in the study of early heart development: Xenopus and zebrafish.* Am J Med Genet, 2000. **97**(4): p. 248-57.
232. Kolker, S.J., U. Tajchman, and D.L. Weeks, *Confocal imaging of early heart development in Xenopus laevis.* Dev Biol, 2000. **218**(1): p. 64-73.
233. Mohun, T.J., et al., *The morphology of heart development in Xenopus laevis.* Dev Biol, 2000. **218**(1): p. 74-88.
234. Warkman, A.S. and P.A. Krieg, *Xenopus as a model system for vertebrate heart development.* Semin Cell Dev Biol, 2007. **18**(1): p. 46-53.
235. Mohun, T., R. Orford, and C. Shang, *The origins of cardiac tissue in the amphibian, Xenopus laevis.* Trends Cardiovasc Med, 2003. **13**(6): p. 244-8.
236. Nakajima, Y., et al., *Heart development before beating.* Anat Sci Int, 2009. **84**(3): p. 67-76.
237. Cai, C.L., et al., *Isl1 identifies a cardiac progenitor population that proliferates prior to differentiation and contributes a majority of cells to the heart.* Dev Cell, 2003. **5**(6): p. 877-89.
238. Abu-Issa, R. and M.L. Kirby, *Heart field: from mesoderm to heart tube.* Annu Rev Cell Dev Biol, 2007. **23**: p. 45-68.
239. Meilhac, S.M., et al., *The clonal origin of myocardial cells in different regions of the embryonic mouse heart.* Dev Cell, 2004. **6**(5): p. 685-98.
240. Bondue, A., et al., *Mesp1 acts as a master regulator of multipotent cardiovascular progenitor specification.* Cell Stem Cell, 2008. **3**(1): p. 69-84.
241. Kitajima, S., et al., *MesP1 and MesP2 are essential for the development of cardiac mesoderm.* Development, 2000. **127**(15): p. 3215-26.
242. Brand, T., *Heart development: molecular insights into cardiac specification and early morphogenesis.* Dev Biol, 2003. **258**(1): p. 1-19.
243. Harvey, R.P., *Patterning the vertebrate heart.* Nat Rev Genet, 2002. **3**(7): p. 544-56.
244. Gessert, S. and M. Kuhl, *The multiple phases and faces of wnt signaling during cardiac differentiation and development.* Circ Res, 2010. **107**(2): p. 186-99.
245. Schultheiss, T.M., J.B. Burch, and A.B. Lassar, *A role for bone morphogenetic proteins in the induction of cardiac myogenesis.* Genes Dev, 1997. **11**(4): p. 451-62.

246. Park, M., et al., *The wingless signaling pathway is directly involved in Drosophila heart development.* Dev Biol, 1996. **177**(1): p. 104-16.
247. Marvin, M.J., et al., *Inhibition of Wnt activity induces heart formation from posterior mesoderm.* Genes Dev, 2001. **15**(3): p. 316-27.
248. Schneider, V.A. and M. Mercola, *Wnt antagonism initiates cardiogenesis in Xenopus laevis.* Genes Dev, 2001. **15**(3): p. 304-15.
249. Lickert, H., et al., *Formation of multiple hearts in mice following deletion of beta-catenin in the embryonic endoderm.* Dev Cell, 2002. **3**(2): p. 171-81.
250. Nakamura, T., et al., *A Wnt- and beta -catenin-dependent pathway for mammalian cardiac myogenesis.* Proc Natl Acad Sci U S A, 2003. **100**(10): p. 5834-9.
251. Ueno, S., et al., *Biphasic role for Wnt/beta-catenin signaling in cardiac specification in zebrafish and embryonic stem cells.* Proc Natl Acad Sci U S A, 2007. **104**(23): p. 9685-90.
252. Naito, A.T., et al., *Developmental stage-specific biphasic roles of Wnt/beta-catenin signaling in cardiomyogenesis and hematopoiesis.* Proc Natl Acad Sci U S A, 2006. **103**(52): p. 19812-7.
253. Huelsken, J., et al., *Requirement for beta-catenin in anterior-posterior axis formation in mice.* J Cell Biol, 2000. **148**(3): p. 567-78.
254. Lindsley, R.C., et al., *Canonical Wnt signaling is required for development of embryonic stem cell-derived mesoderm.* Development, 2006. **133**(19): p. 3787-96.
255. Liu, P., et al., *Requirement for Wnt3 in vertebrate axis formation.* Nat Genet, 1999. **22**(4): p. 361-5.
256. Vonica, A. and B.M. Gumbiner, *Zygotic Wnt activity is required for Brachyury expression in the early Xenopus laevis embryo.* Dev Biol, 2002. **250**(1): p. 112-27.
257. Yamaguchi, T.P., et al., *T (Brachyury) is a direct target of Wnt3a during paraxial mesoderm specification.* Genes Dev, 1999. **13**(24): p. 3185-90.
258. Kemp, C., et al., *Expression of all Wnt genes and their secreted antagonists during mouse blastocyst and postimplantation development.* Dev Dyn, 2005. **233**(3): p. 1064-75.
259. Kouskoff, V., et al., *Sequential development of hematopoietic and cardiac mesoderm during embryonic stem cell differentiation.* Proc Natl Acad Sci U S A, 2005. **102**(37): p. 13170-5.
260. Chen, V.C., et al., *Notch signaling respecifies the hemangioblast to a cardiac fate.* Nat Biotechnol, 2008. **26**(10): p. 1169-78.
261. Kwon, C., et al., *A regulatory pathway involving Notch1/beta-catenin/Isl1 determines cardiac progenitor cell fate.* Nat Cell Biol, 2009. **11**(8): p. 951-7.
262. Afouda, B.A., et al., *GATA transcription factors integrate Wnt signalling during heart development.* Development, 2008. **135**(19): p. 3185-90.
263. Pandur, P., et al., *Wnt-11 activation of a non-canonical Wnt signalling pathway is required for cardiogenesis.* Nature, 2002. **418**(6898): p. 636-41.
264. Eisenberg, C.A. and L.M. Eisenberg, *WNT11 promotes cardiac tissue formation of early mesoderm.* Dev Dyn, 1999. **216**(1): p. 45-58.
265. Eisenberg, C.A., R.G. Gourdie, and L.M. Eisenberg, *Wnt-11 is expressed in early avian mesoderm and required for the differentiation of the quail mesoderm cell line QCE-6.* Development, 1997. **124**(2): p. 525-36.
266. Fraidenraich, D., et al., *Rescue of cardiac defects in id knockout embryos by injection of embryonic stem cells.* Science, 2004. **306**(5694): p. 247-52.

267. Lindsley, R.C., et al., *Mesp1 coordinately regulates cardiovascular fate restriction and epithelial-mesenchymal transition in differentiating ESCs.* Cell Stem Cell, 2008. **3**(1): p. 55-68.
268. Pinson, K.I., et al., *An LDL-receptor-related protein mediates Wnt signalling in mice.* Nature, 2000. **407**(6803): p. 535-8.
269. Tamai, K., et al., *LDL-receptor-related proteins in Wnt signal transduction.* Nature, 2000. **407**(6803): p. 530-5.
270. Wehrli, M., et al., *arrow encodes an LDL-receptor-related protein essential for Wingless signalling.* Nature, 2000. **407**(6803): p. 527-30.
271. Jackson, B.M. and D.M. Eisenmann, *beta-catenin-dependent Wnt signaling in C. elegans: teaching an old dog a new trick.* Cold Spring Harb Perspect Biol, 2012. **4**(8): p. a007948.
272. Niehrs, C., *On growth and form: a Cartesian coordinate system of Wnt and BMP signaling specifies bilaterian body axes.* Development, 2010. **137**(6): p. 845-57.
273. Swarup, S. and E.M. Verheyen, *Wnt/Wingless signaling in Drosophila.* Cold Spring Harb Perspect Biol, 2012. **4**(6).
274. Wang, J., T. Sinha, and A. Wynshaw-Boris, *Wnt signaling in mammalian development: lessons from mouse genetics.* Cold Spring Harb Perspect Biol, 2012. **4**(5).
275. Wray, J. and C. Hartmann, *WNTing embryonic stem cells.* Trends Cell Biol, 2012. **22**(3): p. 159-68.
276. Barker, N. and H. Clevers, *Catenins, Wnt signaling and cancer.* Bioessays, 2000. **22**(11): p. 961-5.
277. Bienz, M. and H. Clevers, *Linking colorectal cancer to Wnt signaling.* Cell, 2000. **103**(2): p. 311-20.
278. Monroe, D.G., et al., *Update on Wnt signaling in bone cell biology and bone disease.* Gene, 2012. **492**(1): p. 1-18.
279. Polakis, P., *Wnt signaling in cancer.* Cold Spring Harb Perspect Biol, 2012. **4**(5).
280. van Amerongen, R., A. Mikels, and R. Nusse, *Alternative wnt signaling is initiated by distinct receptors.* Sci Signal, 2008. **1**(35): p. re9.
281. He, X., et al., *LDL receptor-related proteins 5 and 6 in Wnt/beta-catenin signaling: arrows point the way.* Development, 2004. **131**(8): p. 1663-77.
282. Niehrs, C. and J. Shen, *Regulation of Lrp6 phosphorylation.* Cell Mol Life Sci, 2010. **67**(15): p. 2551-62.
283. Minami, Y., et al., *Ror-family receptor tyrosine kinases in noncanonical Wnt signaling: their implications in developmental morphogenesis and human diseases.* Dev Dyn, 2010. **239**(1): p. 1-15.
284. Peradziryi, H., N.S. Tolwinski, and A. Borchers, *The many roles of PTK7: a versatile regulator of cell-cell communication.* Arch Biochem Biophys, 2012. **524**(1): p. 71-6.
285. Fradkin, L.G., J.M. Dura, and J.N. Noordermeer, *Ryks: new partners for Wnts in the developing and regenerating nervous system.* Trends Neurosci, 2010. **33**(2): p. 84-92.
286. Jing, L., et al., *Wnt signals organize synaptic prepattern and axon guidance through the zebrafish unplugged/MuSK receptor.* Neuron, 2009. **61**(5): p. 721-33.
287. Kikuchi, A., et al., *New insights into the mechanism of Wnt signaling pathway activation.* Int Rev Cell Mol Biol, 2011. **291**: p. 21-71.
288. Cruciat, C.M. and C. Niehrs, *Secreted and transmembrane wnt inhibitors and activators.* Cold Spring Harb Perspect Biol, 2013. **5**(3).

289. Niehrs, C., *The complex world of WNT receptor signalling.* Nat Rev Mol Cell Biol, 2012. **13**(12): p. 767-79.
290. Kuhl, M., et al., *Ca(2+)/calmodulin-dependent protein kinase II is stimulated by Wnt and Frizzled homologs and promotes ventral cell fates in Xenopus.* J Biol Chem, 2000. **275**(17): p. 12701-11.
291. Pereira, C., et al., *Wnt5A/CaMKII signaling contributes to the inflammatory response of macrophages and is a target for the antiinflammatory action of activated protein C and interleukin-10.* Arterioscler Thromb Vasc Biol, 2008. **28**(3): p. 504-10.
292. Blumenthal, A., et al., *The Wingless homolog WNT5A and its receptor Frizzled-5 regulate inflammatory responses of human mononuclear cells induced by microbial stimulation.* Blood, 2006. **108**(3): p. 965-73.
293. Mikels, A.J. and R. Nusse, *Purified Wnt5a protein activates or inhibits beta-catenin-TCF signaling depending on receptor context.* PLoS Biol, 2006. **4**(4): p. e115.
294. MacDonald, B.T. and X. He, *Frizzled and LRP5/6 receptors for Wnt/beta-catenin signaling.* Cold Spring Harb Perspect Biol, 2012. **4**(12).
295. Dale, T.C., *Signal transduction by the Wnt family of ligands.* Biochem J, 1998. **329 (Pt 2)**: p. 209-23.
296. Gumbiner, B.M., *Propagation and localization of Wnt signaling.* Curr Opin Genet Dev, 1998. **8**(4): p. 430-5.
297. Wodarz, A. and R. Nusse, *Mechanisms of Wnt signaling in development.* Annu Rev Cell Dev Biol, 1998. **14**: p. 59-88.
298. Simons, M. and M. Mlodzik, *Planar cell polarity signaling: from fly development to human disease.* Annu Rev Genet, 2008. **42**: p. 517-40.
299. De, A., *Wnt/Ca2+ signaling pathway: a brief overview.* Acta Biochim Biophys Sin (Shanghai), 2011. **43**(10): p. 745-56.
300. Sheldahl, L.C., et al., *Protein kinase C is differentially stimulated by Wnt and Frizzled homologs in a G-protein-dependent manner.* Curr Biol, 1999. **9**(13): p. 695-8.
301. Clark, C.E., C.C. Nourse, and H.M. Cooper, *The tangled web of non-canonical Wnt signalling in neural migration.* Neurosignals, 2012. **20**(3): p. 202-20.
302. van den Heuvel, M., et al., *Distribution of the wingless gene product in Drosophila embryos: a protein involved in cell-cell communication.* Cell, 1989. **59**(4): p. 739-49.
303. Strigini, M. and S.M. Cohen, *Wingless gradient formation in the Drosophila wing.* Curr Biol, 2000. **10**(6): p. 293-300.
304. Dubois, L., et al., *Regulated endocytic routing modulates wingless signaling in Drosophila embryos.* Cell, 2001. **105**(5): p. 613-24.
305. Rives, A.F., et al., *Endocytic trafficking of Wingless and its receptors, Arrow and DFrizzled-2, in the Drosophila wing.* Dev Biol, 2006. **293**(1): p. 268-83.
306. Blitzer, J.T. and R. Nusse, *A critical role for endocytosis in Wnt signaling.* BMC Cell Biol, 2006. **7**: p. 28.
307. Seto, E.S. and H.J. Bellen, *Internalization is required for proper Wingless signaling in Drosophila melanogaster.* J Cell Biol, 2006. **173**(1): p. 95-106.
308. Davidson, G., et al., *Casein kinase 1 gamma couples Wnt receptor activation to cytoplasmic signal transduction.* Nature, 2005. **438**(7069): p. 867-72.

309. Tolwinski, N.S. and E. Wieschaus, *Rethinking WNT signaling.* Trends Genet, 2004. **20**(4): p. 177-81.
310. Zeng, X., et al., *A dual-kinase mechanism for Wnt co-receptor phosphorylation and activation.* Nature, 2005. **438**(7069): p. 873-7.
311. Bilic, J., et al., *Wnt induces LRP6 signalosomes and promotes dishevelled-dependent LRP6 phosphorylation.* Science, 2007. **316**(5831): p. 1619-22.
312. MacDonald, B.T., K. Tamai, and X. He, *Wnt/beta-catenin signaling: components, mechanisms, and diseases.* Dev Cell, 2009. **17**(1): p. 9-26.
313. Zeng, X., et al., *Initiation of Wnt signaling: control of Wnt coreceptor Lrp6 phosphorylation/activation via frizzled, dishevelled and axin functions.* Development, 2008. **135**(2): p. 367-75.
314. Dequeant, M.L. and O. Pourquie, *Segmental patterning of the vertebrate embryonic axis.* Nat Rev Genet, 2008. **9**(5): p. 370-82.
315. Pourquie, O., *Vertebrate somitogenesis.* Annu Rev Cell Dev Biol, 2001. **17**: p. 311-50.
316. Buckingham, M., et al., *The formation of skeletal muscle: from somite to limb.* J Anat, 2003. **202**(1): p. 59-68.
317. Pourquie, O., *Building the spine: the vertebrate segmentation clock.* Cold Spring Harb Symp Quant Biol, 2007. **72**: p. 445-9.
318. Palmeirim, I., et al., *Avian hairy gene expression identifies a molecular clock linked to vertebrate segmentation and somitogenesis.* Cell, 1997. **91**(5): p. 639-48.
319. Aulehla, A., et al., *Wnt3a plays a major role in the segmentation clock controlling somitogenesis.* Dev Cell, 2003. **4**(3): p. 395-406.
320. Ishikawa, A., et al., *Mouse Nkd1, a Wnt antagonist, exhibits oscillatory gene expression in the PSM under the control of Notch signaling.* Mech Dev, 2004. **121**(12): p. 1443-53.
321. Niwa, Y., et al., *The initiation and propagation of Hes7 oscillation are cooperatively regulated by Fgf and notch signaling in the somite segmentation clock.* Dev Cell, 2007. **13**(2): p. 298-304.
322. Dale, J.K., et al., *Oscillations of the snail genes in the presomitic mesoderm coordinate segmental patterning and morphogenesis in vertebrate somitogenesis.* Dev Cell, 2006. **10**(3): p. 355-66.
323. Dequeant, M.L., et al., *A complex oscillating network of signaling genes underlies the mouse segmentation clock.* Science, 2006. **314**(5805): p. 1595-8.
324. Holley, S.A., et al., *her1 and the notch pathway function within the oscillator mechanism that regulates zebrafish somitogenesis.* Development, 2002. **129**(5): p. 1175-83.
325. Holley, S.A., R. Geisler, and C. Nusslein-Volhard, *Control of her1 expression during zebrafish somitogenesis by a delta-dependent oscillator and an independent wave-front activity.* Genes Dev, 2000. **14**(13): p. 1678-90.
326. Dale, J.K., et al., *Periodic notch inhibition by lunatic fringe underlies the chick segmentation clock.* Nature, 2003. **421**(6920): p. 275-8.
327. Bessho, Y., et al., *Periodic repression by the bHLH factor Hes7 is an essential mechanism for the somite segmentation clock.* Genes Dev, 2003. **17**(12): p. 1451-6.
328. Kolter, T. and K. Sandhoff, *Principles of lysosomal membrane digestion: stimulation of sphingolipid degradation by sphingolipid activator proteins and anionic lysosomal lipids.* Annu Rev Cell Dev Biol, 2005. **21**: p. 81-103.

329. Platt, F.M., B. Boland, and A.C. van der Spoel, *The cell biology of disease: lysosomal storage disorders: the cellular impact of lysosomal dysfunction.* J Cell Biol, 2012. **199**(5): p. 723-34.
330. Hodis, E., et al., *A landscape of driver mutations in melanoma.* Cell, 2012. **150**(2): p. 251-63.
331. Chen, C., et al., *Snx3 regulates recycling of the transferrin receptor and iron assimilation.* Cell Metab, 2013. **17**(3): p. 343-52.
332. Nusse, R. and H.E. Varmus, *Many tumors induced by the mouse mammary tumor virus contain a provirus integrated in the same region of the host genome.* Cell, 1982. **31**(1): p. 99-109.
333. Rijsewijk, F., et al., *The Drosophila homolog of the mouse mammary oncogene int-1 is identical to the segment polarity gene wingless.* Cell, 1987. **50**(4): p. 649-57.
334. Nishisho, I., et al., *Mutations of chromosome 5q21 genes in FAP and colorectal cancer patients.* Science, 1991. **253**(5020): p. 665-9.
335. Kinzler, K.W., et al., *Identification of FAP locus genes from chromosome 5q21.* Science, 1991. **253**(5020): p. 661-5.
336. Su, L.K., B. Vogelstein, and K.W. Kinzler, *Association of the APC tumor suppressor protein with catenins.* Science, 1993. **262**(5140): p. 1734-7.
337. Caldwell, G.M., et al., *The Wnt antagonist sFRP1 in colorectal tumorigenesis.* Cancer Res, 2004. **64**(3): p. 883-8.
338. Lee, A.Y., et al., *Expression of the secreted frizzled-related protein gene family is downregulated in human mesothelioma.* Oncogene, 2004. **23**(39): p. 6672-6.
339. Suzuki, H., et al., *Epigenetic inactivation of SFRP genes allows constitutive WNT signaling in colorectal cancer.* Nat Genet, 2004. **36**(4): p. 417-22.
340. Fukui, T., et al., *Transcriptional silencing of secreted frizzled related protein 1 (SFRP 1) by promoter hypermethylation in non-small-cell lung cancer.* Oncogene, 2005. **24**(41): p. 6323-7.
341. Zou, H., et al., *Aberrant methylation of secreted frizzled-related protein genes in esophageal adenocarcinoma and Barrett's esophagus.* Int J Cancer, 2005. **116**(4): p. 584-91.
342. Rhee, C.S., et al., *Wnt and frizzled receptors as potential targets for immunotherapy in head and neck squamous cell carcinomas.* Oncogene, 2002. **21**(43): p. 6598-605.
343. Wong, S.C., et al., *Expression of frizzled-related protein and Wnt-signalling molecules in invasive human breast tumours.* J Pathol, 2002. **196**(2): p. 145-53.
344. Milovanovic, T., et al., *Expression of Wnt genes and frizzled 1 and 2 receptors in normal breast epithelium and infiltrating breast carcinoma.* Int J Oncol, 2004. **25**(5): p. 1337-42.
345. Okino, K., et al., *Up-regulation and overproduction of DVL-1, the human counterpart of the Drosophila dishevelled gene, in cervical squamous cell carcinoma.* Oncol Rep, 2003. **10**(5): p. 1219-23.
346. Kageshita, T., et al., *Loss of beta-catenin expression associated with disease progression in malignant melanoma.* Br J Dermatol, 2001. **145**(2): p. 210-6.
347. Maelandsmo, G.M., et al., *Reduced beta-catenin expression in the cytoplasm of advanced-stage superficial spreading malignant melanoma.* Clin Cancer Res, 2003. **9**(9): p. 3383-8.
348. Bachmann, I.M., et al., *Importance of P-cadherin, beta-catenin, and Wnt5a/frizzled for progression of melanocytic tumors and prognosis in cutaneous melanoma.* Clin Cancer Res, 2005. **11**(24 Pt 1): p. 8606-14.
349. Chien, A.J., et al., *Activated Wnt/beta-catenin signaling in melanoma is associated with decreased proliferation in patient tumors and a murine melanoma model.* Proc Natl Acad Sci U S A, 2009. **106**(4): p. 1193-8.

350. Dorsky, R.I., D.W. Raible, and R.T. Moon, *Direct regulation of nacre, a zebrafish MITF homolog required for pigment cell formation, by the Wnt pathway.* Genes Dev, 2000. **14**(2): p. 158-62.
351. Hornyak, T.J., et al., *Transcription factors in melanocyte development: distinct roles for Pax-3 and Mitf.* Mech Dev, 2001. **101**(1-2): p. 47-59.
352. Gamallo, C., et al., *beta-catenin expression pattern in stage I and II ovarian carcinomas : relationship with beta-catenin gene mutations, clinicopathological features, and clinical outcome.* Am J Pathol, 1999. **155**(2): p. 527-36.
353. Horvath, L.G., et al., *Lower levels of nuclear beta-catenin predict for a poorer prognosis in localized prostate cancer.* Int J Cancer, 2005. **113**(3): p. 415-22.
354. Elzagheid, A., et al., *Nuclear beta-catenin expression as a prognostic factor in advanced colorectal carcinoma.* World J Gastroenterol, 2008. **14**(24): p. 3866-71.
355. Matushansky, I., et al., *Derivation of sarcomas from mesenchymal stem cells via inactivation of the Wnt pathway.* J Clin Invest, 2007. **117**(11): p. 3248-57.
356. Heiser, P.W., et al., *Stabilization of beta-catenin induces pancreas tumor formation.* Gastroenterology, 2008. **135**(4): p. 1288-300.
357. Morris, J.P.t., et al., *Beta-catenin blocks Kras-dependent reprogramming of acini into pancreatic cancer precursor lesions in mice.* J Clin Invest, 2010. **120**(2): p. 508-20.
358. Zimmerman, Z.F., R.T. Moon, and A.J. Chien, *Targeting Wnt pathways in disease.* Cold Spring Harb Perspect Biol, 2012. **4**(11).
359. Blackwood, D.H., et al., *Schizophrenia and affective disorders--cosegregation with a translocation at chromosome 1q42 that directly disrupts brain-expressed genes: clinical and P300 findings in a family.* Am J Hum Genet, 2001. **69**(2): p. 428-33.
360. Mao, Y., et al., *Disrupted in schizophrenia 1 regulates neuronal progenitor proliferation via modulation of GSK3beta/beta-catenin signaling.* Cell, 2009. **136**(6): p. 1017-31.
361. Kang, D.E., et al., *Presenilin couples the paired phosphorylation of beta-catenin independent of axin: implications for beta-catenin activation in tumorigenesis.* Cell, 2002. **110**(6): p. 751-62.
362. Shah, S.P., et al., *Mutational evolution in a lobular breast tumour profiled at single nucleotide resolution.* Nature, 2009. **461**(7265): p. 809-13.
363. Deardorff, M.A., et al., *Frizzled-8 is expressed in the Spemann organizer and plays a role in early morphogenesis.* Development, 1998. **125**(14): p. 2687-700.